



NTNU – Trondheim
Norwegian University of
Science and Technology

Modeling and Analysis of a Frost Proof Leisure Building with Active Solar Heating and Heat Exchange with the Ground

Ragnhild Haukland Løge

Master of Energy and Environmental Engineering

Submission date: Januar 2014

Supervisor: Per Olaf Tjelflaat, EPT

Co-supervisor: Rasmus Høseggen, EPT

Norwegian University of Science and Technology
Department of Energy and Process Engineering

EPT-M-2013-79

MASTEROPPGAVE

for

Stud.techn. Ragnhild Løge

Høsten 2013

**Modellering og analyse av energibruk for en frostsikker fritidsbolig
med aktiv soloppvarming og varmelagring i grunnen***Modeling and analyses of a frost proof leisure building with active solar heating and heat
exchange with the ground***Bakgrunn og målsetting**

De fleste fritidsboliger som bygges i dag har sanitæranlegg. I ubenyttede vinterperioder er bygningene vanligvis elektrisk oppvarmet til 5-10 °C for å unngå frostskafer på installasjonene. En slik bruk av elektrisitet, og relaterte klimagassutslipp, synes unødvendig og burde kunne unngås. Det er fokus på fritidsboliger beliggende ved 60° nord.

I meget kalde perioder vil slik oppvarming, for å frostsikre fritidsboliger, også føre til unødig effektbelastning på kraftlinjene.

Det er en visjon å utvikle en prototype fritidsbolig hvor sanitærinstallasjonene kan sikres mot frost uten bruk av elektrisitet eller andre former for primærenergi. I dette arbeidet er målet å utvikle en simuleringsmodell som realistisk modellerer varmeoverføring fra et solvarmepanel til lagring i grunnen gjennom sommermånedene. Den lagrede varmen ledes tilbake til bygningen gjennom vintermånedene slik at sanitærinstallasjonene holdes frostfrie.

I denne oppgaven fokuseres det på å utvikle en tilfredsstillende løsning for solvarmesystemet for fritidsboligen.

Oppgaven bearbeides ut fra følgende punkter

- 1 Litteraturstudie av aktuelle solfangerløsninger og hvordan disse kan integreres i bygningen.
- 2 En ubebodd bygning med installasjoner modelleres i beregningsprogrammet ESP-r. Det fokuseres spesielt på modellering av solfangersystemet..
- 3 Det skal gjennomføres analyse av varmeutveksling mellom fritidsboligen, solvarmepanelet og grunnen for å oppnå frostsikre tekniske løsninger. Det må gjennomføres parameterstudier, og slik at både typisk beliggenhet i fjellområde og kysten i Sør-Norge blir undersøkt.

Senest 14 dager etter utlevering av oppgaven skal kandidaten levere/sendte instituttet en detaljert fremdrift- og eventuelt forsøksplan for oppgaven til evaluering og eventuelt diskusjon med faglig ansvarlig/veiledere. Detaljer ved eventuell utførelse av dataprogrammer skal avtales nærmere i samråd med faglig ansvarlig.

Besvarelsen redigeres mest mulig som en forskningsrapport med et sammendrag både på norsk og engelsk, konklusjon, litteraturliste, innholdsfortegnelse etc. Ved utarbeidelsen av teksten skal kandidaten legge vekt på å gjøre teksten oversiktlig og velskrevet. Med henblikk på lesning av besvarelsen er det viktig at de nødvendige henvisninger for korresponderende steder i tekst, tabeller og figurer anføres på begge steder. Ved bedømmelsen legges det stor vekt på at resultatene er grundig bearbeidet, at de oppstilles tabellarisk og/eller grafisk på en oversiktlig måte, og at de er diskutert utførlig.

Alle benyttede kilder, også muntlige opplysninger, skal oppgis på fullstendig måte. For tidsskrifter og bøker oppgis forfatter, tittel, årgang, sidetall og eventuelt figurnummer.

Det forutsettes at kandidaten tar initiativ til og holder nødvendig kontakt med faglærer og veileder(e). Kandidaten skal rette seg etter de reglementer og retningslinjer som gjelder ved alle (andre) fagmiljøer som kandidaten har kontakt med gjennom sin utførelse av oppgaven, samt etter eventuelle pålegg fra Institutt for energi- og prosesssteknikk.


Risikovurdering av kandidatens arbeid skal gjennomføres i henhold til instituttets prosedyrer. Risikovurderingen skal dokumenteres og inngå som del av besvarelsen. Hendelser relatert til kandidatens arbeid med uheldig innvirkning på helse, miljø eller sikkerhet, skal dokumenteres og inngå som en del av besvarelsen. Hvis dokumentasjonen på risikovurderingen utgjør veldig mange sider, leveres den fulle versjonen elektronisk til veileder og et utdrag inkluderes i besvarelsen.

I henhold til ”Utfyllende regler til studieforskriften for teknologistudiet/sivilingeniørstudiet” ved NTNU § 20, forbeholder instituttet seg retten til å benytte alle resultater og data til undervisnings- og forskningsformål, samt til fremtidige publikasjoner.

Besvarelsen leveres digitalt i DAIM. Et faglig sammendrag med oppgavens tittel, kandidatens navn, veileders navn, årstall, instituttnavn, og NTNUs logo og navn, leveres til instituttet som en separat pdf-fil. Etter avtale leveres besvarelse og evt. annet materiale til veileder i digitalt format.

- Arbeid i laboratorium (vannkraftlaboratoriet, strømningsmeknikk, varmeteknikk)
- Feltarbeid

NTNU, Institutt for energi- og prosesssteknikk, 9. september 2013


Olav Bolland
Instituttleder


Per O. Tjellfaat
Faglig ansvarlig/veileder

Medveileder: Førsteamanuensis II Rasmus Høseggen

Preface

This master thesis was written during the fall semester of 2013 at the Norwegian University of Science and Technology (NTNU) in Trondheim. The thesis was written at the Department of Energy and Process Engineering (EPT) during the 10th semester of the master program in Energy- and Environmental Engineering.

The thesis is a continuation of the project work report written during the fall semester of 2012 in collaboration with Ida Karin Auråen.

I would like to thank my supervisor Per Olaf Tjelflaat for good guidance and advice along the way and co-supervisor Rasmus Z. Høseggen for much needed help with the simulation program ESP-r. I would also like to thank Eugen Uthaug and the rest of the IT department at EPT for IT related assistance. Finally I would like to thank Ida Karin Auråen for good teamwork in the preparation of the project work report which is the basis for this master thesis.

Abstract

Requirements regarding efficient energy use in buildings are becoming more and more strict. New ideas and technologies are constantly sought to face the challenge of reducing global CO₂ emissions. The building sector accounts for a large part of energy use. The potential for more efficient energy use in this sector is significant and will also contribute towards reduced CO₂ emissions.

This master thesis is a continuation of a project work report written in collaboration with Ida Karin Auråen during the fall semester of 2012. A prototype of a leisure home was developed where sanitary installations were kept frost proof throughout the year without the use of primary energy. This was achieved by placing sanitary installations within well-insulated internal zones, and by using an active solar heating system and heat exchange with the ground.

The goal of this thesis is to improve the model developed in the project work report. The main focus is to improve the design of the solar heating system to better approximate a realistic situation. Auråen's master thesis focused on the interaction between the leisure building and surrounding ground, and the ground model developed in her report is further used in this thesis.

The leisure building consists of two floors and is constructed of poorly insulated log walls. Each floor has a thermally insulated internal zone where sanitary installations are deemed installed. The goal is to maintain frost proof conditions throughout the year within the internal zones to avoid damages to sanitary installations. The idea is to promote seasonal heat storage by storing heat collected during sunny periods in thermal mass located below the building. The desired effect is that the heat transfer is reversed during cold, dark winter months, so that stored heat is released upwards and into the leisure building, preventing formation of frost in the internal zones.

The dynamic simulation tool ESP-r (Environmental System Performance Research) is used to analyze the leisure building. The interactions between the building and the ground are modeled using a submerged basement zone defined with a BASESIMP

configuration. BASESIMP performs quasi 3-dimensional heat transfer calculations between a building and the ground. BASESIMP does not account for heat storage. The heat storage potential in the ground is analyzed through the internal ground floor construction. The floor is modeled as a thermally massive concrete slab with high density and high specific heat capacity. Heat storage calculations are performed based on heat stored in this concrete slab.

The solar heating system is built up using the plants and systems network in ESP-r. The system contains three components; flat plate solar collector, circulation pump and hydronic floor. The hydronic floor component is a water-based floor heating circuit and is embedded within the concrete slab. Heat from the solar collector is transferred to the hydronic floor heating the slab below the internal zones. Towards the end of the winter, the remaining energy stored in the slab, and the incoming solar radiation injected to the slab, are too limited to make a significant heat contribution to the internal zones. Therefore, heat collected from January 1st to April 30th is injected directly to zone air of the internal first floor.

The leisure home is planned located in southern mountain regions in Norway. ESP-r does not have available climate data for this area, and therefore climate data from Östersund, Sweden has been used as an approximation. The building has also been tested with climate data from Fornebu, Norway which is a typical coastal region in the south of Norway. Different parameters have been altered to optimize the model with regards to raising the minimum temperatures in the internal zones. Results show that the internal zones maintain much more stable conditions throughout the year than the outer zones. This shows that isolating sanitary installations within well-insulated internal zones can be a major advantage in the design process to reduce the amount of energy needed to keep the facilities frost free.

A south-oriented solar collector with an area of 2 m², and an slope of 70 ° achieves sufficient energy for frost proof conditions for both locations. The minimum temperatures in the internal ground- and first floor are 5.29 °C and 3.10 °C with Östersund climate data. The delivered energy from the hydronic floor component to the concrete slab, turns out to be 482 kWh with Östersund climate data, and 547 kWh with Fornebu climate data, with a collector efficiency of 68 %.

Results show that heat collected in the spring and summer significantly affect the minimum temperatures occurring around mid-February in the following year.

For further studies and optimization of the model, the interactions between the heat storage and surrounding ground should be studied more thoroughly. The effect which snow may have on the ground conditions should also be studied. Evacuated tube solar collectors are probably more suited for Scandinavian climate than flat plate collectors as used in this thesis. The plant database in ESP-r has no option to model evacuated tube collectors. The effect of such could be studied with another simulation tool.

Sammendrag

Stadig strengere krav stilles til effektiv energibruk i bygninger. Nye ideer og teknologier ettersøkes for å kunne møte utfordringen om å redusere globale CO₂ utslipp. Bygningssektoren står for en stor andel av årlig energibruk. Det er et stort potensial for å utvikle mer energieffektive bygninger, noe som vil bidra til reduserte CO₂ utslipp.

Denne masteroppgaven er en fortsettelse på en prosjektoppgave skrevet i samarbeid med Ida Karin Auråen høsten 2012. I prosjektoppgaven ble det utviklet en prototype av en fritidsbolig hvor sanitærinstallasjoner ble holdt frostfrie gjennom året uten å bruke primærenergi. Dette ble oppnådd ved å plassere sanitærinstallasjoner i meget godt isolerte indre soner, og ved å bruke et aktivt solvarmeanlegg og varmeutveksling med grunnen.

Målet med denne masteroppgaven er å forbedre modellen som ble utviklet i prosjektet. Det vil bli lagt vekt på å forbedre modelleringen av solvarmeanlegget slik at det blir mer tilnærmet en realistisk modell. Auråen sin masteroppgave fokuserte på å utbedre grunnmodelleringen og studere interaksjonen mellom fritidsboligen og omgivende grunnforhold. Auråen sin grunnmodell vil bli brukt videre i denne masteroppgaven.

Fritidsboligen består av to etasjer og er bygget av dårlig isolerte laftede yttervegger. Hver etasje har en velisolert indre sone hvor sanitærinstallasjoner skal plasseres. Målet er å opprettholde frostfrie forhold gjennom året inni de velisolerte indre sonene for å unngå frostskaider på sanitærinstallasjoner. Ideen er å fremme sesonglagring av varme ved å lagre varme hentet fra solanlegget i solrike perioder i termisk masse under bygningen. Den ønskede effekten er at den lagrede varmen skal stige i kaldere, mindre solrike perioder og bidra til å holde de indre sonene i fritidsboligen frostfrie gjennom året.

Det dynamiske simuleringsverktøyet ESP-r (Energy System Performance Research) brukes til å analysere fritidsboligen. Samspillet mellom bygningen og omgivende grunn er modellert ved hjelp av en nedsenket kjellersone definert med en BASESIMP

konfigurasjon. BASESIMP utfører varmetransportberegninger tilnærmet 3-dimensjonalt mellom en bygning og grunnen. BASESIMP tar ikke hensyn til varmelagring. Varmelagringspotensialet i grunnen blir derfor analysert ved hjelp av den indre gulvkonstruksjonen i den nederste etasjen. Gulvkonstruksjonen er modellert som en termisk massiv betongkloss med høy tetthet og høy spesifikk varmekapasitet. Varmelagring i grunnen beregnes ut i fra lagret varme i denne betongklossen.

Solvarmeanlegget er bygget opp ved å bruke nettverk og system valget i ESP-r. Solvarmeanlegget består av tre komponenter; plan solfanger, sirkulasjonspumpe og en vannbåren gulvkomponent. Den vannbårne gulvkomponenten er integrert i et av lagene i betongklossen. Varme fra solfangeren overføres til gulvkomponenten som videre varmer opp betongklossen under de indre sonene. Mot slutten av vinteren er mengden gjenværende varme i klossen, i tillegg til begrenset tilgjengelig solenergi injisert i betongklossen, så lite at det ikke bidrar til noe vesentlig temperaturløft i de indre sonene. Varmen fra solvarmeanlegget blir derfor injisert direkte til romluften i den indre sonen i øverste etasje i perioden 1. januar til 30. april.

Fritidsboligens plassering er i sørlige fjellområder i Norge. ESP-r har ikke tilgjengelig klimadata for dette området, og derfor har klimadata fra Östersund i Sverige blitt brukt som en tilnærming. Bygningen har også blitt simulert med klimadata fra Fornebu, som er et typisk kystområde sør i Norge. Ulike systemparametere har blitt endret på for å optimalisere modellen slik at minimumstemperaturene i de indre sonene blir høyest mulig. Resultatene viser at de indre sonene opprettholder mye mer stabile temperaturer gjennom året enn de ytre sonene. Dette viser at å plassere sanitærinstallasjoner i velisolerte indre soner kan være en stor fordel i prosjekteringsfasen for å redusere mengden energi som kreves for å opprettholde frostfrie forhold.

Med en sørvendt solfanger med et solfangerareal på 2 m^2 og en vinkel på 70° , oppnås tilstrekkelig med energi for å frostsikre de indre sonene, både i Fornebu og Östersund. Minimumstemperaturene i den nedre- og øvre indre sonen er 5.29°C og 3.10°C med klimadata fra Östersund. Levert energi fra den vannbårne gulvkomponenten til betongklossen ble beregnet til 482 kWh for Östersund og 547 kWh for Fornebu med en solfanger virkningsgrad på 68 %.

Resultatene viser at oppsamlet varme fra solfangeranlegget om våren og sommeren har stor effekt på minimumstemperaturene som inntreffer i midten av februar etterfølgende år.

Til videre arbeid og optimalisering av modellen, foreslås det å se nærmere på samspillet mellom varmelagringen og omgivende grunn. Det ville også være av interesse å se på hvilken effekt snødekke har på grunnforholdene. Vakuumrør solfangere er generelt bedre egnet for skandinavisk klima enn plane solfangere som er brukt i denne oppgaven. I systemkomponentdatabasen i ESP-r er det ikke mulig å modellere vakuumrørsolfangere. Effekten av å endre fra plane solfangere til vakuumrørsolfangere kunne blitt studert med et tilsvarende simuleringsprogram.

Table of Contents

Preface	i
Abstract	iii
Sammendrag	vii
List of Figures	xiii
List of tables	xvi
1 Introduction	1
2 Background	3
2.1 Statistics	3
2.2 Building requirements for leisure homes.....	6
3 Introduction to ESP-r	8
4 The leisure home model	10
4.1 Project work model and Auråen’s master thesis	10
4.2 Improved leisure home model.....	13
4.3 Building construction elements.....	13
5 Solar energy	17
5.1 Availability.....	17
5.2 Solar radiation.....	17
5.3 Solar radiation in Norway.....	19
5.4 Direct- and diffuse radiation.....	20
6 Solar heating	21
6.1 Components of a solar heating system	21
6.1.1 Solar collectors.....	21
6.1.2 Hot water storage tanks for solar systems.....	26
6.1.3 Heat storage in the ground	29
6.1.4 Heat exchangers	33
6.1.5 Distribution systems.....	33
6.1.6 Circulation pump.....	34
6.2 Collector efficiency.....	34
6.3 Collector area	37

6.4	Solar heating systems.....	37
6.4.1	Passive solar systems	37
6.4.2	Active solar systems.....	39
7	Integration of solar thermal collectors.....	43
7.1	On-roof integration	43
7.2	In-roof integration.....	44
7.3	Façade integration.....	45
7.3.1	Façade integrated evacuated tube collectors with tilted absorbers	46
8	Dynamic simulation tool ESP-r.....	47
8.1	Ground modeling	47
8.2	BASESIMP	47
8.2.1	BASESIMP inputs	49
8.3	Solar collector model in ESP-r.....	50
9	Solar heating system: possible design solutions.....	54
9.1	Design 1: Storage tank and hydronic floor.....	54
9.2	Design 2: Hydronic floor	55
9.3	Design 3: Storage tank.....	56
9.4	Design 4: Water-based radiator.....	57
10	Chosen system, Design 2: Hydronic floor	59
10.1	Hydronic floor with control loop.....	59
10.2	Old design from the project work report	60
11	Plants and systems model in ESP-r	61
11.1	Defining the solar heating system.....	61
11.2	Defining control strategy.....	67
12	Control loop for heat injection.....	71
12.1	Defining control loop for zone air heating.....	71
13	Simulations.....	76
13.1	Model inputs for the solar heating system components	76
13.1.1	Solar collector inputs	76
13.1.2	Pump inputs	78
13.1.3	Hydronic floor inputs.....	79
13.2	BASESIMP inputs	80

13.3	Start-up days	81
13.4	Climate	81
13.4.1	Östersund climate data	82
13.4.2	Fornebu climate data	84
14	Results and discussion.....	86
14.1	Case simulations with Östersund climate data	88
14.1.1	Case 1	88
14.1.2	Case 2	90
14.1.3	Case 3	91
14.1.4	Case 4	95
14.1.5	Case 5	99
14.1.6	Case 6	101
14.1.7	Case 7	102
14.2	Case simulations with Fornebu Climate data	106
14.2.1	Case 8	106
14.2.2	Case 9	107
14.2.3	Case 10	109
14.3	Solar heating system	110
14.4	Delivered energy to concrete slab from hydronic floor	112
14.5	Heat transfer	114
14.5.1	Energy balance for the concrete slab	115
14.5.2	Energy balance for the basement zone	119
14.6	Cross-section temperatures in the concrete slab.....	123
15	Comparison between Case 6 and Ida Auråen's results	125
16	Conclusion.....	128
17	Proposals for further work.....	131
18	Bibliography	133
	Appendix.....	136

List of Figures

Figure 2-1: Leisure homes in Norway	3
Figure 2-2: New leisure homes and average use area.....	4
Figure 2-3: Electricity use.....	5
Figure 2-4: Number of leisure homes and electricity consumption.....	6
Figure 4-1: Old leisure home model	11
Figure 4-2: Floor plan area with division of zones	12
Figure 4-3: Cross section of the building.....	12
Figure 4-4: New leisure home model.....	13
Figure 4-5: Leisure home.....	16
Figure 4-6: Cross section view of the leisure home.....	16
Figure 5-1: The path of the sun at central European latitude [11].....	18
Figure 5-2: Average annual insolation worldwide, based on [12].....	19
Figure 5-3: Average daily incoming radiation on a horizontal surface in Norway, based on [14].....	20
Figure 5-4: Radiation principles, based on [11].....	20
Figure 6-1: Solar heating system principle, based on [15]	21
Figure 6-2: Flat plate collector, based on [17].....	23
Figure 6-3: Evacuated heat pipe tube [20].....	25
Figure 6-4: Direct-flow evacuated tube collector [22]	26
Figure 6-5: Solar hot water tank, Ecoline Sun [24]	27
Figure 6-6: Solar hot water tank, Ecoline Twin Coil [25]	28
Figure 6-7: Water tank thermal storage, based on [1]	30
Figure 6-8: Water-gravel pit storage, based on [1].....	31
Figure 6-9: Aquifer thermal energy storage, based on [1].....	32
Figure 6-10: Borehole thermal energy storage, based on [1].....	33
Figure 6-11: Typical collector efficiencies [26]	36
Figure 6-12: Direct gain passive system, based on [27]	38
Figure 6-13: Indirect gain passive system, based on [27].....	38
Figure 6-14: Isolated gain passive system, based on [27]	39
Figure 6-15: Direct circulation system, based on [14].....	40
Figure 6-16: Indirect circulation system, based on [14]	41

Figure 7-1: On-roof installation with flat plate collectors [30].....	43
Figure 7-2: Flat on-roof installation with support frames [31].....	44
Figure 7-3: Flat on-roof evacuated tube installation with tilted absorbers [32]	44
Figure 7-4: In-roof integration of solar collectors [33].....	45
Figure 7-5: In-roof integrated solar collectors [34]	45
Figure 7-6: Façade integrated solar thermal panels [32]	46
Figure 8-1: basement.....	48
Figure 8-2: Slab-on-grade	48
Figure 8-3: The collector model	52
Figure 8-4: Parameters for the collector model	53
Figure 9-1: System with storage tank and hydronic floor.....	55
Figure 9-2: System with hydronic floor.....	56
Figure 9-3: System with storage tank	57
Figure 9-4: System with radiator mimicking floor heating	58
Figure 10-1: Cross section of leisure home illustrating point of heat injection.....	59
Figure 11-1: Network definition	62
Figure 11-2: Component types.....	63
Figure 11-3: Input parameters for <i>variable speed domestic WCH pump</i>	63
Figure 11-4: Input parameters for <i>slab-on-grade hydronic floor</i>	64
Figure 11-5: Concrete slab with nodes and layers	65
Figure 11-6: Connection types.....	65
Figure 11-7: Connections in the solar heating system	66
Figure 11-8: Containment types.....	66
Figure 11-9: Containments for system components	67
Figure 11-10: Editing options	68
Figure 11-11: Plant sensor	68
Figure 11-12: Plant component for actuator	69
Figure 11-13: Controller types.....	70
Figure 12-1: Control loop for heat injection.....	72
Figure 12-2: Control law.....	73
Figure 12-3: Zone control period data	74
Figure 12-4: Zone controls.....	75
Figure 13-1: Map showing Fornebu and Östersund [44].....	82
Figure 13-2: Dry bulb temperature Östersund	83

Figure 13-3: Direct and diffuse solar radiation Östersund.....	83
Figure 13-4: Dry bulb temperature Fornebu.....	85
Figure 13-5: Direct and diffuse solar radiation Fornebu	85
Figure 14-1: Dry bulb temperatures for Case 1	89
Figure 14-2: Dry bulb temperatures for Case 2	90
Figure 14-3: Dry bulb temperatures for Case 3a	92
Figure 14-4: Dry bulb temperatures for Case 3b	93
Figure 14-5: Dry bulb temperatures for Case 3c	95
Figure 14-6: Dry bulb temperatures for Case 4	97
Figure 14-7: Dry bulb temperatures for Case 4, based on daily averages	98
Figure 14-8: Dry bulb temperatures for Case 5	100
Figure 14-9: Dry bulb temperatures for Case 6, based on daily averages	101
Figure 14-10: Dry bulb temperatures for Case 7a, based on daily averages	103
Figure 14-11: Dry bulb temperatures for Case 7b, based on daily averages	105
Figure 14-12: Dry bulb temperatures for Case 8	106
Figure 14-13: Dry bulb temperatures for Case 9, based on daily averages	108
Figure 14-14: Dry bulb temperatures for Case 10, based on daily averages	109
Figure 14-15: Operation of solar heating system.....	111
Figure 14-16: Hydronic floor temperature.....	112
Figure 14-17: Delivered energy from hydronic floor to concrete slab	114
Figure 14-18: Concrete slab control volume and heat fluxes	116
Figure 14-19: Energy balance for concrete slab	118
Figure 14-20: Direction of heat fluxes to and from concrete slab	119
Figure 14-21: Basement control volume and heat fluxes	120
Figure 14-22: Energy balance for basement zone.....	122
Figure 14-23: Direction of heat fluxes to and from basement zone	123
Figure 14-24: Cross section through concrete slab on July 1 st	123
Figure 14-25: Cross section through the concrete slab on December 1 st	124
Figure 15-1: Dry bulb temperatures from Ida Auråen’s model, based on [7]	126
Figure 17-1: Advanced control system for the solar heating system.....	131

List of tables

Table 2-1: Minimum requirements	7
Table 2-2: Requirements for buildings with log walls.....	7
Table 4-1: Building construction elements	14
Table 4-2: Concrete slab construction properties	15
Table 4-3: Basement construction elements	15
Table 6-1: Freezing point of propylene glycol water solutions, based on [28]	41
Table 9-1: System Designs	54
Table 13-1: Solar collector inputs.....	76
Table 13-2: Pump inputs.....	78
Table 13-3: Hydronic floor inputs	79
Table 13-4: Electrical control loop inputs	80
Table 13-5: Inputs for BASESIMP configuration BCIB_6.....	80
Table 14-1: Simulations with Östersund climate data	86
Table 14-2: Simulations with Fornebu climate data	87
Table 14-3: Time axis dates	88
Table 14-4: Peak values for Case 1.....	90
Table 14-5: Peak values for Case 2.....	91
Table 14-6: Peak values for Case 3a.....	92
Table 14-7: Peak values for Case 3b.....	94
Table 14-8: Power input and time of heat injection from Jan-01 to Apr-30.....	96
Table 14-9: Peak values for Case 4.....	99
Table 14-10: Power input and time of heat injection from Nov-01 to Dec-31	99
Table 14-11: Peak values for Case 5.....	100
Table 14-12: Peak values for Case 6.....	102
Table 14-13: Peak values for Case 7a.....	103
Table 14-14: Zone dry bulb temperatures 31-Dec and 1-Jan	104
Table 14-15: Peak values for Case 7b.....	106
Table 14-16: Peak values for Case 8.....	107
Table 14-17: Peak values for Case 9.....	109
Table 14-18: Peak values for Case 10.....	110
Table 14-19: Delivered energy from hydronic floor.....	113

Table 14-20: Heat fluxes to and from concrete slab	117
Table 14-21: Heat fluxes to and from basement zone	121
Table 15-1: Old and new control loop	125
Table 15-2: Control loop if Case 6 has a collector area of 4m ²	126
Table 15-3: Peak values for temperatures in Auråen's case	127

1 Introduction

The building sector accounts for a significant part of the total energy use in Norway. Approximately 40 % of the total energy use from the European Union countries originates from the building sector [1]. Requirements regarding efficient energy use in buildings are becoming more and more strict, both for permanent residences and leisure homes.

The number of leisure homes in Norway has increased dramatically during the last decades. Leisure homes in Norway have traditionally been built as primitive, simple wooden houses with short heating seasons, whereas modern leisure homes are normally equipped with sanitary installations and electricity. Even though the modern ones are better insulated, this trend has resulted in increased energy demand. A major factor contributing to the increased demand is that leisure homes are often left partly heated throughout the year to avoid frost damages to sanitary installations. Such heating is close to 100 % electrical.

Norway is currently in a situation where it is partly dependent on imported energy and power. Especially during the heating season, parts of this electricity production may come from highly polluting coal fired plants. An alternative heating solution, focusing on utilization of renewable energy sources has been studied in this report. The report will demonstrate how an active solar heating system can be used to maintain frost proof conditions for sanitary installations throughout the year in leisure homes. The result is less use of energy and the marginal contribution to reduced CO₂ emissions. The model will be analyzed for a typical mountain region and a coastal region in the southern parts of Norway.

The first part of the report is a literature study with statistics regarding existing leisure homes, an introduction to solar energy and different heat storage possibilities. The second part applies this knowledge with the aim to maintain frost proof conditions for sanitary installations in leisure homes, while minimizing the use of primary energy. This has been addressed in several previous project work reports and master theses. This report is a continuation of the project work report *Analyses of energy use for a*

frost proof leisure building with solar heating and heat exchange with the ground, written during the fall semester 2012 at NTNU. The goal is to improve the model from the project, with emphasis on creating a more realistic active solar heating system. The dynamic simulation tool ESP-r is used for modeling and analyzing possible solutions.

It is assumed that the reader has basic knowledge regarding building engineering, heat and mass transfer and relevant technical terminology.

2 Background

2.1 Statistics

As of November 2013 there are 445 918 buildings in Norway used for leisure and holiday purposes, whereof 413 318 are listed as leisure homes and 32 600 as residential buildings used as leisure homes. Figure 2-1 presents the distribution of leisure homes in the different Norwegian counties. The three counties with the highest number of leisure homes are Oppland, Buskerud and Hedmark respectively [2].

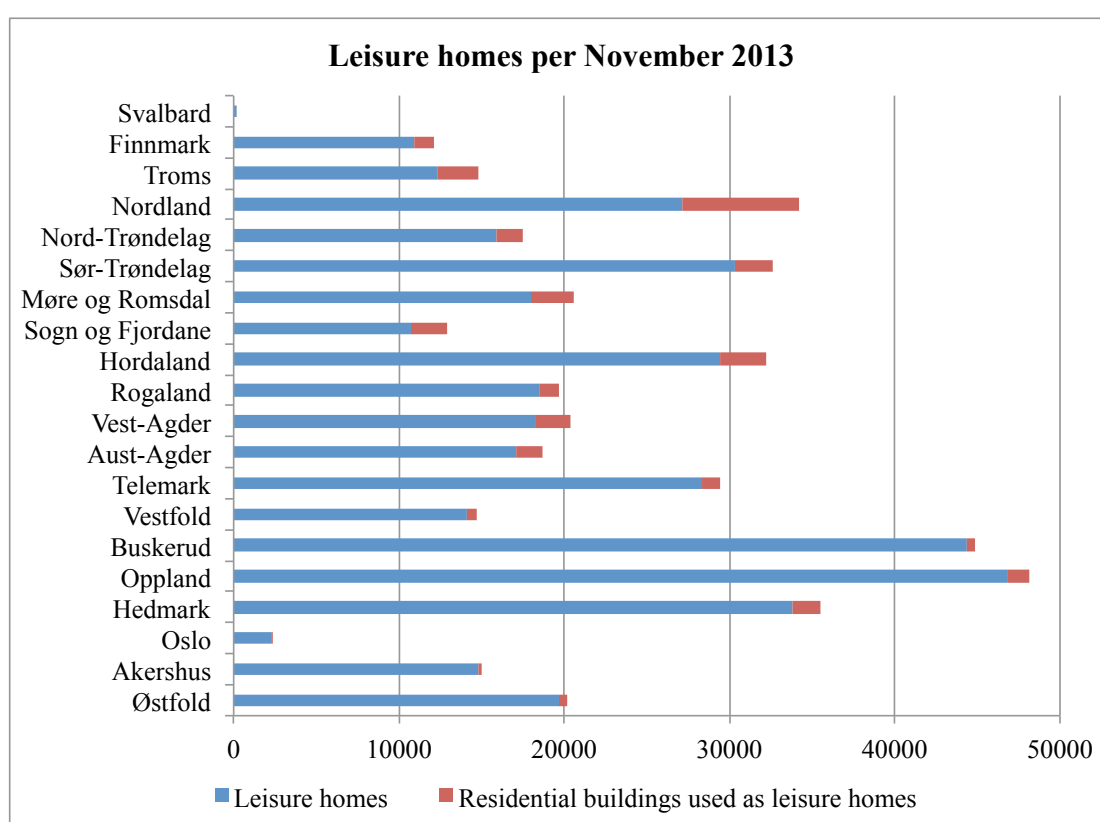


Figure 2-1: Leisure homes in Norway

The number of leisure homes in Norway is increasing rapidly. Consequently, so is the energy consumption originating from this building category. From 1993 to 2006 the net electricity consumption in Norwegian leisure homes increased by approximately 85 % from 0.7 TWh to 1.3 TWh. During the same period, the number of leisure homes increased by only 15 % [2]. This indicates that the increased electricity consumption is not only a consequence of the development of new leisure homes, but must also be attributed several other factors. The most obvious is that the average use area per leisure building has increased. Figure 2-2 shows the development of new

leisure homes along with the average use area of new leisure homes from 1983 to 2012. The data is collected from Statistics Norway [3].

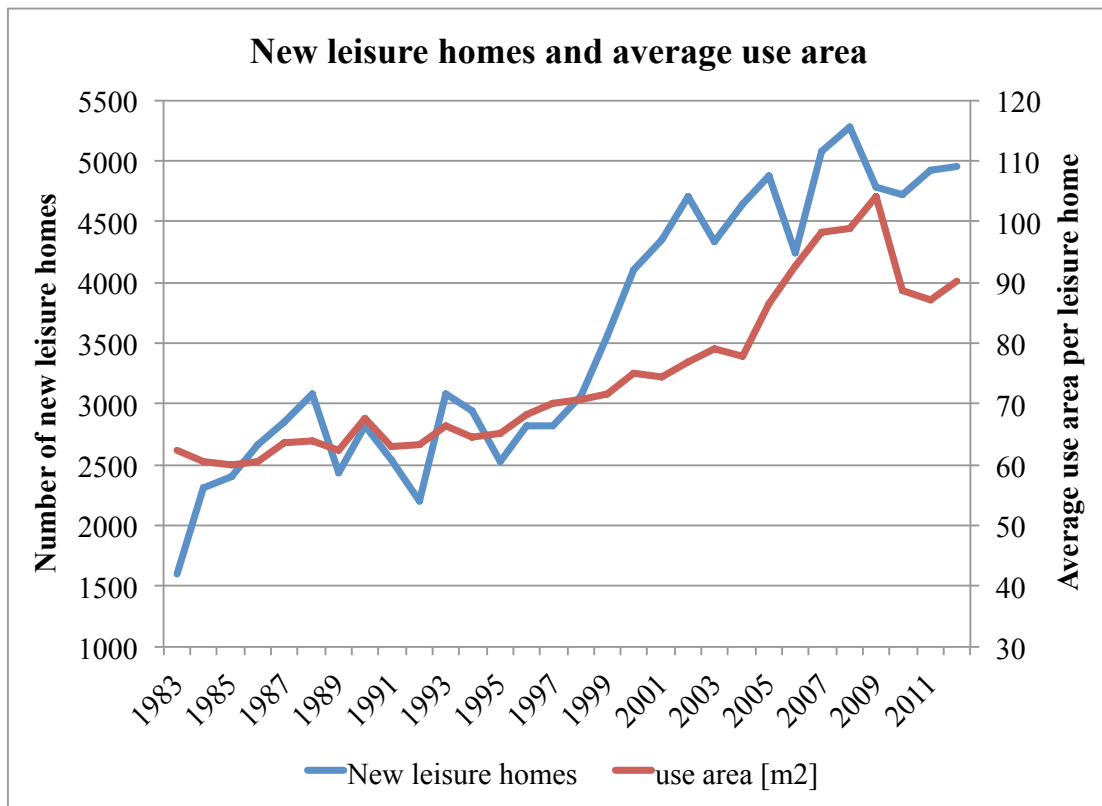


Figure 2-2: New leisure homes and average use area

Many conventional leisure homes have been modernized with installed electricity. More leisure homes are kept partially heated during the winter. There is in general an increased use of various electrical equipment as ever more electrical gadgets are developed. Such and other factors contribute towards increased energy use. Figure 2-3 shows the electricity consumption in Norwegian residential buildings and leisure homes from 1990 to 2009. Even though the electricity consumption in leisure homes is still a relatively small part of a households total energy use, it is clear that this consumption has increased during the past decades.

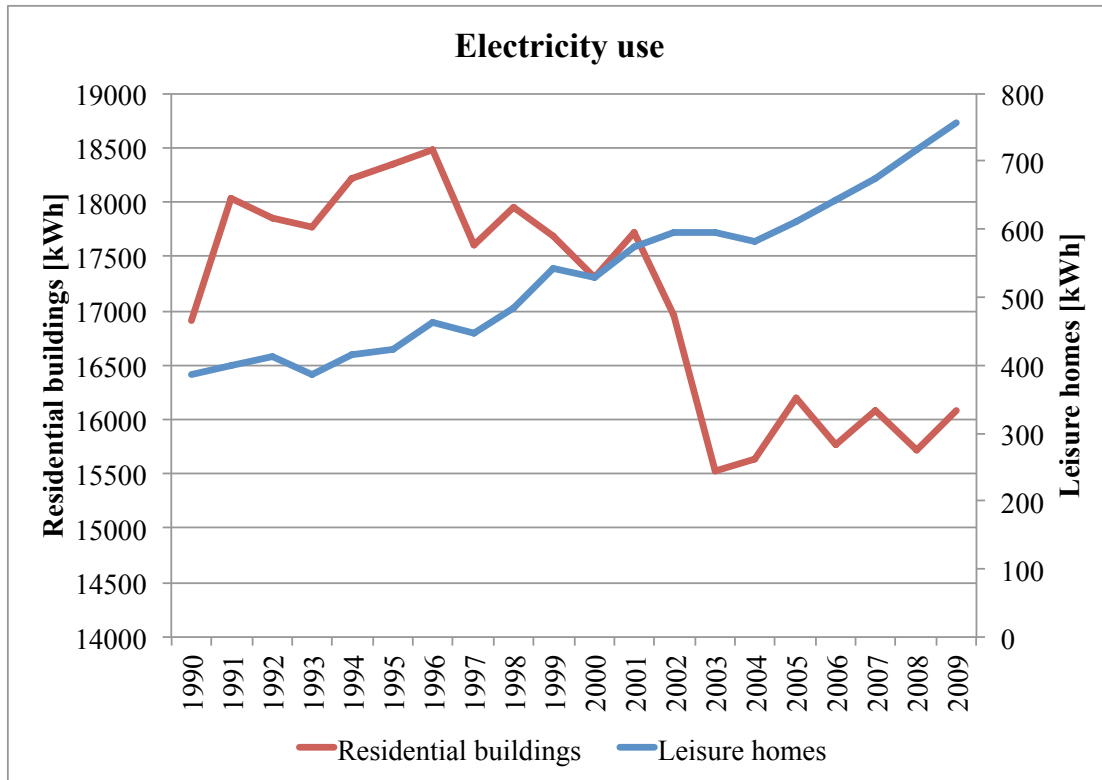


Figure 2-3: Electricity use

Leisure homes are often left partially heated throughout the winter to avoid frost damages to sanitary installations. SINTEF recommends to maintain a minimum temperature of 10 °C inside leisure homes throughout the year to avoid such damages, which annually cost Norwegian insurance companies approximately 100 million NOK [4].

Figure 2-4 shows the number of leisure homes, and the electricity consumption in leisure homes, from 2001 to 2010. It is evident that the electricity consumption is growing at a more rapid rate than the growth rate of the number of new buildings.

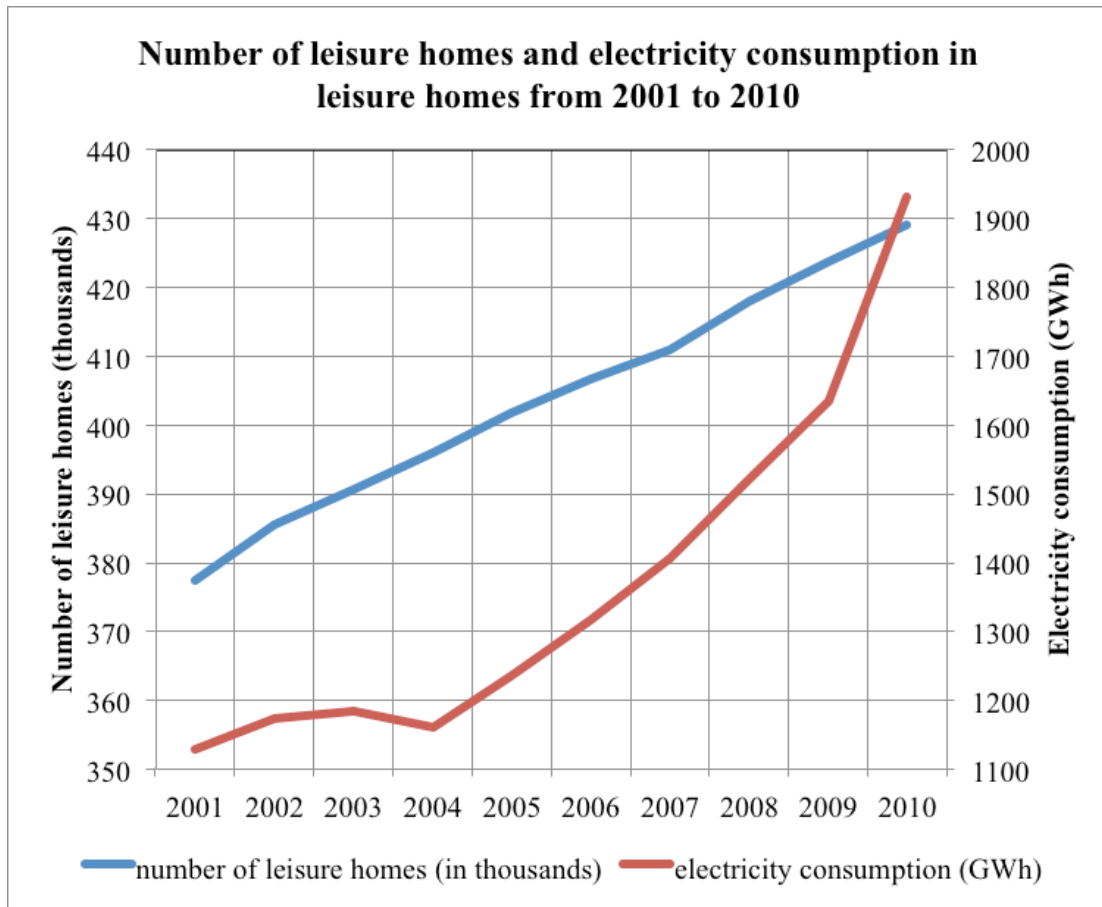


Figure 2-4: Number of leisure homes and electricity consumption

2.2 Building requirements for leisure homes

Traditionally, leisure homes have been built without considering energy efficiency. However, during the last decades, requirements regarding efficient energy use have become more and more strict. According to the Norwegian Building Regulation TEK10 §14-4, leisure homes with a use area larger than 150 m² have the same requirements as residential buildings. Table 2-1 shows minimum requirements for U-values and air infiltration rate for leisure- and residential buildings. Requirements for buildings with log walls are slightly different and can be seen in Table 2-2. For leisure homes with a use area smaller than 50 m² there are no requirements for energy efficiency [5].

Table 2-1: Minimum requirements

U-value external wall [W/m ² K]	U-value roof [W/m ² K]	U-value floor and to the exterior [W/m ² K]	U-value window [W/m ² K]	Air infiltration at 50Pa pressure difference [h ⁻¹]
≤ 0.22	≤ 0.18	≤ 0.18	≤ 1.60	≤ 3.0

Table 2-2: Requirements for buildings with log walls

Building category	Dimension external wall	U-value roof [W/m ² K]	U-value floor and to the exterior [W/m ² K]	U-value window [W/m ² K]
Residential buildings and leisure homes with heated gross area > 150 m ²	≥ 8" logs	≤ 0.13	≤ 0.15	≤ 1.40
Leisure homes with heated gross area < 150 m ²	≥ 6" logs	≤ 0.18	≤ 0.18	≤ 1.60

3 Introduction to ESP-r

The dynamic building simulation tool ESP-r (Environmental System Performance Research) will be used to analyze the test building in this report. ESP-r is an integrated energy-modeling tool for simulating thermal, visual and acoustic performance in buildings, and the energy use and gaseous emissions associated with environmental control systems. ESP-r is developed by the Energy Systems Research Unit (ESRU) at the University of Strathclyde in Glasgow.

ESP-r attempts to simulate the real world as thoroughly as possible and to an extent that is consistent with the current best practice. ESP-r lets the designer explore complex relationships between the shape of a building, materials, airflow, plants and control units. ESP-r is based on a finite volume conservation approach in which a problem (specified in terms of geometric attributes, construction, operation, leakage distribution etc.) is transformed into a set of conservation equations that are further integrated at successive time-steps in response to climate, occupancy and control system influences.

ESP-r comprises a central Project Manager that includes standard default databases for materials, constructions, climate data etc., a simulator, various performance assessment tools and a selection of third party applications for CAD, visualization and report generation [6]. The default databases can either be used as is, or be altered at the user level.

Detailed theory regarding possibilities in ESP-r will not be included in this report. Information about the program can be found on the website <http://www.esru.strath.ac.uk/Programs/ESP-r.htm>. ESP-r is a free open-source license program and can be downloaded from the internet. Theory relevant for this report will be described further in chapter 8.

The modeling possibilities within ESP-r are large, and because of the open-source policy, new elements are frequently added to the program allowing for more accurate models. ESP-r has the ability to simulate innovative and leading technologies in addition to standard simulation features. A weakness with ESP-r is that the threshold

for new users is high in part due to complicated specialist features and a less developed user interface. It is important to note that a simulation tool will never fully represent a real situation. It is merely an approximation to the real case and the degree of accuracy depends on the quality of the program as well as the user's knowledge and effort.

4 The leisure home model

4.1 Project work model and Auråen's master thesis

A simple box-shaped leisure home building was developed and analyzed in the project work report written by Ida Karin Auråen and myself during the fall semester of 2012 at NTNU. The goal of the project was to obtain frost proof conditions for sanitary installations placed in well-insulated internal zones, based on energy from an active solar heating system and heat storage in the ground. Auråen has further studied the model in her master thesis written in the spring of 2013. Auråen's master thesis focused on improving the ground model from the project, studying possibilities for seasonal heat storage in the ground. The main goal of this thesis is to achieve frost proof conditions for the sanitary installations in the leisure home with an improved and more realistic model of the solar heating system. The same building envelope has been studied in several prior project work reports and master theses. The original box-shaped building consists of two floors and a total of six zones (Figure 4-1). Each floor has three zones, one south and one north zone facing the exterior, and one internal zone. The internal zones have no external walls, are very well insulated and are the main points of attention in the analysis. As a simplification, all sanitary installations are deemed placed within the internal zones. Therefore, achieving frost proof conditions within these zones is the main focus area of this thesis.

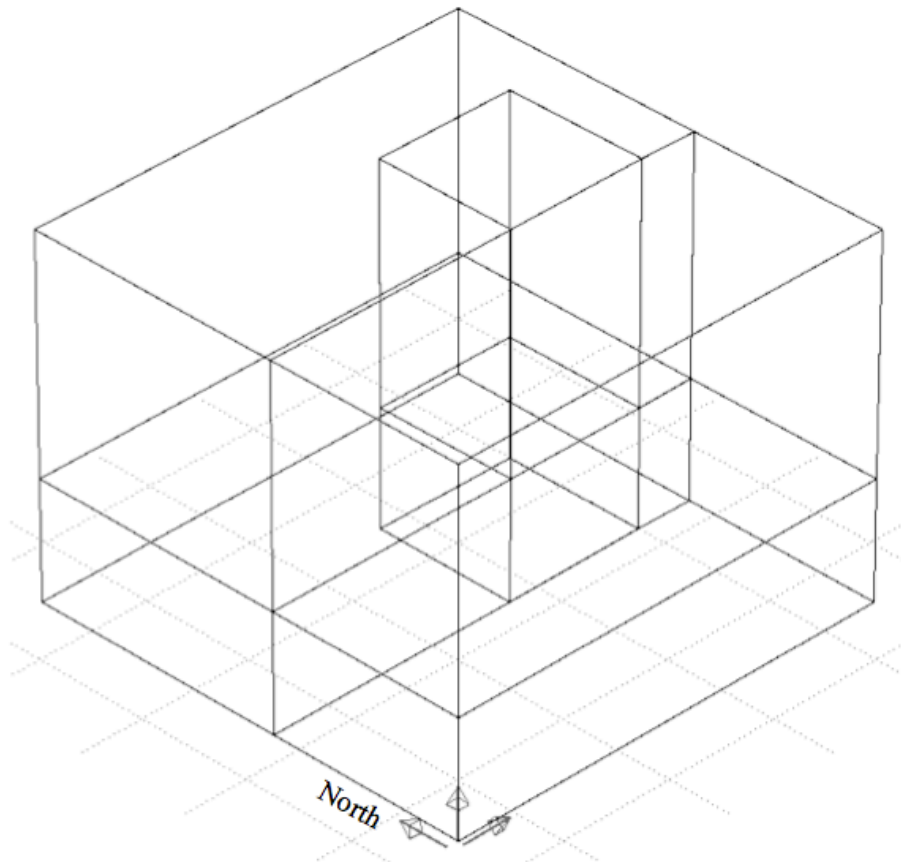


Figure 4-1: Old leisure home model

The division of zones and a cross section of the leisure home are shown in Figure 4-2 and Figure 4-3 respectively.

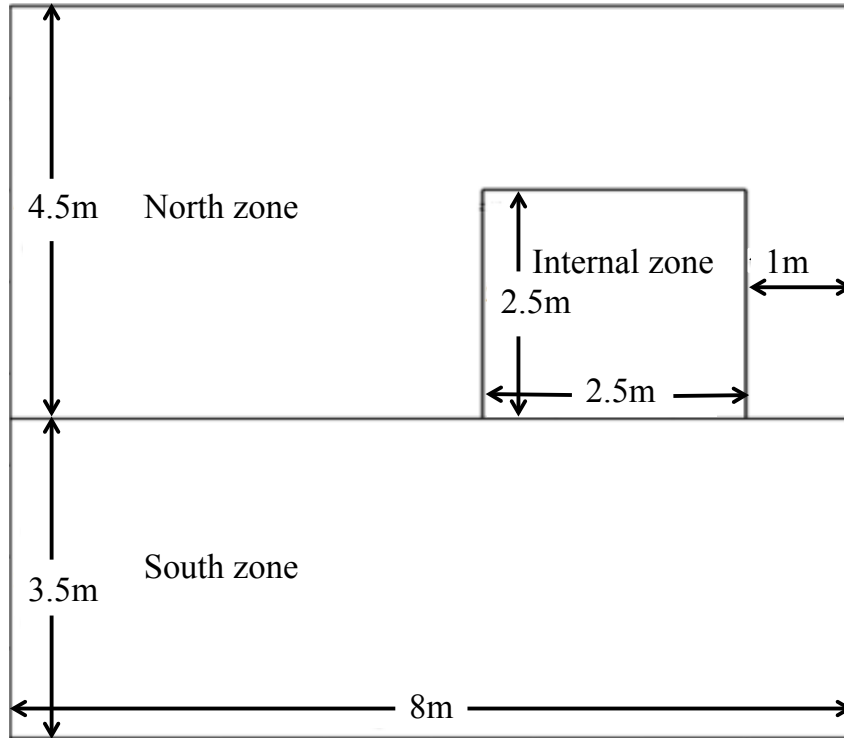


Figure 4-2: Floor plan area with division of zones

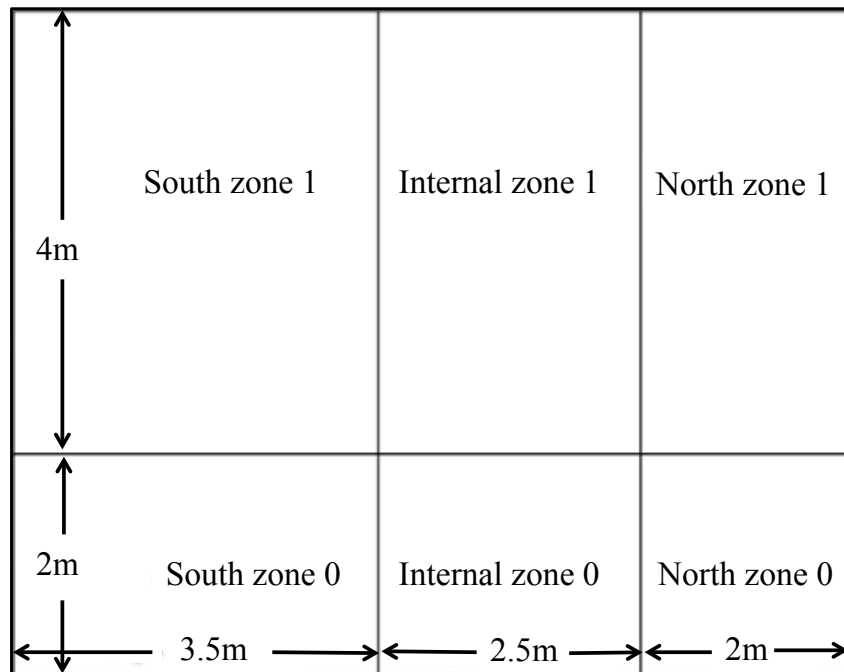


Figure 4-3: Cross section of the building

4.2 Improved leisure home model

Auråen developed a new and improved model of the leisure home in her master thesis [7]. Major improvements were carried out in relation to the ground modeling. A new basement zone was created to better account for foundation heat losses. The basement zone is placed directly below the leisure home with a width of 8 m, length of 8 m and height of 2 m. The basement zone is submerged 1.9 m into the ground. Figure 4-4 shows the improved leisure home model with the extra basement zone. This thesis will use the same building envelope as the one shown in the figure below.

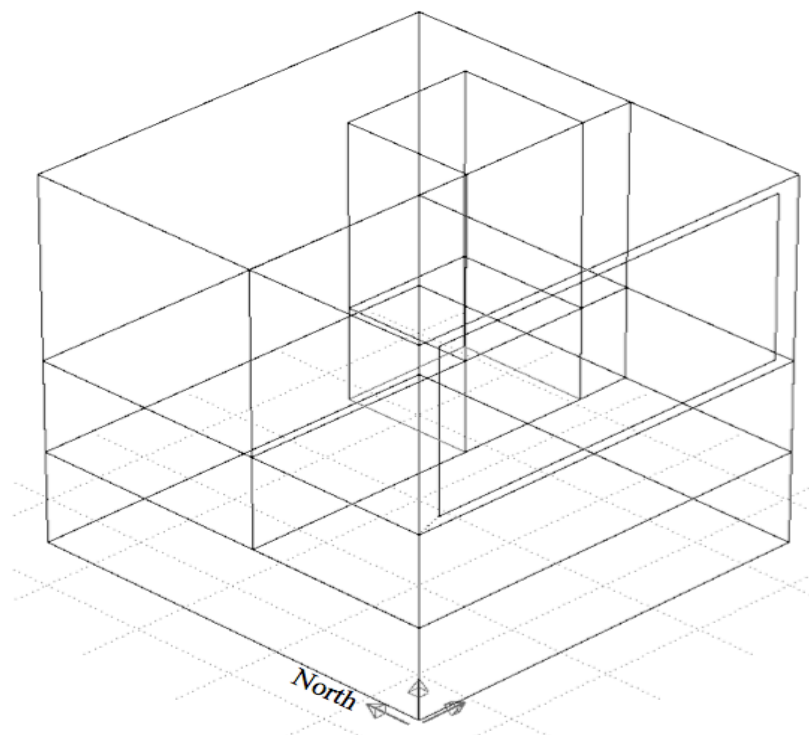


Figure 4-4: New leisure home model

4.3 Building construction elements

A construction database was created in ESP-r and the materials in each construction element are presented in Table 4-1. Each construction element is made up of predefined or user-defined materials and given a thickness. The resulting U-values for each construction element are also shown.

Table 4-1: Building construction elements

Construction	ESP-r name	Material	Thickness [mm]	U-value [W/m ² K]
External wall ground floor	0ext_wall	Heavy mix concrete	200	0.128
		Glass wool	300	
External wall first floor	1ext_wall	Fir	150	0.806
Internal zone wall	int_wall	Polyurethane foam	250	0.117
		Heavy mix concrete	100	
Partition wall between north and south zone	part_wall	Plate glass	6	2.811
		Air	12	
		Plate glass	6	
Partition floor	part_floor	Heavy mix concrete	150	3.608
Ground floor	floor	Flooring	100	0.106
		EPS	250	
		Heavy mix concrete	250	
Roof	roof	Snow	300	0.052
		Fir	160	
		Polyurethane foam	350	
South-facing window	window	Plate glass	6	1.458
		Air	16	
		Plate glass	6	
Internal zone ground floor* (concrete slab)	massive_floor	Massive concrete	1500	0.806

* The internal ground floor construction is made up of five layers of a user-defined material called *massive concrete*, each with a thickness of 0.3 m. This construction is created to represent thermal mass below the building and is made from a standard material in ESP-r called *heavy mix concrete*, but with modified values for the specific heat capacity and the density. The construction will be referred to as “concrete slab” in the text.

The properties of the user-defined *massive concrete* material and the standard *heavy mix concrete* provided by ESP-r are shown in Table 4-2. The thermal properties of *heavy mix concrete* were in the project work report found not to be sufficient to obtain frost proof conditions. In the project it was found that if the product of the two parameters were multiplied by 10, sufficient thermal mass was achieved. The result is the mentioned *massive concrete* material. This is a very rough simplification, but is further used for the purpose of seasonal heat storage calculations. In the simulations, the slab has the thermal properties of *massive concrete* for the most part. To get a comparison with *massive concrete* and “normal” thermal properties, some simulations will also be run with the *heavy mix concrete* material in the concrete slab.

Table 4-2: Concrete slab construction properties

Material	Density [kg/m ³]	Specific heat [J/kgK]
Heavy mix concrete	2100	653
Massive concrete	9000	1524

The construction elements database presented in Table 4-1 will be used for the leisure home in this report along with construction elements for the submerged basement zone given in Table 4-3.

Table 4-3: Basement construction elements

Construction	ESP-r name	Material	Thickness [mm]	U-value [W/m ² K]
Basement walls	base_wall	Glass wool	100	0.356
		Heavy mix concrete	200	
Basement floor	base_floor	Heavy mix concrete	100	4.142

Figure 4-5 shows a sketch of the leisure home and Figure 4-6 shows a cross section view of the leisure home illustrating the submerged basement zone and the concrete

slab. The concrete slab together with the submerged basement zone are designed to represent thermally massive ground conditions.

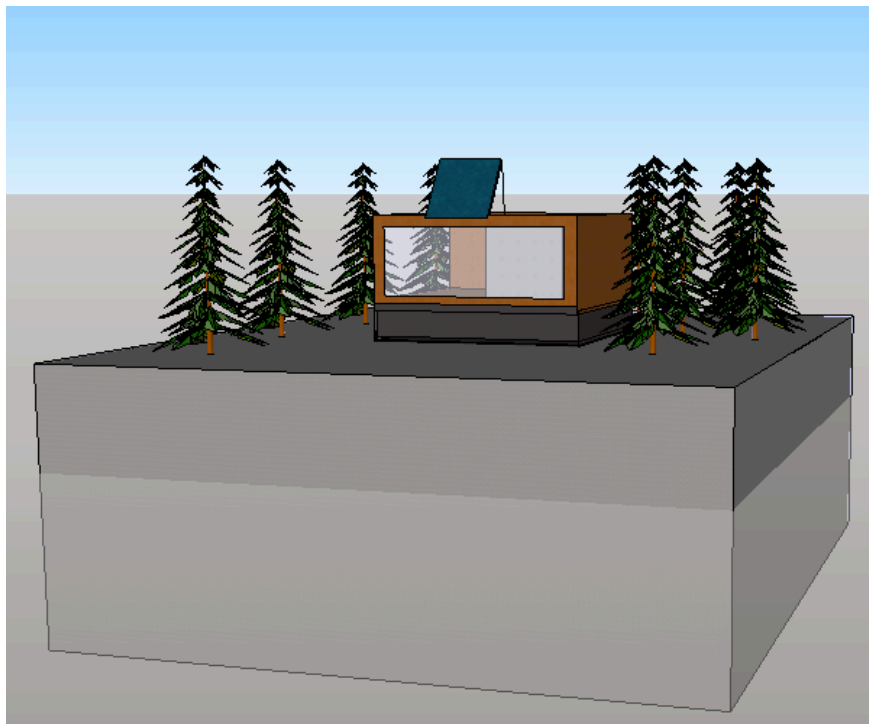


Figure 4-5: Leisure home

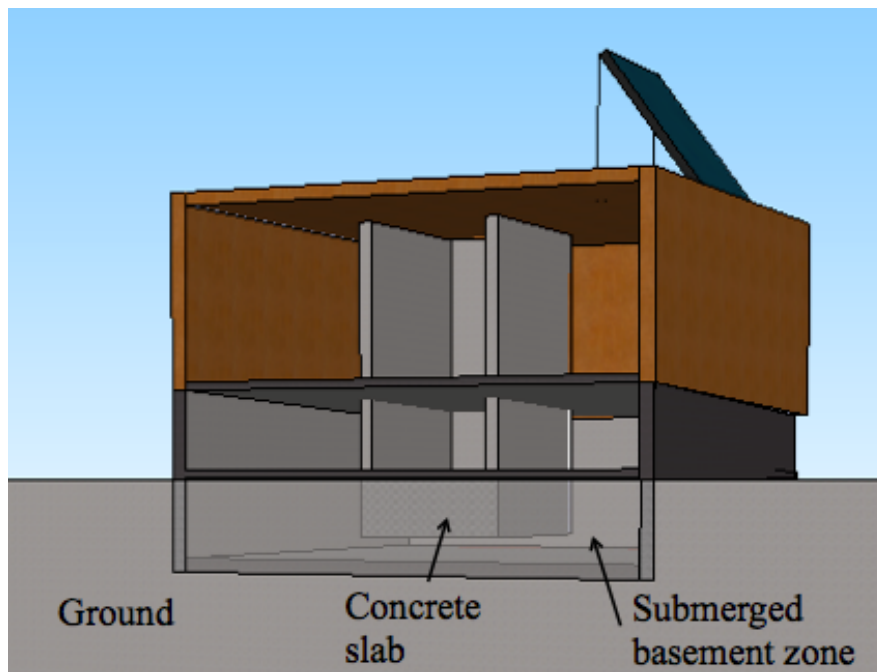


Figure 4-6: Cross section view of the leisure home

5 Solar energy

5.1 Availability

Solar energy can be transformed in photovoltaic solar panels and solar collectors into electricity and heat, respectively. This thesis focuses on thermal exploitation of solar energy and only solar collectors will be discussed further.

Utilizing the sun's energy as a heat source is not a new idea. Technologies regarding solar water heating have been used for many years. More than one hundred years ago, black painted water tanks were used as simple solar water heaters. Today, more than 30 million m² of solar collectors are installed around the world, and the technologies have improved greatly during the past century [8].

The sun is the source of life on earth and, indirectly or directly, the fuel for most renewable energy sources. Solar energy is available in great amounts all over the earth. Annually, the earth receives 15 000 times more energy from the sun than the global energy use [9]. Incoming solar radiation depends on geographical location and in the sunniest areas on the globe, solar radiation could potentially deliver up to 2500 kWh/m² evenly distributed throughout the year [10].

5.2 Solar radiation

Solar irradiance is defined as the rate at which radiant energy is incident upon a surface per m² of surface area. Solar irradiance outside the earth's atmosphere is approximately constant and equal to 1367 W/m² with a variation of $\pm 3\%$. The variation of $\pm 3\%$ is due to the changing distance between the earth and the sun. On average, approximately 30 % of the solar radiation is reflected before reaching the surface of the earth [11]. Solar radiation is scattered by the atmosphere, spreading light and mitigating certain wavelengths. The mitigation varies according to the atmospheric content of gases. The main factors influencing the amount of solar radiation that can be utilized as useful energy are geographical location, time of the year and local conditions. The sun is lower on the horizons on the northern- and southern hemispheres compared to close to the equator. Far from the equator, solar rays have to pass through more air to reach the ground, thus increasing the scattering.

The sun is higher on the horizon in the summer than in the winter, except in tropical areas, and hence the incoming radiation will depend on the time of year. Local cloud formation and shadows from nearby nature and buildings will contribute to increased scattering and less incoming radiation will reach the surface. Figure 5-1 shows the path of the sun at different times of the year at central European latitude.

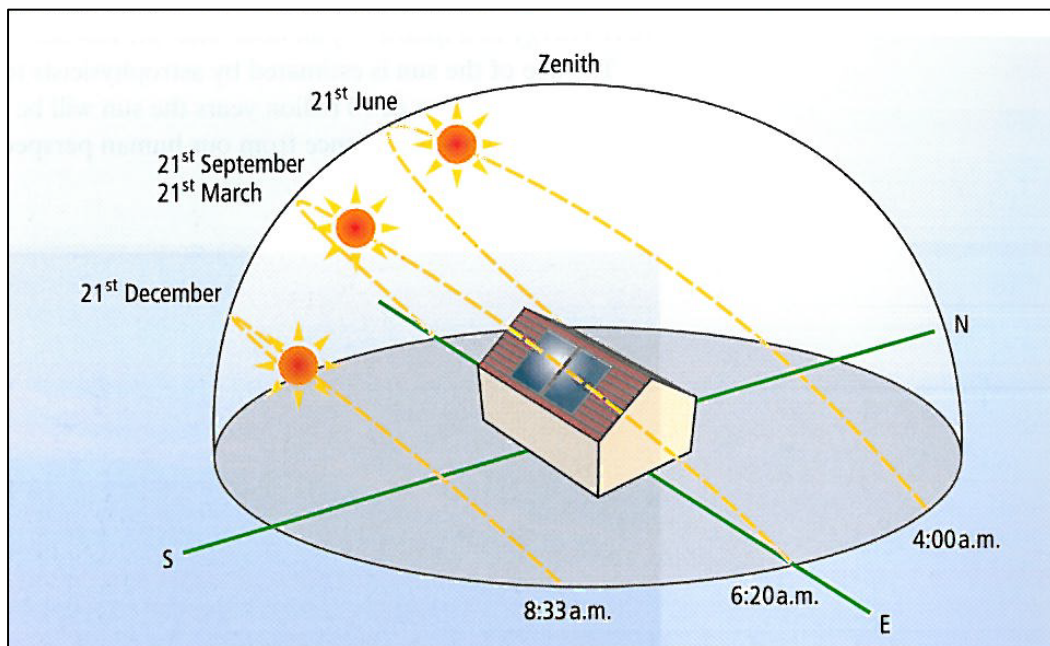


Figure 5-1: The path of the sun at central European latitude [11]

With an ever increasing awareness regarding energy use and resulting greenhouse gas emissions, solar energy is considered to be one of the potential ways to limit or reduce the use of fossil fuels. Solar thermal technologies are being further developed by a growing industry. However, the development resources as well as the current solar generating capacity are still small-scale compared to the resources devoted to the oil- and gas industry. Figure 5-2 shows annual incoming solar radiation on a horizontal surface.

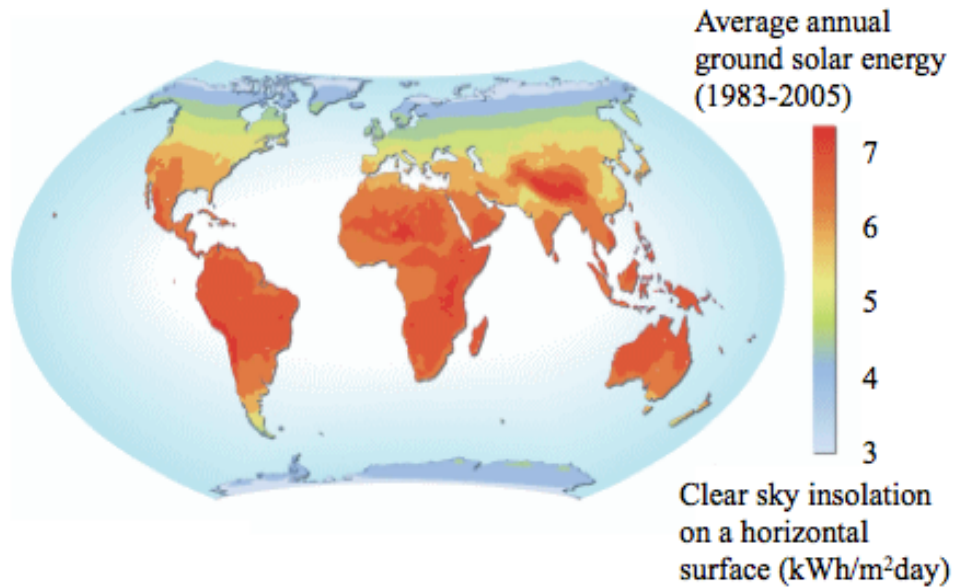


Figure 5-2: Average annual insolation worldwide, based on [12]

5.3 Solar radiation in Norway

In Norway, solar radiation varies significantly throughout the year depending on the season and the latitude. The annual incoming solar radiation on a horizontal plate in Norway varies from approximately 700 kWh/m² in the north to approximately 1100 kWh/m² in the south. This is equivalent to 30-50 % of the incoming solar radiation at the equator. Nevertheless, according to Norsk Solenergiforening (Norwegian Solar Energy Association), the sun annually provides the Norwegian building sector with 3-4 TWh of useful heat by passive solar heating (heat supplied to the building through windows and building elements) [13]. A distribution of average daily incoming solar radiation on a horizontal surface in Norway is shown for January and July in Figure 5-3.

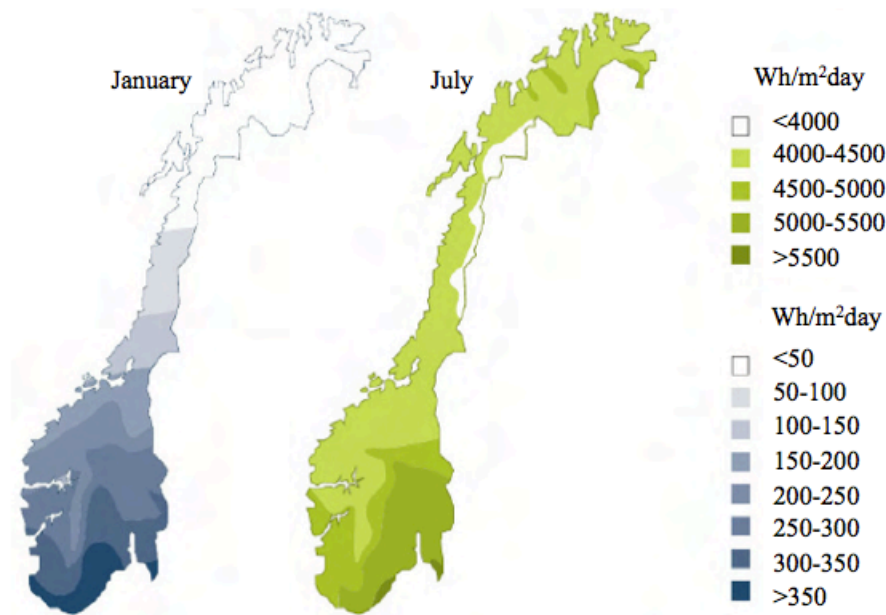


Figure 5-3: Average daily incoming radiation on a horizontal surface in Norway, based on [14]

5.4 Direct- and diffuse radiation

The solar radiation reaching the surface of the earth consists of two main components: direct and diffuse radiation. Direct solar radiation is radiant energy received directly from the sun, while diffuse radiation is scattered from the sky and surroundings in all directions. Scattered radiation from surroundings depends on the local albedo, defined as the ratio of reflected radiation from the surface, to incident radiation upon it. The principles are illustrated below.

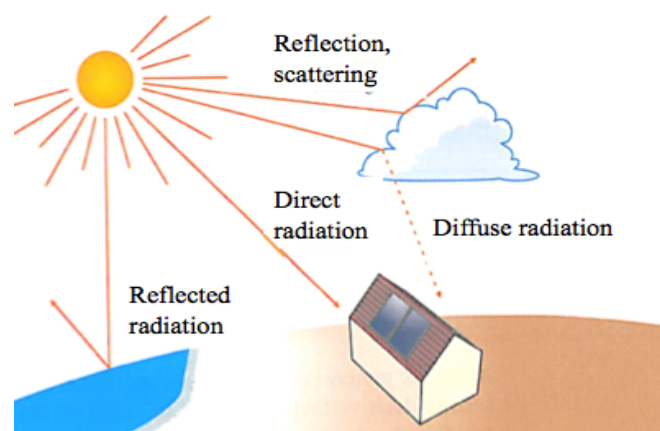


Figure 5-4: Radiation principles, based on [11]

6 Solar heating

6.1 Components of a solar heating system

The main components of a solar heating system are solar collectors, heat-storage, heat exchangers, distribution system, and a control system. A heat-storage is necessary because the sun cannot supply sufficient heat directly at all times. Usually a solar heating system cannot meet the total energy demand and therefore an auxiliary- or back-up energy source is needed. Figure 6-1 shows a principal sketch of a solar water heating system for a house. The back-up system is connected to the upper/hot part of the storage tank.

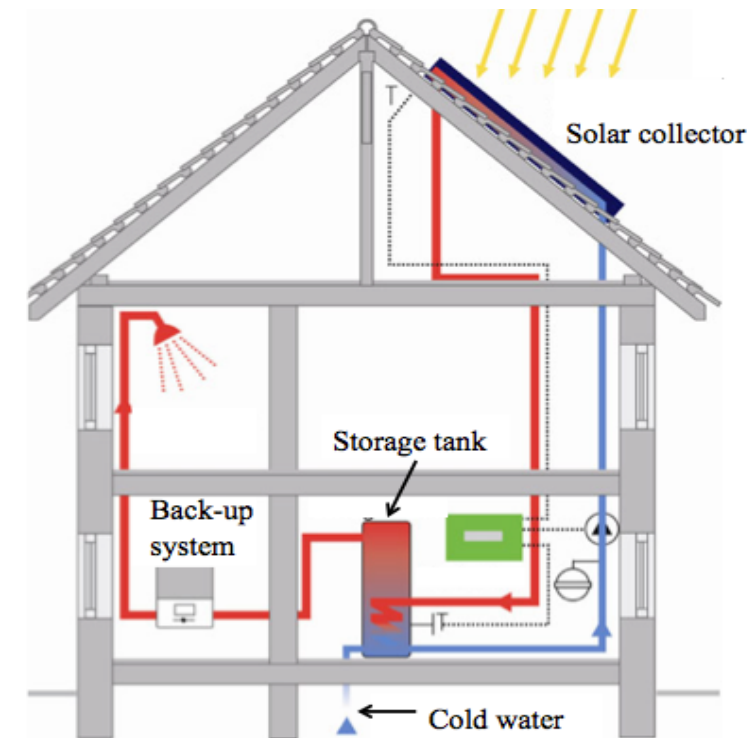


Figure 6-1: Solar heating system principle, based on [15]

6.1.1 Solar collectors

A solar collector is the heart of a solar heating system. In the collector, solar irradiance is absorbed and converted to thermal energy. A heat transfer fluid transfers the heat from the collector through the distribution system to an accumulator tank. For active solar systems the most common collector types are either air-based collectors or water-based collectors. Air-based collector systems are primarily designed for

preheating of ventilation air or for space heating. Water-based collector systems, also known as hydraulic collectors, are suitable for domestic hot water production and space heating and allow for easy storage of solar gains. There are four main types of hydraulic collectors. These are evacuated tube collectors, glazed flat plate collectors, unglazed flat plate collectors and unglazed plastic collectors. The different collectors have different strengths and weaknesses, and the choice of collector is often based on climatic conditions. Traditionally the glazed flat plate collector is the most widely used in Norway. Eventually the evacuated tube collector has become a larger part of the market as well.

Most solar collectors consist of an absorber, a translucent coating layer often referred to as glazing, and insulation. The sun shines through the glazing, hits the absorber, and heats the working fluid inside the tubes. The absorber is the key component in the solar collector. This is where solar irradiance is converted to thermal energy. The absorber is usually a thin metal plate with a black color or a selective surface. A selective surface absorbs a large part of visible light, around 98 %, in the same way as a black painted surface does, but it emits less infrared radiation [14]. This means that by using a selective surface, heat loss from the solar collector is reduced, resulting in a more efficient collector. The task of a solar collector is to achieve the highest possible thermal yield. The absorber is therefore provided with a high light-absorption capacity and the lowest possible thermal emissivity.

Glazing is used to protect the collector from climatic conditions, and to utilize the greenhouse effect that occurs. Glazing is especially useful for collectors used in cold and windy areas. The layer acts as a “heat trap” by taking up short wave solar radiation while preventing long wave heat radiation from escaping. Usually the glazing layer is made of glass or plastic. Using a glazing layer with a low emitting coating or with transparent insulation materials can further reduce the heat loss. Measures taken to reduce the heat loss from the solar collector will however often result in a reduction of the transmission properties in the glazing, and it is therefore necessary to consider what the optimal combination is for each individual case.

To increase the performance of the solar collector, it is essential to insulate the collector. This will reduce the thermal conduction and the heat loss to surroundings. A

common insulation material used for solar collectors is mineral fiber, as it can withstand temperatures up to 150-200 °C [11]. To avoid precipitation onto the glass pane and damaging of the light-transmitting capacity, it is important to choose an insulation material that will not vaporize at the given temperatures.

Glazed flat plate collectors

Figure 6-2 shows a cross section through a traditional flat plate fluid based solar collector. Flat plate solar collectors are made with an insulated robust frame, glazing attached to the front of the collector and a solid back. An absorber plate lies just beneath the glazing, and metal tubes are positioned under the absorber. A heat transfer fluid flows through the metal tubes and transfers heat either directly or via a heat exchanger to a storage tank. Flat plate collectors are not the most efficient solar collectors in cold climates because they suffer from more heat loss than other types of collectors. However, flat plate collectors can use antifreeze working fluids and are thus suited for a wider range of climates. Flat plate collectors have an operating range from well below -20 °C to around 80 °C [16].

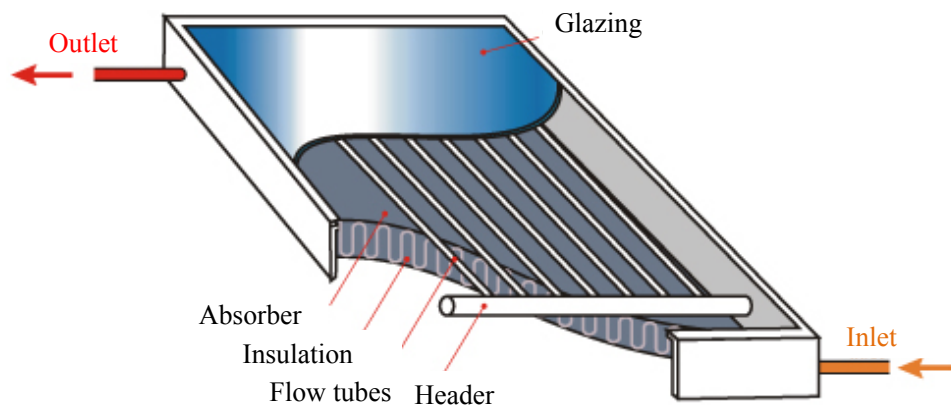


Figure 6-2: Flat plate collector, based on [17]

Evacuated tube collectors

Unlike flat plate collectors, evacuated tube collectors vary widely in their construction and operation. Evacuated tube collectors are constructed of several individual glass tubes where each tube contains an absorber plate. All the air is removed from the tubes creating a vacuum. The absence of air in the tubes creates excellent insulation, allowing higher temperatures to be achieved in the absorber plate. Evacuated tube

collectors generally perform better than flat plate collectors in cold climates because they mostly rely on the light they receive and less the ambient temperature. Tubes come in different qualities. High quality tubes can efficiently absorb diffuse solar radiation in cloudy conditions and are almost unaffected by wind [18]. There are several different types of evacuated tube collectors. Two examples are evacuated heat-pipe collectors and direct-flow evacuated tube collectors.

Evacuated heat pipe collectors

A heat-pipe collector consists of several vacuum-sealed copper tubes, each containing a small amount of fluid. The reason for evacuating the heat pipe is to promote a change of state of the liquid it contains. A heat pipe is an evaporating-condensing device for rapid heat transfer. The vacuum enables the fluid to evaporate at low temperatures, around 30 °C [14]. Latent heat from the vaporization process is transferred when evaporating a water-based liquid in the solar heat inlet region, and condensing its vapor in the discharge region. The heat source is the absorber plate inside the tubes. The condenser (heat discharge region of the heat pipe) is in direct contact with a distributor that serves as a heat exchange/sink. In a heat pipe, the heat transfer is always unidirectional, from absorber to distributor and never reverse [19]. Heat-pipe collectors have to be mounted at a certain angle above the horizontal to allow the internal fluid of the heat pipe to return to the hot absorber. Evacuated heat pipe tubes are ideal for solar water heating and solar space heating because of their high operative temperatures and very low radiant heat losses. The glass tubes and vacuum within protect the absorber coating and structure materials from corrosion and climatic conditions. An illustration of an evacuated heat pipe tube is shown in Figure 6-3.

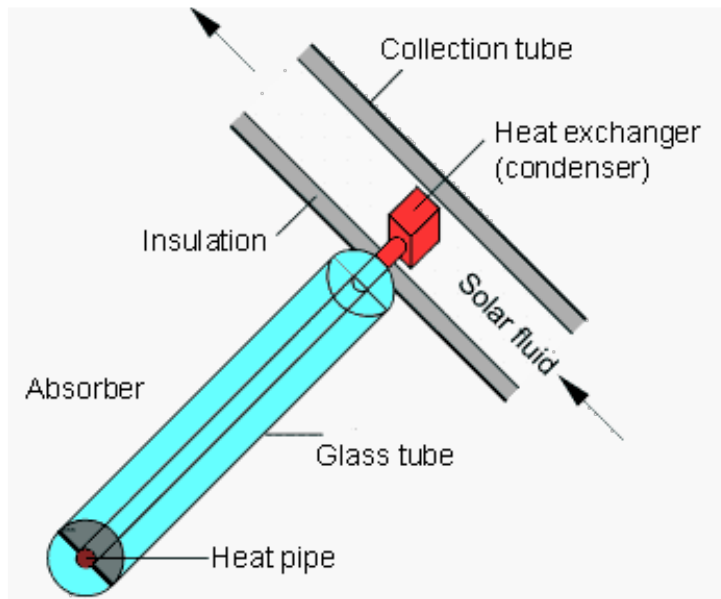


Figure 6-3: Evacuated heat pipe tube [20]

Direct-flow evacuated tube collectors

This collector type consists of a group of glass tubes each of which is a flat or curved aluminum fin attached to a metal or glass absorber plate. The fin is covered with a selective coating that absorbs solar radiation well while inhibiting radiant heat loss.

Inside each tube there are two pipes where the heat transfer fluid circulates in the inlet pipe and the outlet pipe. Direct-flow evacuated tube collectors come in different varieties distinguished by the arrangement of the inlet- and outlet pipes [21]. One example is shown in Figure 6-4.

- Concentric fluid inlet and outlet (glass-metal) pipes use a single glass tube. Inside each glass tube there is a copper heat pipe or water flow pipe with an attached fin. With this type of construction, each single pipe can easily be rotated to achieve the desired tilt angle even if the collector is mounted horizontally. A downfall of this type of direct-flow collector is that the different heat expansion rates of the glass and metal tubes can cause them to weaken and fail, resulting in a loss of vacuum, and hence losses in efficiency.
- Separated inlet and outlet (glass-metal) pipes are the traditional type of evacuated tube collectors. The absorbers can be flat or curved. As for the concentric fluid design, the efficiency can be very high, especially at relatively low working

temperatures. The same weakness applies for this type of design; the potential for loss of vacuum can lead to a reduction in collector efficiency.

- A third design is to have two glass tubes fused together at one end (glass-glass). The inner tube is coated with an integrated cylindrical metal absorber. Glass-glass tubes are generally not as efficient as glass-metal tubes but tend to be more reliable. For very high temperature applications however, glass-glass tubes can in some cases be more efficient than the glass-metal designs.

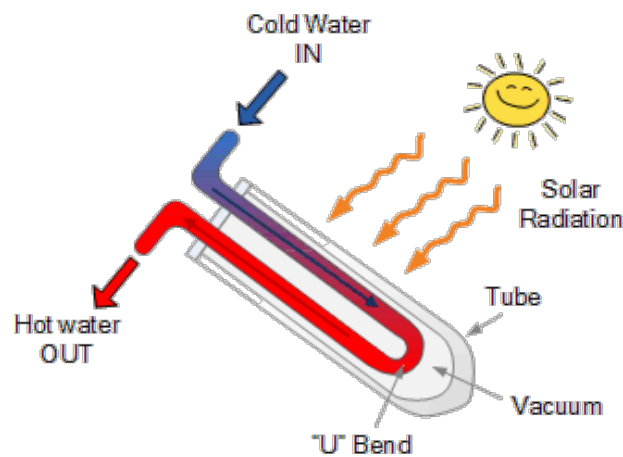


Figure 6-4: Direct-flow evacuated tube collector [22]

Overlooking practical installation and maintenance issues, the evacuated heat pipe collector will function better at lower levels of solar radiation than a direct-flow evacuated tube collector. This is because the heat transfer fluid conducts heat much faster in a heat pipe collector. [23].

6.1.2 Hot water storage tanks for solar systems

The path of the sun changes throughout the year and the amount of incoming solar radiation varies from day to day. A solar heating system cannot directly deliver sufficient heat at all times, and consequently, all solar water heating systems require a storage system. Hot water tanks connected to solar water heating systems normally have one or two built-in heat exchangers. For domestic hot water production, an important factor is to ensure that the temperature in the potable water tank is above 60-65 °C to avoid bacteria growth such as legionella.

OSO HOTWATER has purpose-designed domestic hot water tanks for utilizing solar energy. One example of such a design is the Ecoline Sun (Figure 6-5). The tank is suitable for all types of solar collectors, can handle up to 8 m² of solar collectors, and can save up to 60 % of annual energy consumption for domestic hot water. The tank has a number of features specially suited for solar energy. It includes an electric booster that provides heat if the solar collectors are not yet installed, or in periods with little or no solar energy available. The electric heater ensures sufficiently high temperatures to avoid bacteria growth and is placed above the heating coil to provide two temperature zones, optimally utilizing the solar energy [24].

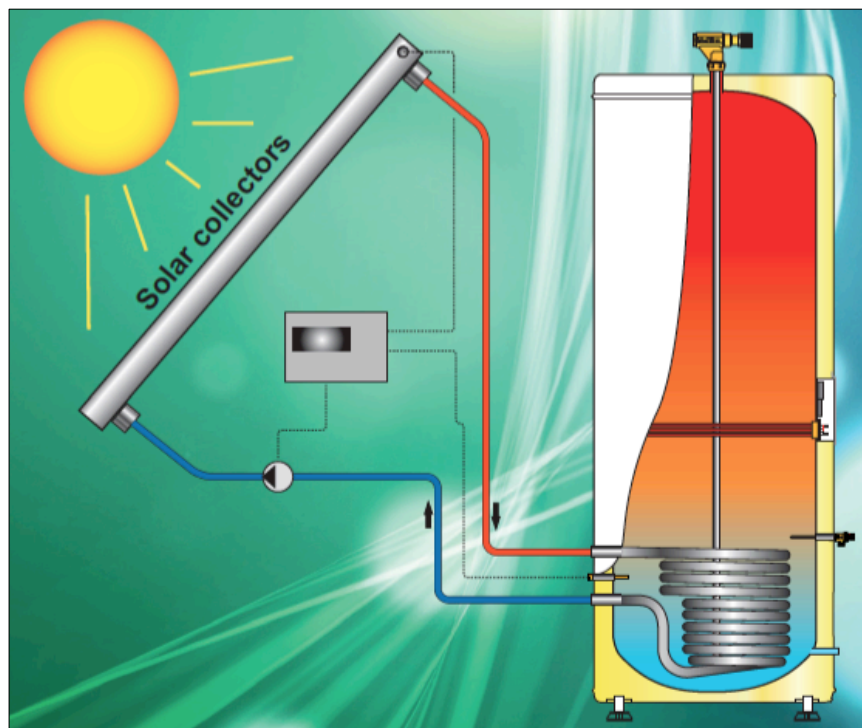


Figure 6-5: Solar hot water tank, Ecoline Sun [24]

To minimize heat loss, the tank must be well insulated. The tank has suitable connections to fit the water supply, heat exchanger and a drainage system.

Because incoming solar irradiance varies significantly throughout the year and from day to day, a secondary energy source is often used in combination with the solar heating system to ensure sufficient heat supply. The accumulator tank then has two built-in heat exchangers, one connected to the solar circuit and one connected to the secondary energy supply. Figure 6-6 shows a purpose-designed storage tank combining two energy sources for domestic hot water production. In addition, an

electric heater is included as backup if either of the two energy sources is not operating [25].

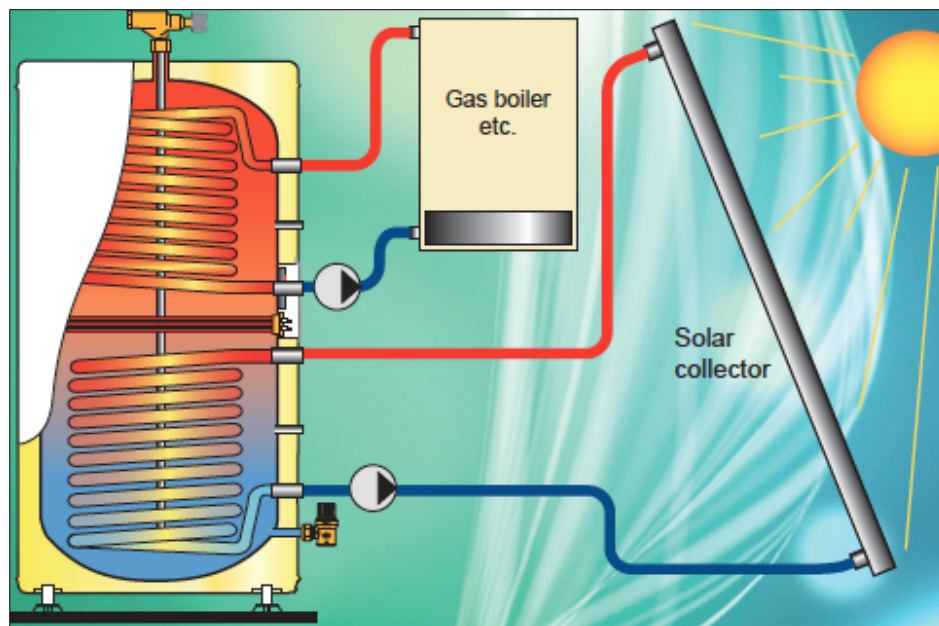


Figure 6-6: Solar hot water tank, Ecoline Twin Coil [25]

Temperature layering

For efficiency reasons, the temperature in the storage tank should be divided between a hot side and a cold side. In a temperature-layered tank, hot water stays at the top of the tank and cold water at the bottom. A tall tank is preferable as the mixing is minimal compared to a short, wide tank. The solar collector efficiency increases with a lower inlet temperature. The hot water at the top of the tank is used to heat domestic hot water. An auxiliary energy source should be connected to the upper hot part of the tank to further raise the temperature to the desired level before leaving the system. An alternative to using a tall tank is to connect several small tanks in series. This alternative can be easier to install and requires less maintenance.

Insulation of the storage tank

To avoid significant heat losses to surroundings, proper heat insulation of the tank is essential. In total, the heat loss rate from the storage tank should be less than 2 W/K. Normally the insulation consists of CFC- and PVC-free materials with a thermal conductivity, $\lambda < 0.035$ W/mK. As for a collector, a k-value (W/m²K) can also be defined for a storage system as the ratio of the thermal conductivity to insulation thickness ($k = \lambda/D$, where D is the insulation thickness). The product of the k-value

and the surface area of the storage tank, A , gives the heat loss rate, kA (W/K) of the tank [11].

6.1.3 Heat storage in the ground

The main issue avoiding solar thermal systems from achieving their full potential for heating purposes is related to the fact that the energy source has a periodic nature and its effective exploitation is dependent on the availability of efficient and effective energy storage systems. This is particularly true at high latitude locations such as in Norway and Sweden, where seasonal variations of solar radiation are significant. The greatest amount of energy is collected during the summer when the heating demand is at the lowest. Because a tank has a finite storage capacity, surplus energy from the solar heating system in sunny periods cannot be utilized to its full potential by only using an accumulator tank.

Another type of storage system that can be used in solar heating systems is seasonal heat storage in the ground. Energy from solar collectors during sunny periods can be stored in the ground beneath the building. During cold periods, this heat can heat up the building either by using a heat pump, or by passive heat exchange from a warm zone to a cold zone. A ground heat storage system can also be used in combination with an accumulator tank. If the storage tank is full, surplus energy can be transferred to the ground.

There are several different concepts for storing thermal energy. The principle methods available for seasonal storage of solar thermal energy mainly store energy in the form of sensible heat. Storage of sensible heat results in energy losses during the storage time. The losses depend on the storage time, temperature, storage volume and geometry, and thermal properties of the storage medium. Thermal Energy Storage (TES) systems are important technologies for minimizing the mismatch between thermal energy availability and demand. The most promising technologies for seasonal energy storage are found to be in the ground [1]. Such systems are known as Underground Thermal Energy Storage (UTES) systems. The four main types of UTES systems are:

- Water tank thermal storage
- Water-gravel pit storage

- Aquifer thermal energy storage (ATES)
- Borehole thermal energy storage (BTES)

Water tank thermal storage

A water tank thermal storage normally consists of a reinforced concrete tank either partially or fully buried in the ground (Figure 6-7). This type of storage system is flexible in the sense that it can be built almost independently of geological conditions. The walls and roof area are often thermally insulated and steel liners are used in the structure to guarantee water tightness and to reduce heat losses caused by vapor transport through walls. From a thermodynamic point of view, this method appears to be the most favorable because of the high specific heat of water and the possibility for high capacity rates for charging and discharging [1].

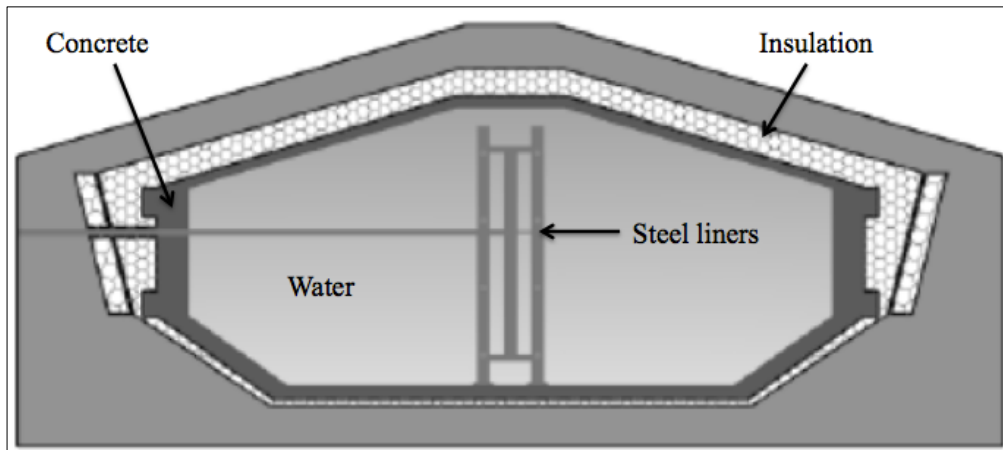


Figure 6-7: Water tank thermal storage, based on [1]

Water-gravel pit storage

Water-gravel pits are usually buried in the ground (Figure 6-8). The walls and top of the pit need to be insulated and waterproofed. Heat is charged and discharged into and out of the pit either by direct water exchange or by plastic piping installed in different layers inside the store. Water has a higher specific heat capacity than the water-gravel mixture and therefore the volume of the basin has to be larger compared to hot water heat storages to achieve the same heat storage capacity [1].

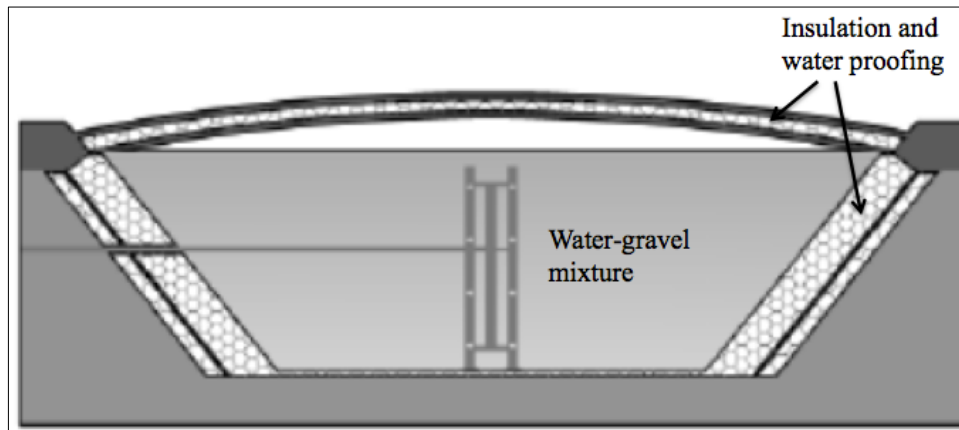


Figure 6-8: Water-gravel pit storage, based on [1]

Aquifer thermal energy storage

Aquifers are below-grade widely distributed layers of water-bearing permeable rock or unconsolidated materials such as sand, gravel, sandstone or limestone. If there are no impervious layers above and below, and no or low groundwater flow, they can be used for heat storage. Groundwater can be extracted or injected from the porous materials using water wells. In charging periods, cold water is extracted from cold wells, heated by the solar heating system and injected into hot wells. In discharging periods the cycle is reversed. In an aquifer system, good knowledge regarding mineralogy, geochemistry and microbiology in the ground is essential to prevent system damages [1].

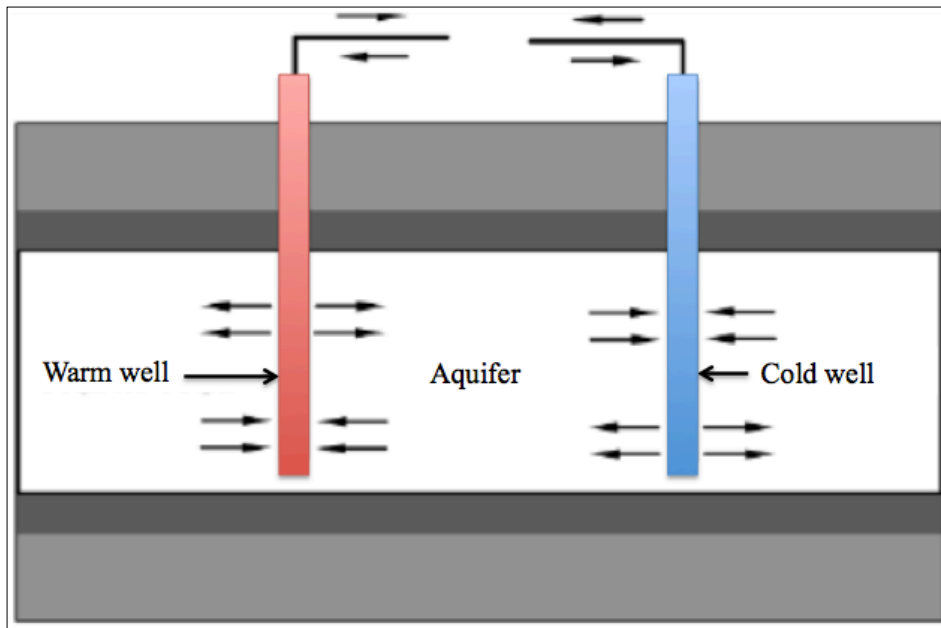


Figure 6-9: Aquifer thermal energy storage, based on [1]

Borehole thermal energy storage

In BTES systems heat is stored directly in the ground. Examples of suitable geological formations include rock or water-saturated soils. Ground heat exchangers (U-pipes) are placed in vertical boreholes, at a depth of 30-200 m below grade. Depending on geographical location, the boreholes are usually filled with groundwater, quartz sand or thermally enhanced grouts. Water runs through the U-pipes and feeds heat in or out of the ground. The heated ground volume constitutes the volume of the storage facility. To reduce heat losses to the surface, there is usually an insulation layer at the top of the storage. An advantage of using BTES systems is that the storage capacity can easily be expanded by connecting additional boreholes. However, the size of the store has to be three to five times larger than that of a hot water heat storage to obtain the same heat capacity. Because the capacity at charging and discharging is lower for such a system, normally a buffer store (water tank) is integrated into the system [1].

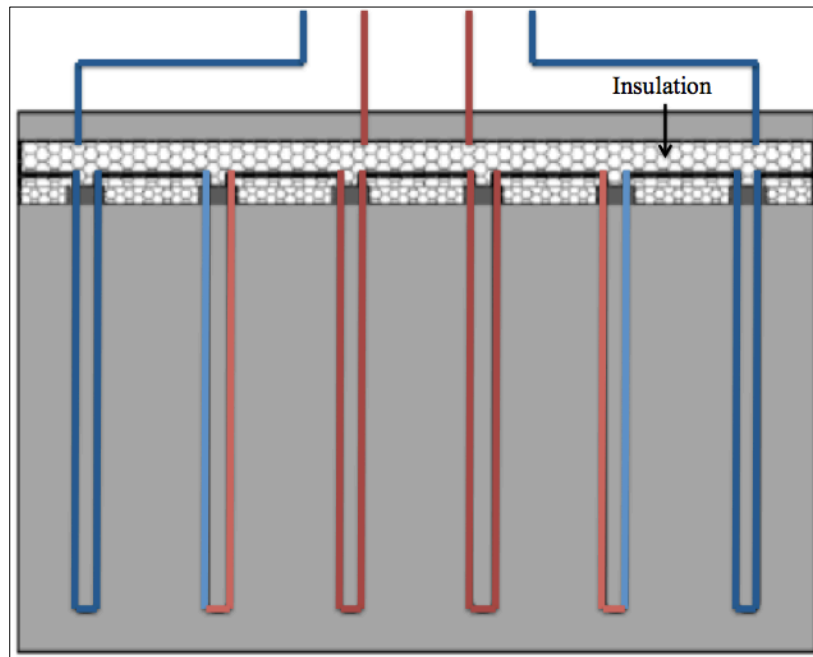


Figure 6-10: Borehole thermal energy storage, based on [1]

6.1.4 Heat exchangers

Liquid-to-liquid heat exchangers are used in solar water heating systems to transfer heat from the working fluid to the potable water. These can either be single-walled or double-walled. Single-walled heat exchangers have a single membrane between the two fluids and are the most efficient heat exchangers. Double-walled heat exchangers are also used in solar water heating system where domestic hot water is needed. They require an extra layer of protection for the consumption water to avoid leakage. However there is no need for double-walled heat exchangers unless a toxic solar fluid is being used, which is usually not the case.

6.1.5 Distribution systems

Normally either copper tubes or steel tubes are used in the solar heating circuit. The distribution system must withstand the pressure and the temperature gradient it is subject to, and should be well insulated. According to the European standard; EN 12976 the minimum heat insulation should be approximately 20-30 mm depending on the tube diameter [11]. The distribution system contains a number of components such as circulation pump, thermostat, manometer, expansion vessel, safety valves, particle filter and control valves for filling and discharging the heat medium. These components are often integrated in one operational unit.

An antifreeze water-glycol mix is normally used as the working fluid to provide sufficient temperature difference. The thermal properties will differ depending on the mass fraction of glycol in the mixture. If the viscosity increases, a more powerful pump is needed, and operating costs will increase. Fluids that can be used as heat transfer mediums include water, salt solutions, glycol solutions and alcohol.

6.1.6 Circulation pump

A circulation pump is necessary to ensure that the working fluid is circulating through the system. Operation of the pump requires electricity. If the building is not connected to the grid, photovoltaic panels could be installed to produce electricity for this purpose. Another solution could be to use a generator if the building is not connected to the electric grid.

The operation of the pump should be based on the temperature difference between the solar collector and the storage system, ensuring that the working fluid is circulating only when there is a positive heat gain to the system. If the temperature in the outlet of the solar collector is less than or equal to the temperature in the storage system, there would not exist a positive heat gain to the system.

There are different types of control strategies for circulation pumps. With an on-off controller the mass flow is constant and independent of the temperature level as long as the pump is operating. A frequency controlled pump is more energy efficient, because the mass flow rate can vary depending on the temperature level when the pump is operating, requiring less electricity at lower mass flow rates.

6.2 Collector efficiency

Any hot object eventually loses its heat back to the surroundings. The efficiency of a solar collector is directly related to heat loss, mainly from convection and radiation. Thermal insulation is used to slow down the heat loss process. In general, the efficiency of a solar collector can be described by the following equations [11]:

$$\eta = \frac{\dot{Q}_A}{G} \quad (6-1)$$

where \dot{Q}_A is the available thermal power (W/m^2) and G is the irradiance incident on the glass pane (W/m^2). The available power is calculated from the available irradiance at the absorber, converted into thermal energy, minus the losses due to convection, conduction and radiation:

$$\dot{Q}_A = G_A - \dot{Q}_L \quad (6-2)$$

where G_A is the available irradiance (W/m^2) at the absorber, and \dot{Q}_L represents the thermal losses (W/m^2). The available irradiance G_A is defined as the product of the irradiance incident on the glass pane, the degree of transmission of the glass τ and the degree of absorption of the absorber α :

$$G_A = G \cdot \tau \cdot \alpha \quad (6-3)$$

The thermal losses depend on the temperature difference between the absorber and ambient air $\Delta\theta$. This relationship can as a first approximation be considered linear and can be described by the heat loss coefficient k ($\text{W}/\text{m}^2\text{K}$):

$$\dot{Q}_L = k \cdot \Delta\theta \quad (6-4)$$

With the equations mentioned above, the collector efficiency can be written as:

$$\eta = \frac{G \cdot \tau \cdot \alpha - k \cdot \Delta\theta}{G} = \frac{G \cdot \eta_0 - k \cdot \Delta\theta}{G} \quad (6-5)$$

where η_0 describes the optical efficiency. At higher absorber temperatures the thermal losses no longer increase linearly with the temperature difference. This is because of

increasing thermal radiation. The equation for the second order approximation for higher absorber temperatures can be written as:

$$\eta = \eta_0 - \frac{k_1 \cdot \Delta\theta}{G} - \frac{k_2 \cdot \Delta\theta}{G} \quad (6-6)$$

where k_1 is the linear heat loss coefficient ($\text{W}/\text{m}^2\text{K}$) and k_2 is the quadratic heat loss coefficient ($\text{W}/\text{m}^2\text{K}$).

Figure 6-11 shows typical efficiency curves and areas of application with the same global solar irradiance for the following collector types: unglazed collector, glazed flat-plate collector, and evacuated tube collector. The efficiency is given as a function of the temperature difference between collector and surroundings.

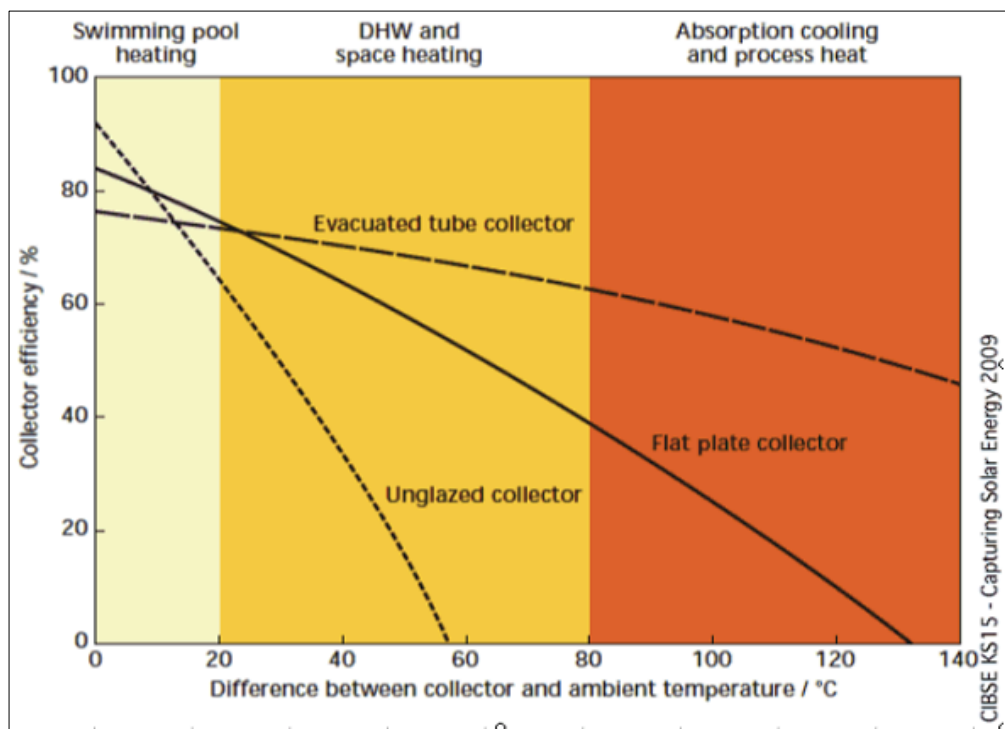


Figure 6-11: Typical collector efficiencies [26]

Figure 6-11 shows that as the temperature difference between the collector and the surroundings increases, eventually the evacuated tube collector is the most efficient collector type. Hence, in cold climates, evacuated tube collectors are generally the best solution. The average annual efficiency of a system with evacuated tube collectors is between 45 % and 50 % [11].

6.3 Collector area

The required collector area depends on several factors, the main ones being:

- Heat loss from the building
- Climatic conditions
- Desired heat ratio covered by the solar heating system

The collector area can be calculated using the following equation:

$$A = \frac{Q_{tot} \cdot SF}{E_G \cdot \eta_{sys}} \quad (6-7)$$

where A is the required collector area (m^2), Q_{tot} is the total annual heating demand (kWh/year), SF is the desired ratio of coverage by the solar collector (typically 40-70 %), E_G is annual solar irradiance per m^2 of collector area (kWh/ m^2 year), and η_{sys} is the average system efficiency (accounts for losses in the collector, pipes and heat storage) [11].

6.4 Solar heating systems

There are three main principles for utilizing energy from the sun. Photovoltaic cells convert solar energy to electricity. Passive- and active solar systems convert solar energy into thermal energy. Active systems rely on pumps to move liquid between collector and storage tank, while passive systems rely on gravity and the tendency for water to naturally circulate as it is heated. Photovoltaic cells will not be discussed further in this report.

6.4.1 Passive solar systems

Passive solar heating refers to the use of the sun's energy for heating and cooling purposes in buildings. Passive systems are simple with few moving parts and require minimal maintenance and no mechanical systems. In a passive solar heating system, energy from the sun is utilized through building constructions. Two primary elements of passive solar heating are south facing windows, and thermal mass to absorb, store and distribute heat. The goal of all passive solar heating systems is to capture heat from the sun within building elements and release heat in periods when the sun is not shining.

There are three categories of passive solar heating: direct gain, indirect gain, and isolated gain. A system with direct gain (Figure 6-12) uses the actual living space as a solar collector, absorber and distribution system. When the sun shines through the window, heat is absorbed and emitted to the interior space. In an indirect gain system (Figure 6-13), thermal mass absorbs the sunlight and heat is transferred through building constructions into the interior space by conduction. An isolated gain system (Figure 6-14) receives energy from the sun through an isolated part separate from the main living area. Examples are sunrooms and convective loops through air collectors to a storage system in the house [27].

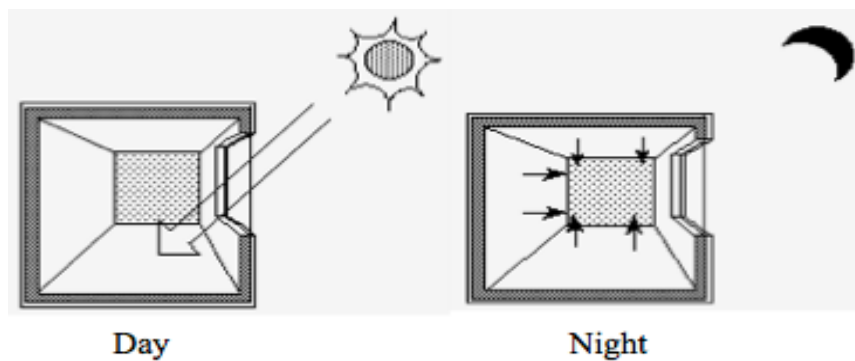


Figure 6-12: Direct gain passive system, based on [27]

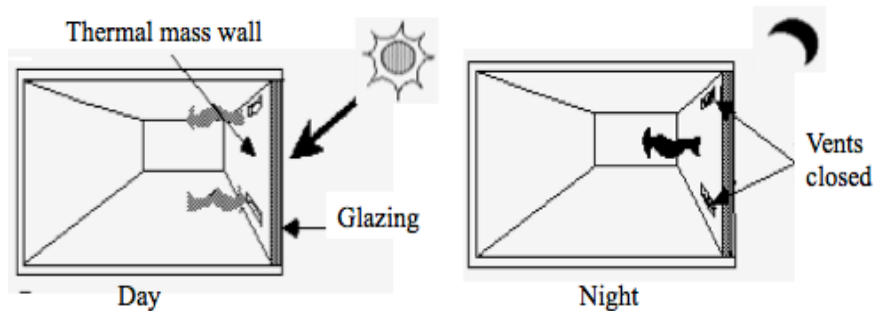


Figure 6-13: Indirect gain passive system, based on [27]

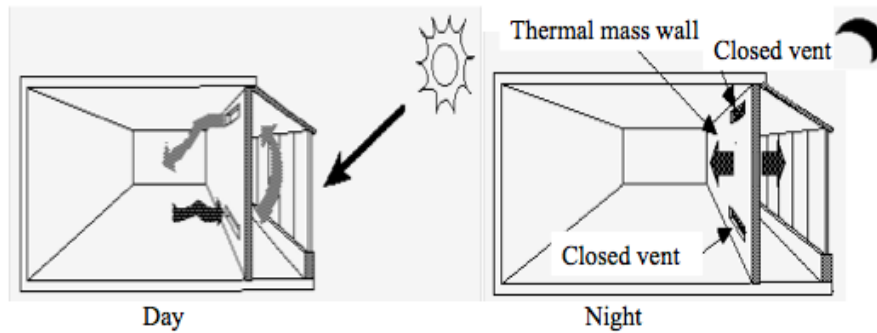


Figure 6-14: Isolated gain passive system, based on [27]

6.4.2 Active solar systems

An active solar heating system requires a pump to circulate the working fluid through the system. A control unit is also needed to assure that the working fluid only circulates through the collector when the useful energy gain for the system is positive. As mentioned, solar heating systems normally need a secondary energy source to maintain sufficiently high temperatures. Typical excess energy supplies include electrical resistances in the storage system, heat pumps and boilers.

For domestic hot water heating, an important factor to consider is to avoid the risk of bacteria such as legionella. The legionella bacteria has its optimal growing condition between 30 °C and 40 °C. The cold water temperature should therefore not exceed 25 °C and the water in the hot water tank should be kept at minimum 60-65 °C. Active solar heating systems can be constructed in various ways. Two examples follow below.

Direct open loop circulation system

In a direct circulation system, a pump circulates potable water through the solar collector and directly to the storage tank in the building. It is possible to integrate an extra hot water tank to a direct system to separate the water in the solar collector circuit from the potable water. The extra hot water tank can be integrated into the storage tank. To prevent system components from destructing, a drainage system is necessary to remove water from the collector circuit when the ambient temperature falls below freezing level. Figure 6-15 shows the principle of a direct circulation system for hot water heating.

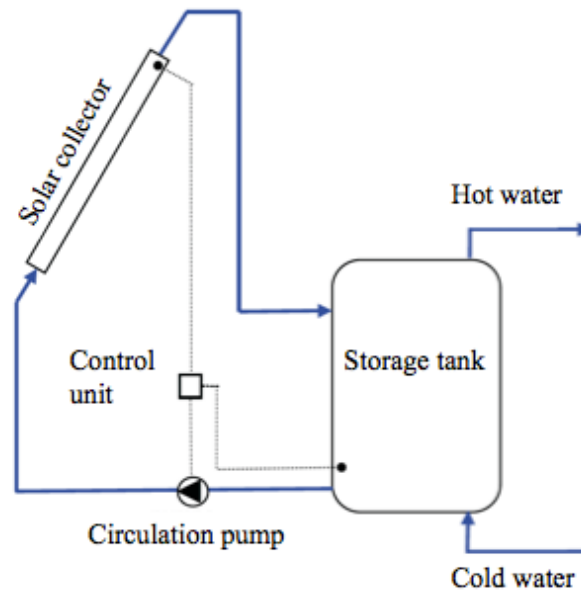


Figure 6-15: Direct circulation system, based on [14]

One variant of the direct circulation system is a drain-down system. In a drain-down system, the fluid in the storage tank is pumped from the tank to the collector array where it is heated. The control unit is programmed to switch off the pump if freezing conditions occur or if the useful energy gain for the system is negative. The water in the collector circuit can then be drained to avoid component damages. The solar collectors and exterior piping must be carefully sloped for the fluid to drain when the circulation pump stops. Because direct open loop systems use water as the working fluid through the solar circuit, they are not well suited for cold climates as frost can damage the system components.

Indirect circulation system

In an indirect circulation system, heat from the solar collector is transferred to the storage system via a heat exchanger. The working fluid used in an indirect system is normally an antifreeze water-glycol mix allowing for much lower temperature applications. The percentage of glycol in the mix depends on the expected ambient temperature. Table 6-1 shows the freezing point of different propylene glycol water-based solutions.

Table 6-1: Freezing point of propylene glycol water solutions, based on [28]

Propylene glycol solution by mass (%)	0	10	20	30	40	50	60
Freezing point [°C]	0	-3	-8	-14	-22	-34	-48

An indirect circulation system is shown in Figure 6-16. The heat exchanger can either be placed outside the tank, be integrated within the tank or as a mantle around the tank. The pump is controlled by a thermostat based on a positive temperature difference between the solar collector and the bottom of the storage tank. To minimize the risk of legionella growth, it is important to maintain sufficient circulation in and out of the hot water tank. Placing the heat exchanger on the user side of the tank instead of the collector circuit side as in Figure 6-16 can further decrease this risk of bacteria growth. The system would then be a closed system.

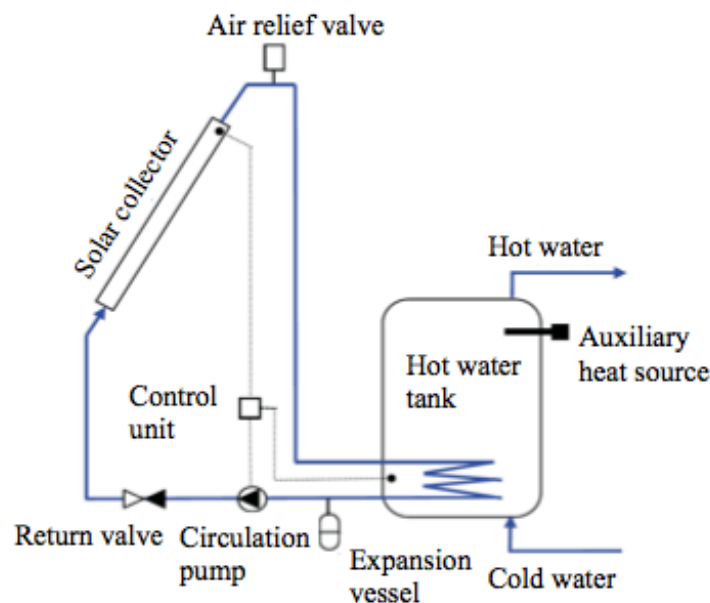


Figure 6-16: Indirect circulation system, based on [14]

A solution often used in an indirect circulation system is a drain-back system. As for the drain-down system explained for the direct circulation system, the circulation pump is switched off if freezing conditions occur or if the useful energy gain is negative. In a drain-back system however, the fluid in the collector circuit is not connected to a floor drain. Instead, the fluid in the collector and exterior piping is

drained by gravity to a drain-back tank. In drain-back systems, water can be used as the heat transfer medium since the system is secured for frost protection, although it is most common to use an antifreeze medium.

7 Integration of solar thermal collectors

When installing solar thermal collectors there are several factors that need to be taken into account. The collectors should be positioned at an appropriate orientation and angle from the horizontal in order to generate a significant energy yield. The installation should be carefully planned considering the collector and further equipment typically have a lifetime of 25 years. In addition, the system normally needs maintenance within one to two years and costs related to maintenance are minimized if the system parts are easily accessible [29].

From an architectural point of view solar collectors should not only answer to technical constraints of their specific solar thermal technology. Collectors can also be integrated into the building design in a way that aesthetically satisfies the architect. Solar collectors can be integrated in roof constructions as on-roof elements or in-roof elements as well as in the building façade.

7.1 On-roof integration

In on-roof constructions, collectors are installed over existing roof tiles on construction rails (Figure 7-1). For flat-roof installations, specially designed support frames can be used to achieve the optimal orientation and inclination of the collectors (Figure 7-2). This solution tends to be more expensive and the visual impact may not satisfy the architect's point of view. An alternative solution when a tilted collector might have an undesirable visual impact on a flat roof is to use evacuated tube collectors and have only the absorber part in the tubes tilted (Figure 7-3) [29].



Figure 7-1: On-roof installation with flat plate collectors [30]



Figure 7-2: Flat on-roof installation with support frames [31]



Figure 7-3: Flat on-roof evacuated tube installation with tilted absorbers [32]

7.2 In-roof integration

Solar collectors can be used as multifunctional elements in buildings replacing conventional building elements and contributing to clean energy use. Collectors can be delivered in a wide range of and shapes and sizes and can be designed to fit the exact shape of a roof (Figure 7-4), or parts of a roof (Figure 7-5).



Figure 7-4: In-roof integration of solar collectors [33]

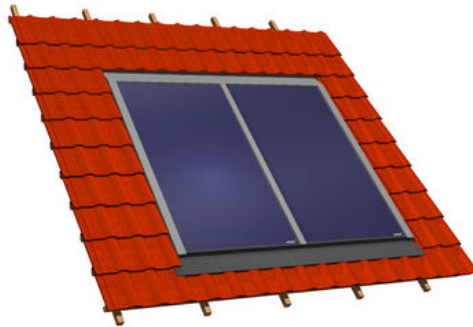


Figure 7-5: In-roof integrated solar collectors [34]

7.3 Façade integration

Due to the vertical installation, façade integration of solar collectors allows for rather evenly distributed irradiation throughout the year. With vertical installations a lot of the irradiation can be used in the winter, when the highest heating demand occurs. Another benefit of façade installation is that there is often not enough space on the roof or no suitable south oriented roof area available. Façade integrated collectors fulfill several functions. They act as solar thermal panels, improve the building's thermal insulation, reducing the heat loss from the building, and protect the façade from climatic conditions as well as working as structural elements. Integration can be on the entire façade (Figure 7-6), or part of the façade while preserving aesthetic building appearance.



Figure 7-6: Façade integrated solar thermal panels [32]

An important issue when integrating solar panels into the façade is to meet the same building requirements as other façade components. In addition, shading from nearby constructions or elements should be minimal, and connections between collector and wall require expertise attention regarding structural calculations and building physics.

The annual global irradiance is approximately 30 % less on a vertical façade surface than on a 45 ° tilted surface. However, vertical collectors are less likely to face problems with snow coverage and they benefit from increased irradiation through reflection from snow. With these factors considered, global irradiance on a vertical surface is only 24 % less than that of a 45 ° tilted surface [29].

7.3.1 Façade integrated evacuated tube collectors with tilted absorbers

As for flat roof installations (Figure 7-3), façade mounted evacuated tube collectors can be installed so that the absorbers inside the tubes are tilted to a desired angle to maximize the solar gain from a vertical installation. This solution can be especially beneficial to use in cold climates and areas subject to great amounts of snowfall in the winter. Such an installation on a flat roof would more likely suffer from snow coverage than if it were mounted on a vertical wall. In addition, evacuated tube collectors allow for higher absorber temperatures as the vacuum enables boiling at lower temperatures.

8 Dynamic simulation tool ESP-r

8.1 Ground modeling

There are a number of different possibilities for ground modeling in ESP-r. Auråen studied possible ways to account for heat loss from the building to the ground in her master thesis and the chosen solution was to use one of the BASESIMP configurations available in ESP-r. A BASESIMP configuration will be used further in this report. Information concerning alternative ground modeling methods will not be included here, as the main focus of this report is to improve the solar heating system. Details regarding alternative ground modeling approaches can be found in Auråen's master thesis *Modeling of heat exchange with the ground and analyses of energy use for a frost proof leisure building with active solar heating*, written during the spring semester 2013 [7].

8.2 BASESIMP

BASESIMP (simplified basement model) is a regression-based algorithm that was developed to improve the state of foundation heat-loss modeling in whole building energy programs. The algorithm covers a broad range of foundation configurations, has minimal processing requirements and is extensible. BASESIMP expresses both above-grade and below-grade time-dependent heat losses. The algorithm was developed from 33 000 runs performed with BASECALC – a finite-element-based program for analyzing foundation heat losses- to generate the database for the BASESIMP regressions [35].

BASESIMP has the capability to model basement and slab-on-grade systems. A basement is defined as a foundation where the floor slab is located 0.65 m to 2.4 m below-grade (Figure 8-1). A slab-on-grade is defined as a foundation whose floor slab is located within 0.1 m of grade (Figure 8-2).

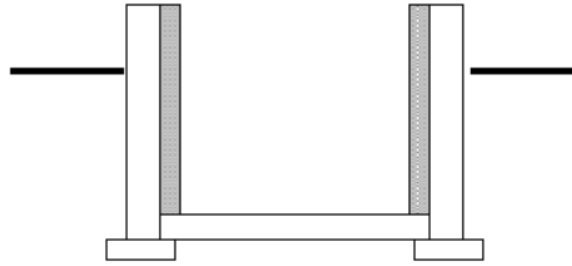


Figure 8-1: basement

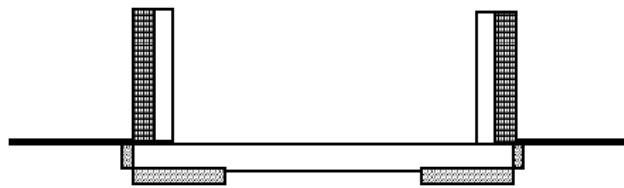


Figure 8-2: Slab-on-grade

BASESIMP calculates the foundation heat loss as a function of thermal and geometric properties (insulation resistance, height, depth, width, length) and site conditions (soil conductivity, water-table depth, and weather). Each system has a unique set of correlation coefficients and BASESIMP uses a single set of correlation equations for all systems. This makes the algorithm easy to implement as limited inputs are required and, having only one set of equations minimizes the risk of error.

Some main attributes offered by BASESIMP follow below [35]:

- BASESIMP covers a large number of foundation systems
- The foundation is treated as a whole rather than broken down into several segments
- BASESIMP treats above-grade heat losses, including effects of thermal bridging from below-grade components to above-grade components
- BASESIMP accounts for thermal bridging to the main-story walls
- No interpolation is required in BASESIMP for the depth of the floor slab and the soil conductivity as these are variables in the correlations.
- In BASESIMP, the water-table depth is a variable
- BASESIMP allows the importation of BASECALC output for the modeling of “custom” foundations

8.2.1 BASESIMP inputs

BASESIMP configurations are implemented in building simulations as a boundary condition for a surface. In the project manager in ESP-r within the menus *zones and composition* and *geometry and attribution*, the different zones and surfaces can be linked to their boundary conditions. By selecting the basement zone, *surface attributes*, and the surface of interest, the boundary condition can be set to *BASESIMP*. By choosing the option *BASESIMP foundation configuration* a new list of basement configurations is presented. Option BCIB_6 was used in Auråen's master thesis, and after discussions with the supervisor the same option will be used for the model in this report. BASESIMP configurations require some inputs from the user. The required input parameters are explained below [36].

Height

The height is defined as the distance from the top of the floor slab to the top of the basement structural wall. This value must be at least 0.1 m greater than the depth, and between 1 and 2.5 m.

Width

The width is the distance between the exterior-of-structural-wall to exterior-of-structural-wall. This value must be less than or equal to the length, and between 2 and 20 m.

Length

The length is the distance between the exterior-of-structural-wall to exterior-of-structural-wall. This value must be greater than or equal to the width, and between 2 and 20 m.

Depth

The depth is the distance from the top of the floor slab to the grade level. This value must be between 0.05 and 2.4 m.

Wall insulation overlap

The wall insulation overlap is the height of the wall covered by both interior and exterior wall insulation. The value must be between 0 and 2.4 m. This parameter is only relevant for BASESIMP configurations BCCN_1 and BCCN_2.

Soil conductivity

The soil conductivity is the thermal conductivity of soil surrounding the foundation and the value must be between 0.1 and 10 W/mK.

Water table

The water table dictates the depth of horizontal thermal boundary. The deeper the water table, the lower the foundation heat loss will be. The value must be between 5 and 20 m.

TG_{avg}

TG_{avg} is the annual average soil temperature and the value must be between -10 and 20 °C.

TG_{amp}

TG_{amp} is the amplitude of the ground-temperature's annual sine wave. Value must be between 0 and 25 °C.

TG_{ps}

TG_{ps} is the phase lag of the ground-temperature's annual sine wave. Value must be between 0 and 1 radians.

Moore method

The parameters TG_{avg}, TG_{amp} and TG_{ps}, representing ground temperatures can either be set by the user or by the Moore method and the climate file in ESP-r. The Moore method was originally developed for the software HOT2000. The method is a soil estimation model that uses average monthly ambient dry bulb temperatures and annual heating degree-days to estimate the temperature of the soil at any depth at any time of the year. The ground temperatures will be set by the Moore method in this report.

8.3 Solar collector model in ESP-r

A new solar collector model was developed in ESP-r within ESP-r's plants and systems network in 2004. The old model required a significant amount of input data that were often too advanced for the typical user. The new model is based on empirical collector performance results and requires limited inputs. The new model allows for an integrated simulation of residential buildings and solar energy systems.

The collector is modeled as a one-node component. The node represents the outlet temperature of the collector. The collector is characterized by its efficiency, and can be expressed as a function of the outlet temperature [37]:

$$\eta = \eta_{0,out} - \eta_{1,out} \frac{(\theta_{out} - \theta_e)}{G} \quad (8-1)$$

where $\eta_{0,out}$ and $\eta_{1,out}$ are two parameter characteristics of the collector, θ_{out} is the collector outlet temperature, θ_e is the ambient temperature and G is the solar radiation incident upon the collector. An energy balance for the collector yields:

$$M\bar{c} \frac{\partial \theta_{out}}{\partial t} = -\dot{m}C_p(\theta_{out} - \theta_{in}) + \eta AG \quad (8-2)$$

where M is the mass of the collector including the fluid in the collector, \bar{c} is the weighted average specific heat capacity of the collector mass, \dot{m} is the mass flow rate through the collector, θ_{in} is the collector inlet temperature, and A is the gross area of the collector [37]. The energy balance is not correct in the sense that the left-hand side of the equation should optimally use an average collector temperature instead of the collector outlet temperature to represent the energy stored in the collector. However, it is assumed that all the mass of the collector is concentrated at the collector's outlet and the validity of these simplifications will not matter because the time dependent term will later be dropped from the equation [37].

Combining equations (8-1) and (8-2), and identifying θ_{out} with the component's node temperature θ_k , and θ_{in} with the node temperature θ_j of the component j which feeds into the collector, the equation can be rewritten as:

$$M\bar{c} \frac{\partial \theta_k}{\partial t} = -\dot{m}C_p(\theta_k - \theta_j) + \eta_{0,out}AG - \eta_{1,out}A(\theta_k - \theta_e) \quad (8-3)$$

Equation (8-3) is ready to be programmed into ESP-r. The one-node component collector model is illustrated in Figure 8-3.

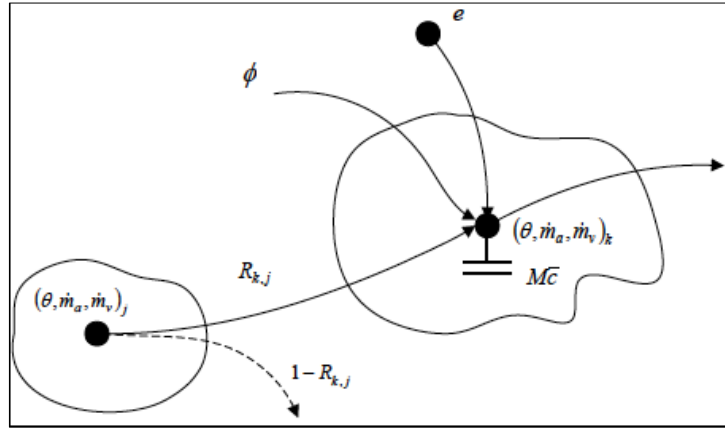


Figure 8-3: The collector model

Collector efficiencies are rarely calculated as a function of the outlet temperature as presented in equation (8-1). North-American test results tend to use the inlet temperature, while European test results are often reported in terms of average collector temperature. Furthermore, test reports generally provide a quadratic equation:

$$\eta = \eta_0 - \eta_1 \frac{\Delta\theta}{G} - \eta_2 \frac{\Delta\theta^2}{G} \quad (8-4)$$

where $\Delta\theta$ is defined by:

$$\Delta\theta = \theta_{in} - \theta_e \quad (\text{North-American efficiency equation})$$

$$\Delta\theta = \theta_{avg} - \theta_e \quad (\text{European efficiency equation})$$

where θ_{avg} is the average temperature of the collector inlet and outlet temperatures:

$$\theta_{avg} = \frac{\theta_{in} + \theta_{out}}{2}$$

It is necessary to convert quadratic equations as (8-4) to equations in the form of (8-1). Further details regarding the collector efficiency equations are found in the article *Development of a New Solar Collector Model in ESP-r*, written by D. Thevenard, K. Haddad and J. Purdy [37]. The solar collector model requires 11 parameters entered by the user. A screenshot of the parameters are shown in Figure 8-4. The values used in this report are presented in section 13.1.1.

Collector area (m ²)	:	2.0000
Type of efficiency equ. (1=North-American,2=Europe)	:	2.0000
Constant coef. of efficiency equ. (-)	:	0.62000
Linear coef. of efficiency equ. (W/m ² /C)	:	3.8700
Quadratic coef. of efficiency equ. (W/m ² /C ²)	:	0.11000E-01
Collector test flow rate (kg/s)	:	0.20000E-01
Heat capacitance of fluid used for test (J/kg/C)	:	3600.0
Inc. angle equation linear term coef. (-)	:	0.20000
Inc. angle equation quadratic term coef. (-)	:	0.0000
Collector slope (deg. from horizontal)	:	70.000
Collector azimuth (deg., N=0, E=90)	:	180.00

Figure 8-4: Parameters for the collector model

9 Solar heating system: possible design solutions

Several different system solutions were attempted simulated in ESP-r. The different ideas for the design of the solar heating system will be presented in this chapter and are summarized in Table 9-1. The chosen design to study further will be design 2: Solar heating system with hydronic floor.

Table 9-1: System Designs

	Solar heating system solutions
Design 1	Storage tank and hydronic floor
Design 2	Hydronic floor embedded in concrete slab
Design 3	Storage tank
Design 4	Water-based radiator embedded in concrete slab

9.1 Design 1: Storage tank and hydronic floor

The first approach was to have a solar heating system consisting of the following four plant components:

- Solar collector
- Storage tank
- Hydronic floor
- Pump

Explanation

A water-glycol mix flows in a closed loop circuit. The water-glycol mix is heated in the solar collector. Thereafter it flows into the storage tank and further to the hydronic floor before being pumped back to the solar collector (Figure 9-1). The operation of the pump is based on the temperature difference between the solar collector and the storage tank. The pump is switched off when this temperature difference is less than 5 °C, hence, when the solar gain is close to zero or negative. The tank is placed in the internal ground floor zone. The hydronic floor is embedded within a layer in the concrete slab in the ground floor of the same zone. The internal ground floor zone is being heated from the floor heating circuit as well as from heat loss from the storage tank.

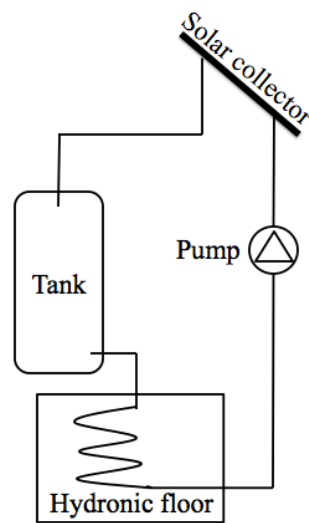


Figure 9-1: System with storage tank and hydronic floor

The system explained above was attempted simulated in ESP-r. The program did not respond and ended with several warning messages. After several attempts under the supervision of an experienced user in addition to contacting program developers for help, it was decided in consultation with the supervisors not pursue this solution and rather look at alternative solutions under this thesis. A related approach is suggested in the chapter for proposals for further work in chapter 16.

9.2 Design 2: Hydronic floor

The second system solution that was attempted simulated in ESP-r consisted of three components:

- Solar collector
- Hydronic floor
- Pump

Explanation

A water-glycol mix flows in a closed loop circuit. The water-glycol mix is heated in the solar collector. Thereafter it flows directly to the hydronic floor before being pumped back to the solar collector. The operating condition for the pump is the same principle as for the first approach, except the temperature difference is now based on the difference between the collector and the hydronic floor. Also here, the hydronic floor is embedded within a layer in the concrete slab. Heat transfer to the internal ground floor zone is from floor heating.

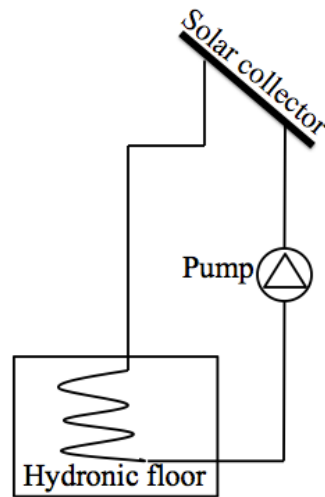


Figure 9-2: System with hydronic floor

When attempting to simulate this model, the same problem was encountered as for the first approach. After several attempts it was decided to evaluate whether the designs mentioned under sections 9.3 and 9.4 might be more feasible. However, the final choice was to nevertheless do the rest of the thesis with design 2 as further discussed in section 9.5.

9.3 Design 3: Storage tank

In the third approach the hydronic floor component was removed and the system consisted of the following three components:

- Solar collector
- Storage tank
- Pump

Explanation

The operation of the pump is based on the temperature difference between the collector and the storage tank. The tank is placed in the internal ground floor zone. With this approach, simulations were working. However, with no heat supply directly to the ground, the principle of seasonal heat storage could not be analyzed in a realistic way.

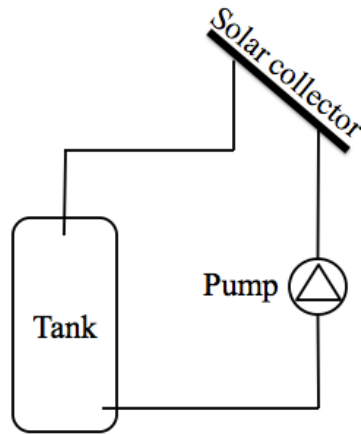


Figure 9-3: System with storage tank

9.4 Design 4: Water-based radiator

After several attempts trying to integrate the hydronic floor component in the solar heating system, as explained under sections 9.1 and 9.2, a water-based radiator was chosen to imitate a water-based floor-heating component. This system solution consisted of three components:

- Solar collector
- Water-based radiator
- Pump

Explanation

The radiator is given a surface area equal to the floor area of the internal zone, 6.25m^2 and placed within the ground floor. The operation of the pump is based on the temperature difference between the collector and the radiator and heat transfer to the room is from floor heating.

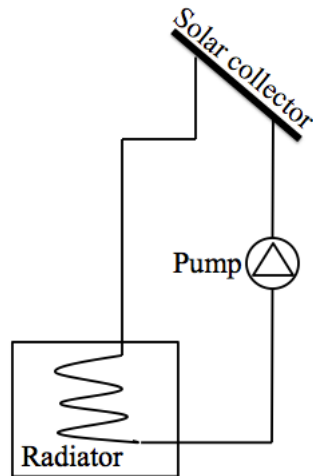


Figure 9-4: System with radiator mimicking floor heating

Design 4 was also tested with a storage tank between the collector and the radiator, but ESP-r did not respond when trying to simulate. Design 4 was at first chosen as the system principle to analyze further. It was very unclear to what degree the radiator would actually act as a floor-heating component, and it was decided to try to implement design 2 one last time.

10 Chosen system, Design 2: Hydronic floor

After having worked through the alternatives mentioned in chapter 9, design 2 with hydronic floor was pursued. To minimize the risk of flaws in the model, everything was built up from scratch. How to implement the design in ESP-r will be explained in detail in the chapter 11. Figure 10-1 shows a cross section sketch of the leisure home with a south oriented solar collector. The point of heat injection to the hydronic floor is within a layer in the concrete slab.

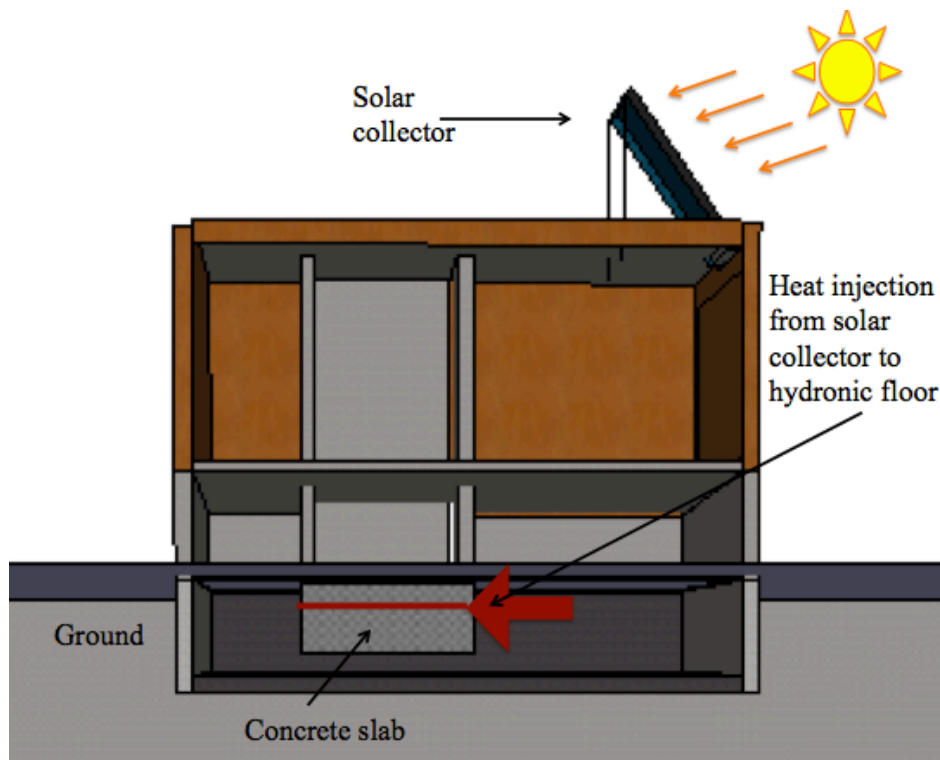


Figure 10-1: Cross section of leisure home illustrating point of heat injection

10.1 Hydronic floor with control loop

The design with heat injection to the hydronic floor in the internal zone will also be tested in combination with heat injected directly to zone air for a chosen time period. Simulations showed that the heat injected to the concrete slab during the darkest months was so limited that it did not make any significant heat contribution to the leisure home. Chapter 12 will describe a system solution with heat injection to the floor combined with heat injection directly to zone air from a control loop in selected periods. Heat to zone air is implemented as electrical heating, but the amount of heat supplied is based on heat that would otherwise be supplied by the solar heating system via the hydronic floor.

10.2 Old design from the project work report

The original goal of the project work report, mentioned in section 4.1 with regards to the solar heating system was to build up a plant network of components, as in design 2. The implementation did not work and a simplification was made to imitate an active solar heating system. In the simplified system, heat was injected to the ground floor from an electrical heating control loop. The amount of heat injected per month was based on calculated average monthly values of irradiance modified for collector area, angle of inclination and collector efficiency. The time period of heat injection was based on average solar hours per day for each month. The same solar heating modeling approach was later used in Auråen's master thesis. Auråen's results with electrical heating imitating an active solar heating system will be compared to the results from design 2, where the solar collector and hydronic floor components are implemented. Chapter 12 describes how control loops for electrical heating are implemented in ESP-r.

11 Plants and systems model in ESP-r

This chapter will present how the plants and systems simulation parameters are integrated into the leisure home model. To allow for a replication of the simulation, the description will be presented in detail.

In ESP-r environmental control systems can be represented as zone/flow controls or as a network of system components, often called a plant system. The solar heating system will be built up as a plant system. This method allows for interactions between components and/or controls, and the psychometric state within components and at points in the network is explicitly computed and available for inspection [38].

When creating a plant system, planning is essential even for a simple model. It is often advantageous to sketch the network, gather component information, and identify the sequence of components before creating the network.

11.1 Defining the solar heating system

Ideally, for efficiency purposes, evacuated tube collectors are most likely the best choice for solar collectors in cold climates. In ESP-r there is no option to model evacuated tube collectors and the collector in the model is the one-node simplified flat plate collector explained in Section 8.3.

The one-node solar collector can be modeled using the following steps:

1. In the *project manager* in ESP-r, select the option *browse/edit/simulate*.
2. In the *browse/edit/simulate* menu, under *networks*, select *plants and systems*.
3. The *plant model* menu has two options: *idealized* or *explicit*. Select *explicit*.
4. The menu *network definition* (Figure 11-1) will appear with a number of selections. To build up a plant network, the user must define system components, connections between system components and links between components and their surrounding environment under containments.

```

Network definition;edit
a Problem name :../nets/test.pln
b Simulation type : Energy + one phase.
c Project title  :
-----
Problem status...
-----
No. of components ...      ( 3 )
d Components
-----
No. of connections ...    ( 3 )
e Connections
-----
No. of containments ...   ( 2 )
f Containments
-----
No. of comp. + electrical data ( 0 )
g Electrical data
-----
h Link to fluid flow network
-----
No. of linked zones ...   ( 1 )
i Link plant to zone(s)
-----
j plant config file format > descriptive
-----
! Update plant config file
? Help
- Exit

```

Figure 11-1: Network definition

5. The next task is to define system components. By selecting *components*, and then the option *add/delete/copy*, and further *add*, a list of possible component types included in ESP-r are presented (Figure 11-2). The components used in the model are found under *wet central heating* and *solar and others*. The chosen solar collector is called *simplified flat plate solar collector*, the pump is called *variable speed domestic WCH pump*, and the hydronic floor is called *slab-on-grade hydronic floor*. Each component has a set of default values for different system parameters provided by ESP-r. These can either be used as is, or be altered by the user. An example of typical component parameters can be seen in Figure 11-3 for the pump.

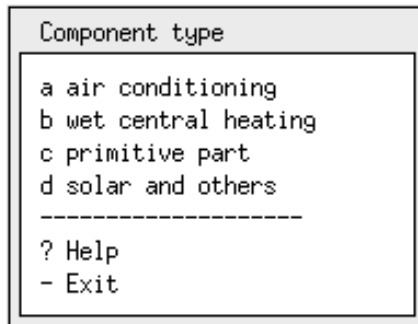


Figure 11-2: Component types

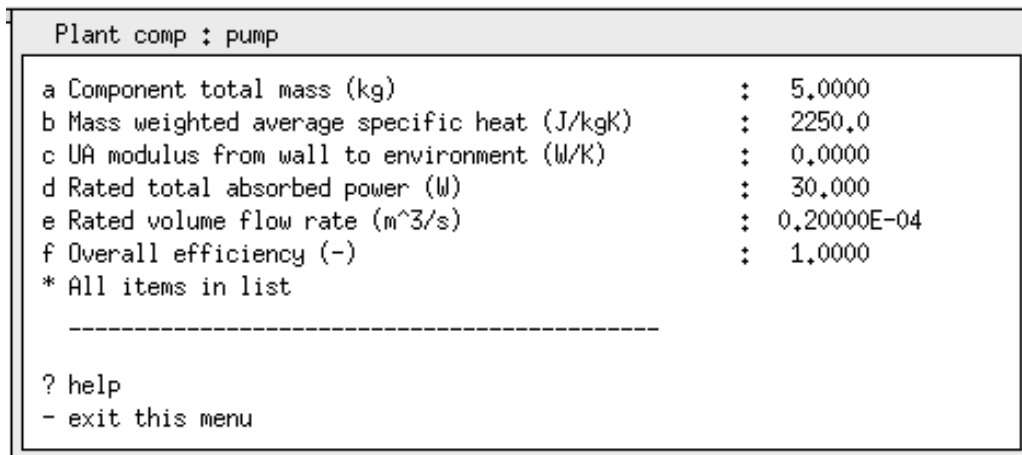


Figure 11-3: Input parameters for *variable speed domestic WCH pump*

The input parameters for the hydronic floor component should be considered carefully. According to the ESP-r user manual, system components are “placed” in the desired zone or construction through the option containments, which will be described in step 7. However, for the hydronic floor component, this must also be defined within component parameters. Figure 11-4 shows a list of the component parameters required for the hydronic floor.

```

Plant comp : hydro_floor

a Number of circuits (integer)           : 1,0000
b Inside diameter of pipe (m)           : 0,17000E-01
c Outside diameter of pipe (m)         : 0,20000E-01
d Pipe spacing (m)                       : 0,30000
e Thermal conductivity of pipe material (W/mK) : 0,38000
f Volumetric specific heat of pipe material - rho*Cp : 0,32000E+07
g Served zone number (integer)         : 3,0000
h Zone surface number (integer)        : 6,0000
i Injection node number (integer)       : 10,000
* All items in list

-----

? help
- exit this menu

```

Figure 11-4: Input parameters for *slab-on-grade hydronic floor*

Options *g*, *h*, and *i* define which zone, surface, and surface layer the heat is injected into. The hydronic floor should be placed in zone *0_intzone* within the surface *0_intground* and in one of the concrete layers in the ground floor. The model has seven zones, listed in the menu from letters *a* to *g*, where *a* represents *served zone number 1*, *b* represents *served zone number 2* etc. The *zone surface number* is found in the same way in the menu *surface lists and edges* for the chosen zone. The *injection node number* describes which layer within the chosen surface the heat is injected to. A construction in ESP-r is built up by a number of layers with chosen materials. Each layer has 3 nodes, one exterior or bordering another layer, one integrated node and one internal node (adjacent to the next layer or inside a zone). Layer 1 represents the exterior layer, while the last layer represent the internal layer adjacent to the zone. The concrete slab in the ground floor consists of five layers of concrete, making a total of 11 nodes (see Figure 11-5). The injection node should be close to the internal ground floor zone, and the node of injection should then be somewhere from 8 to 10. Injecting heat at the lower nodes would create a hot ceiling in the basement, and with the large thermal mass only receiving heat from the solar heating system, it is unlikely that this heat would contribute to any significant heating of the leisure home if it were injected far down in the construction. The principle of nodes and layers within the concrete slab is shown in Figure 11-5.

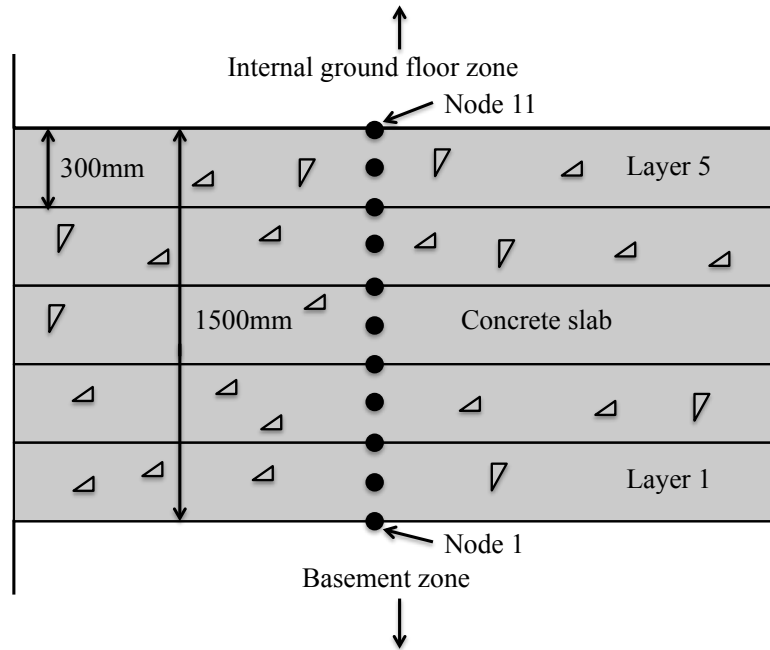


Figure 11-5: Concrete slab with nodes and layers

6. The next step is to connect the components. By selecting *connections*, and then *add/delete/copy*, and further *add*, the components defined in step 5 appear. Select a *receiving* component and next, the component *sending* to the *receiving* component. A list of connection types appears (Figure 11-6), and option *c from another component* is chosen to link the solar collector to the hydronic floor, the hydronic floor to the pump and the pump back to the solar collector.

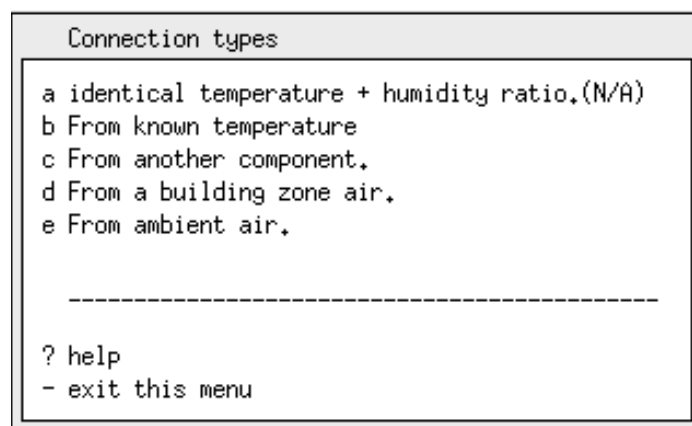


Figure 11-6: Connection types

The connections defined for the model in this report are shown in Figure 11-7. The mass diversion ratio is 1 for all the connections because it is a closed loop system and the mass flow rate is the same throughout the system.

Connections						
Sending comp	@ Node	to	Receiving comp	@ Node	Conn Type	Mass Div
a pump	water node 1	-->	solar_coll	water node 1	to compt	1,000
b solar_coll	water node 1	-->	hydro_floor	water node 1	to compt	1,000
c hydro_floor	water node 1	-->	pump	water node 1	to compt	1,000

+ add/delete/copy

? Help
- Exit

Figure 11-7: Connections in the solar heating system

7. The next step is to define containments. Components exist in a context, such as surrounded by a fixed or ambient temperature, or within a surface. In this step components are attributed containments. The different containment types are shown in Figure 11-8. Containments defined for the solar heating model are presented in Figure 11-9. The solar collector is linked to ambient air and the hydronic floor is linked to a layer within the ground floor in the internal zone. The pump is not linked to anything and is assumed to be adiabatic.

Containments types
a Ambient air temperature.
b A plant component temperature.
c Fixed temperature.
d Zone (air/surface/const) temperature.

? help
- exit this menu

Figure 11-8: Containment types

Containments		
Component	Containment descr.	Type
a solar_coll	outside air	0
b hydro_floor	zone: basement	3

+ Add/Delete/Copy		
? Help		
- Exit		

Figure 11-9: Containments for system components

11.2 Defining control strategy

A control strategy is defined to get a reasonable operation pattern for the pump. The pump will be controlled based on a measured temperature difference between the solar collector and the radiator. The heat transfer fluid should only circulate when there is a positive temperature difference between the collector and the hydronic floor in order to make a heat contribution.

1. In the *project manager* in ESP-r, select the option *browse/edit/simulate*.
2. The control strategy of the solar heating system is defined in the *controls* menu under *plants and systems*. In this step, day types and time periods for when the control loop/loops should be activated are defined.
3. Select the existing control loop or create a new control loop. A list of editing options will appear (Figure 11-10). A control loop is defined with sensor details, actuator details and period data.

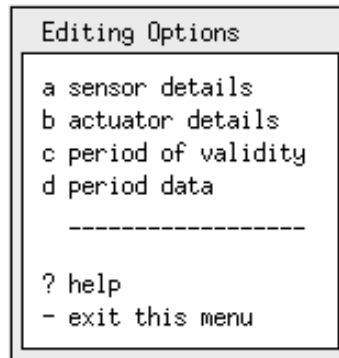


Figure 11-10: Editing options

4. For each defined control loop, one must specify what the sensor(s) in the loop(s) are supposed to register. The type of sensor is defined under *sensor details* (Figure 11-11) and for this model the chosen option is *a senses output of a plant component*. The next step is to select the component you wish to place the sensor at. A follow-up question asking whether you want the sensor to measure a temperature difference between two nodes will appear. In this model we want the temperature difference between the solar collector and the hydronic floor, so the answer is yes.

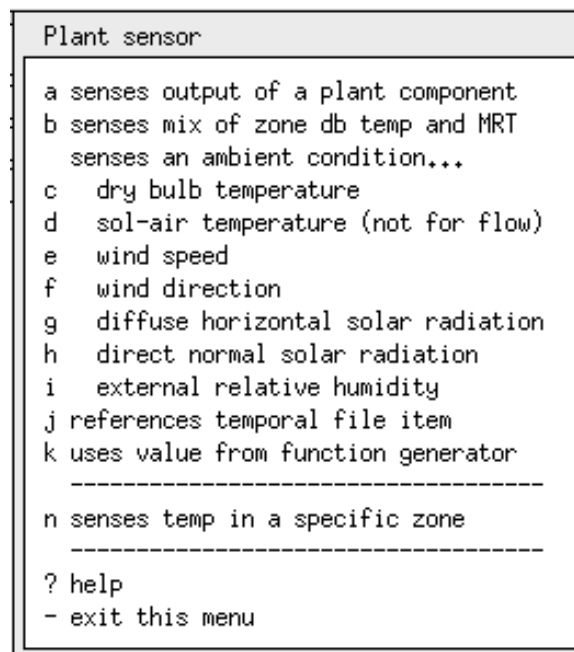


Figure 11-11: Plant sensor

5. The next step is to define actuator details. The actuator is located at a node within a plant component, and the pump is selected as the actuator (Figure 11-12).

Plant component for actuator ?		
Name	Iref no.1	Type
a solar_coll	84	solar and other
b pump	15	water heating
c hydro_floor	63	solar and other

? Help		
- Exit		

Figure 11-12: Plant component for actuator

- The last step that needs to be implemented to have a functioning control loop is to specify details regarding type of control and set point values. This is done in the menu *period data* in Figure 11-10. Figure 11-13 shows available controller types in ESP-r and in this model option *y senses temp diff* is selected to get the temperature difference between the solar collector and the hydronic floor. The control strategy makes sure that the pump is operating only when the temperature in the solar collector is high enough to make a heat contribution to the hydronic floor. The pump is based on on/off control. Realistically, on/off control would most likely not be used, but it will be used for simulation purposes to show that the system is not in operation when there is a negative temperature difference. This means that the mass flow is independent of the temperature level, as long as the pump is operating.

controller type		
a	senses dry bulb	actuates flux
b	senses dry bulb	actuates flow
c	senses enthalpy	actuates flux
d	senses enthalpy	actuates flow
e	senses 1st ph mass flow	actuates flux
f	senses 1st ph mass flow	actuates flow
g	senses 2nd ph mass flow	actuates flux
h	senses 2nd ph mass flow	actuates flow
i	senses adl plant output	actuates flux
j	senses adl plant output	actuates flow
k	senses RH	actuates flux
l	senses RH	actuates flow
m	senses dry bulb	actuates variable
n	senses enthalpy	actuates variable
o	senses 1st ph flow	actuates variable
p	senses 2nd ph flow	actuates variable
q	senses plant output	actuates variable
r	senses RH	actuates variable
s	senses dry bulb	actuates mass ratio
t	senses enthalpy	actuates mass ratio
u	senses 1st ph flow	actuates mass ratio
v	senses 2nd ph flow	actuates mass ratio
w	senses plant o/p	actuates mass ratio
x	senses RH	actuates mass ratio
y	senses temp diff	actuates flow
z	senses abs temp diff	actuates flow
0 Page --- part: 1 of 2 ---		
? help		
- exit this menu		

Figure 11-13: Controller types

12 Control loop for heat injection

The hydronic floor component is embedded within the concrete slab. Because of Sweden and Norway's placement on the northern hemisphere, the amount of incoming solar radiation during the winter is limited. A small heat input into a large thermal mass may not contribute to any significant temperature raise inside the leisure home. To utilize heat collected in periods with limited solar radiation, heat will be attempted injected directly to zone air rather than to the floor. The solar heating system will be switched off in these months and a calculated equivalent amount of heat that would otherwise be supplied by the hydronic floor will be injected straight to zone air by electrical heating. This modeling approach for heat injection to the room during selected months is explained below.

12.1 Defining control loop for zone air heating

A building control unit holds details on sensor and actuator locations and defines the time dependent operation of the active controllers through a simulation. The control strategy is associated with the building zones or constructions to define the time dependent control objectives.

A basic controller for heating and cooling is defined for the purpose of heat injection to zone air. The principle is explained below.

1. In the project manager under *browse/edit/simulate, controls, and zones*, a building control strategy for heat injection to zone air can be defined.
2. The *number of zone control day types* is chosen to be *dates of validity* in order to separate each month. Each day type is then defined from start day to finish day, i.e. day 60 to day 90 for the month of March and so on, and the last day must be day number 365 to cover the whole year.
3. The number of *periods in day type* is chosen to be 3. This means that for each day type (each month in this case) there are three independent time periods per day. The start time for each period must be defined, and the first period always starts at time 00.00. Heat equivalent to heat supply from the hydronic floor is to be injected between the start of period 2 and the start of period 3 and is zero before and after. The start time of each period depends on the month. Each month has

different numbers of solar hours, which has a subsequent effect on the hours of heat supply by the hydronic floor. The principle of heat injection in period 2 is illustrated in Figure 12-1 for one day in March.

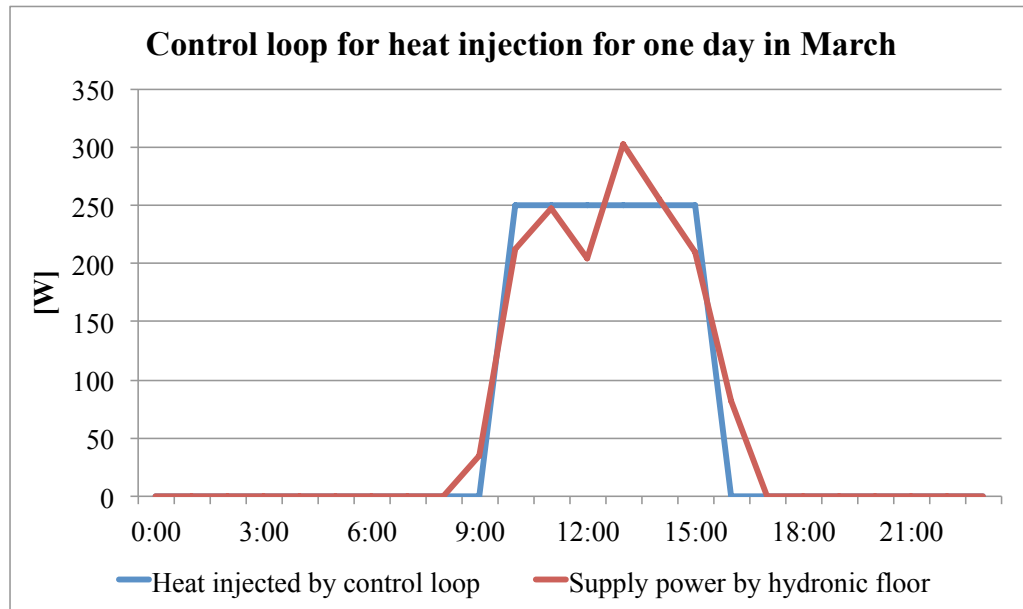


Figure 12-1: Control loop for heat injection

The red line is heat supply from the hydronic floor if the solar heating system is operating. The blue line is a calculated average equivalent amount of electrical heat injected to zone air in period 2.

4. To direct the heat to the zone air, the sensor is set to *senses dry bulb temperature*, and the actuator is set to *air point in zone*.
5. The control law for periods 1 and 3 is set to *free floating*, and period 2 is set to *basic controller for heating/cooling* (Figure 12-2) to obtain the heating pattern shown in Figure 12-1.

```

control law (indented=old or obscure)
a Basic controller for heating/cooling
b Free-float controller
c Basic pre-heat or pre-cool controller
d Fixed heat injection and extraction
e PID control action for heating/cooling
f Flux connection between zone & plant
g Multi-stage control with hysteresis
h CAV variable supply T with constraints
i Heat pipe from `outside` to inside
j Separate flux ON & OFF set points
k Match sensed/recorded value (ideal)
l Match sensed/recorded value (on/off)
m Time-proportioning separate (on/off)
n Floating `three-position` control
o Optimum start (with rewind) control
p Optimum stop control
q Fuzzy Logic PI-PD control
r Null controller.
s Multi-sensor heating/cooling
t Evaporative source (surface)
u Slave Capacity Controller
v VAV cooling with CAV reheat (BETA)
w Match sensed values (ideal;2 setpoints)
x Adaptive human comfort model

-----
? help
- exit this menu

```

Figure 12-2: Control law

6. Zone control period data is defined for the basic controller (Figure 12-3). Since the heat injection is a constant value during a given time period per day, both maximum and minimum heating capacity is set to the calculated supply power per day for the given month (250 W per day in March, as seen in Figure 12-1 and Figure 12-3). No cooling is requested so cooling capacities are set to zero. The heating set point is set to a temperature that will most likely never occur (100 °C in Figure 12-3) to assure that heat is being injected regardless of high temperatures in the zone. The cooling set point is also set to 100 °C to make sure that there is no cooling unless the zone temperature reaches 100 °C which most likely will never happen.

```

Zone control period data

Loop 2 day type: 3 period: 2
Sensed & actuated property is...
db temp > flux

-----
1 Starting at: 11.000
2 Law: basic control
a Choose parameter to edit:
b Maximum heating capacity (W)      : 250.0
c Minimum heating capacity (W)     : 250.0
d Maximum cooling capacity (W)      : 0.0
e Minimum cooling capacity (W)     : 0.0
f Heating setpoint (C)             : 100.000
g Cooling setpoint (C)            : 100.000
h
i
j
k
l RH control >> OFF                : 0.0

-----
+ Shift to earlier or later period
! List details
? Help
- Exit

```

Figure 12-3: Zone control period data

7. During the months when the solar heating system is in operation, the electrical control loop is set to *free floating*, which means that there is no heat injection to zone air during this period.
8. The last step that needs to be done to have a functioning control loop is to *link loop to zone*. The loop will be linked to 0_intzone and 1_intzone in two separate simulations to see which of the two gives the best result. Figure 12-4 shows two building zone control loops. Control loop 2 has five periods of validity, four for each of the first four months where heat is injected directly to zone air, and one for the rest of the year where the zone control is set to *free floating* and the plant control (solar heating system) is on.

```

Controls
a control focus >> zones
b description; no overall control descript
c description; no zone control description
  loops      : 2
d link loops to zones

-----
cntl| sensor |actuator|   day   | valid | periods
loop|location|location|  type   | during| in day
e  1 7 0 0 7 8 2 all daytypes  1 365  1
f  2 6 0 0 6 0 0 all daytypes  1  31  3
g                               all daytypes 32  59  3
h                               all daytypes 60  90  3
i                               all daytypes 91 120  3
j                               all daytypes 121 365  1
-----

+ add/delete/copy control loop
! list or check current control data
> save control data
? help
- exit this menu

```

Figure 12-4: Zone controls

13 Simulations

13.1 Model inputs for the solar heating system components

13.1.1 Solar collector inputs

Table 13-1: Solar collector inputs

Parameter	Symbol	Value
Collector area [m ²]	A	2/4
Collector efficiency [-]	η	0.677
Heat loss coefficient 1 [-]	a_1	2.380
Heat loss coefficient 2 [-]	a_2	0.027
Collector mass flow rate [kg/s]	m	0.02/0.04 (depending on collector area)
Heat capacitance of test fluid [J/kgK]	c_p	3600
Collector slope (deg. from horizontal)	α	70/90
Collector azimuth (deg., N=0, E=90)	β	180
Mass fraction of propylene glycol (%)	-	50

The first four parameters are based on a flat plate solar collector data sheet from Djurs Solvarme [39] with a collector area of 2 m². The collector mass flow rate depends on the collector area and is calculated using the following equation:

$$\dot{m} = \frac{Q_{useful}}{c_p * \Delta T} \quad (13-1)$$

where ΔT (K), is the temperature difference between the inlet and outlet of the solar collector, set to 10 K [11], and Q_{useful} (W) is the useful heat output of the solar collector with a tilt angle of 70 ° and a collector efficiency of 68 %. Q_{useful} is calculated using equation (13-2):

$$Q_{useful} = I_{max,70^\circ} * A * \eta = 680 W \quad (13-2)$$

where $I_{max,70^\circ}$ (W/m^2), is the maximum irradiation per m^2 . assumed to be $500 \text{ W}/\text{m}^2$ for Östersund [40]. The resulting mass flow rate is calculated to $0.01889 \text{ kg}/\text{s}$, and rounded up to $\dot{m} = 0.02 \text{ kg}/\text{s}$.

With a 50/50 mixing ratio of glycol and water, the working fluid will have its freezing point at $-34 \text{ }^\circ\text{C}$ (see Table 6-1). A 40/60 mix could alternatively be used. The freezing point would then be at $-22 \text{ }^\circ\text{C}$. The heat capacity of the working fluid is set to $3600 \text{ J}/\text{kgK}$, based on a 50/50 glycol water mixture [28].

The collector slope from the horizontal and orientation are set to 70 ° and 180 ° respectively based on recommendations from The Spanish Technical Building Code [41]. According to The Spanish Technical Building Code, the optimal orientation is considered to be south (180 °), and the optimal tilt depends on the period of use and is chosen depending on the following scenarios:

- Annual constant demand: tilt = the geographical latitude
- Preferred demand in winter: tilt = the geographical latitude + 10 °
- Preferred demand in summer: tilt = the geographical latitude - 10 °

Östersund is located at latitude 63.18 ° north, and hence the optimal collector slope is approximately 73 ° if winter demand is prioritized, and 53 ° if summer demand is prioritized. A collector slope of 70 ° is chosen to utilize solar contributions during late fall and winter. In addition, a collector placed at such a steep slope, is less likely to be covered by snow during the winter. The model will also be tested with a collector slope of 90 ° .

13.1.2 Pump inputs

Table 13-2: Pump inputs

Parameter	Symbol	Value
Total mass [kg]	m	5
Specific heat capacity [J/kgK]	c_p	2250
UA pump [W/K]	UA	0
Absorbed power [W]	P_{el}	25
Volume flow rate [m ³ /s]	\dot{v}	0.00002/0.00004 (depending on collector area)
Pump efficiency [-]	η_{pump}	0.04

The total mass and specific heat capacity is collected from a model exemplar in ESP-r, *system2_water_glycol*. Heat transfer from the pump to surroundings is assumed negligible. The pump efficiency of small pumps (<100 W) is normally in the range 2-7 % [42] and is set to 4 %. The necessary pump power is calculated based on some rules of thumb for pressure losses. For solar heating systems with collector area smaller than 10m² and total pipe length less than 50m, the pressure loss Δp (Pa) in the solar collector and the remaining solar circuit is assumed not to exceed 0.2x10⁵ Pa and 0.3x10⁵ Pa respectively [42]. With these assumptions considered, the necessary size of the pump is calculated to be 25 W, from equation (13-3).

$$P_{el} = \frac{\dot{v} * \Delta p}{\eta_{pump}} = \frac{(2.0 * 10^{-5}) * (5 * 10^5)}{0.04} = 25 W \quad (13-3)$$

13.1.3 Hydronic floor inputs

Table 13-3: Hydronic floor inputs

Parameter	Symbol	Value
Number of circuits [-]	-	1
Inside diameter of pipe [m]	d_i	0.017
Outside diameter of pipe [m]	d_o	0.020
Pipe spacing [m]	l	0.200
Thermal conductivity of pipe material [W/mK]	k	0.380
Served zone number [-]	-	3
Zone surface number [-]	-	6
Injection node number [-]	-	10

The pipe diameter and pipe spacing is chosen based on recommendations from SINTEF Byggforsk Project Report 39, *Project guide – Simplified system for waterborne heating of residential buildings* (Prosjektveileder – Forenklet anlegg for vannbåren oppvarming av boliger) [43]. The thermal conductivity of the pipe material is collected from the components database in ESP-r. The served zone number is zone number 3: 0_intzone. The zone surface number is surface 6: floor in 0_intzone. The injection node number is 10: layer 10 within floor (concrete slab) in 0_intzone.

13.1.4 Electrical control loop inputs

The table below shows the calculated electrical heat injection for each month and the time period of heat injection for the electrical control loop for Östersund. The electrical heat injection per month is calculated based on what the hydronic floor would supply if the solar heating system was in operation.

Table 13-4: Electrical control loop inputs

Period	Month	Time interval	No of hours	Heat injection [W]
1	Jan	1230-1330	1	110
2	Feb	1100-1500	4	143
3	Mar	1000-1600	6	257
4	Apr	0830-1630	8	250

13.2 BASESIMP inputs

The basement zone below the building, together with the concrete slab are modeled to represent thermally massive ground conditions surrounding the entire building. The model accounts for foundation heat loss and it enables approximated heat loss calculations through the slab. The inputs for the chosen BASESIMP configuration BCIB_6 (explained in Section 8.2.1) are shown in Table 12-4.

Table 13-5: Inputs for BASESIMP configuration BCIB_6

	Input
Height	2 m
Width	8.6 m
Length	8.6 m
Depth	1.9 m
Overlap	0 m
Insulation	2.8 m ² K/W
Soil conductivity	1.9 W/mK
Water table	8 m
TG _{avg}	Set by Moore method
TG _{amp}	Set by Moore method
TG _{ps}	Set by Moore method

The geometric inputs for the BASESIMP configuration are based on the geometry of the basement zone. The basement is defined to be submerged 1.9 m below ground level and the insulation is determined from the materials used in the basement walls. The soil conductivity is set based on the thermal conductivity of rock such as granite,

which is assumed to surround the leisure home. The water table is set to 8 m below the basement zone, which means 9.9 m below ground level. The reason for this is that at around 10 m depth into the ground, the soil temperatures are considered close to stable throughout the year.

Heat transfer is calculated quasi 3-dimensionally between the basement zone and the surrounding ground. BASESIMP does not take storage into account, and therefore the storage is calculated as stored heat in the concrete slab.

13.3 Start-up days

Start-up days is an important simulation parameter that should be given attention when looking at thermal performance in buildings. Start-up days are included in the model to account for previous climatic conditions in the ground. Thermal mass in the ground uses a significant amount of time to be heated and cooled, and to represent this thermal inertia, several start-up days should be included. Ideally, start-up days should represent 1-3 years, to obtain stable conditions in the ground. However, ESP-r allows a maximum of 100 start-up days and therefore this will be used in the simulations.

13.4 Climate

When analyzing the energy demand for a building, one of the most important factors to consider is climatic conditions at the location of the building. Statistics from climate databases can provide historical information about ambient temperatures, which can be used to estimate the heating demand. An issue in the design process is whether to design the system for the average heating demand over a year, the heating demand in a typical winter month, or for the extreme winter month. In this report the main issue is to keep sanitary installations frost proof throughout the year, so for this case the design point should be the extreme winter month with very low ambient temperatures that may not occur every year, but possibly every 5-10 years.

The leisure home is designed to fit the location of the southern mountain regions in Norway. In ESP-r there is no available climate data for this exact area, but climate data from Östersund, Sweden is a good approximation and available in ESP-r. In

addition, the model will be tested with climate data from Fornebu, Norway. Figure 13-1 shows the locations of Fornebu and Östersund.

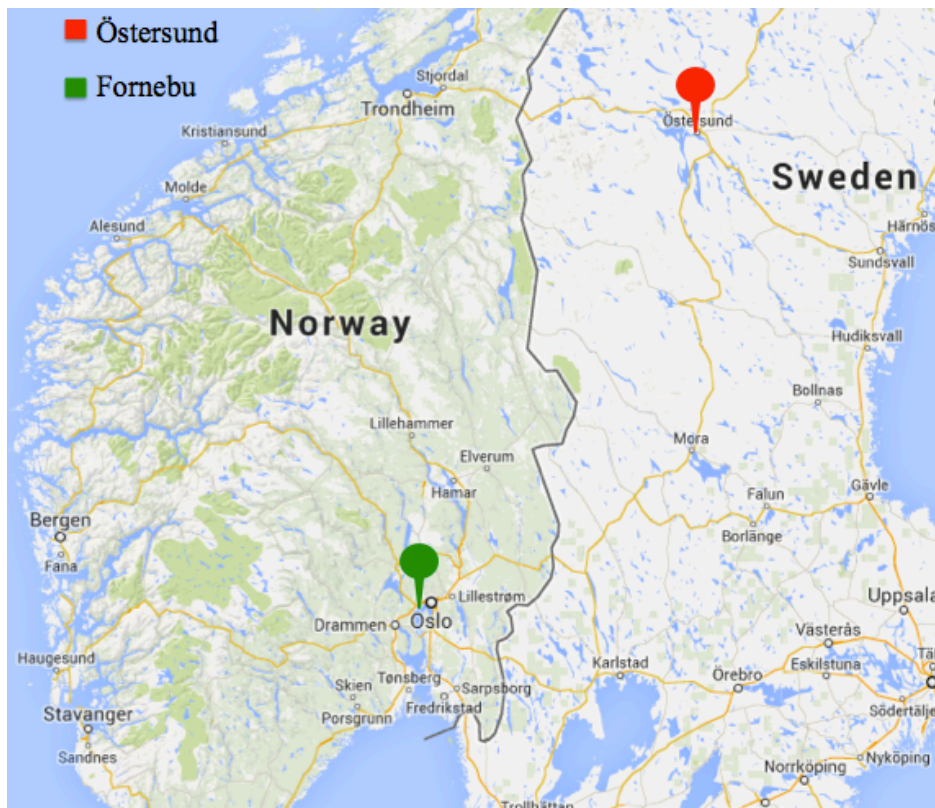


Figure 13-1: Map showing Fornebu and Östersund [44]

13.4.1 Östersund climate data

Östersund is located at a latitude of 63.18° north and longitude of 14.67° east at an elevation of 312 meters above sea level. The location is a typical inland mountain area. Figure 13-2 shows average dry bulb temperatures over a year and Figure 13-3 shows incoming direct- and diffuse radiation on a horizontal plate over a year in Östersund. The data is collected from the climate file in ESP-r as average hourly values.

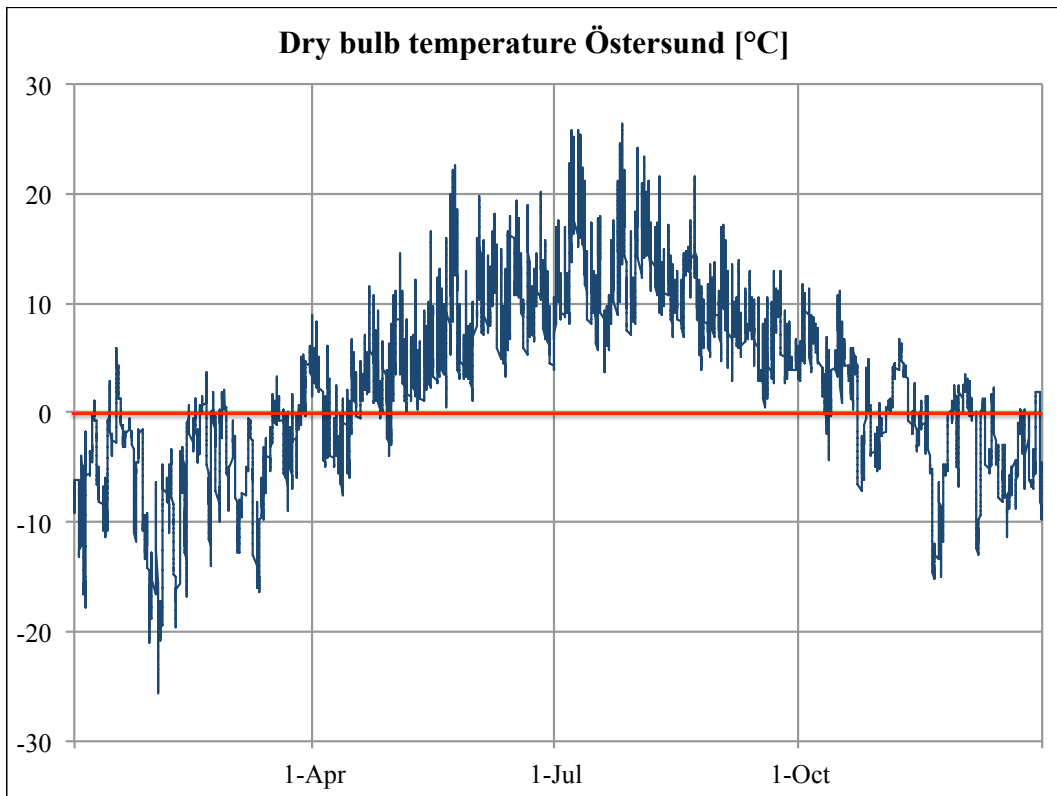


Figure 13-2: Dry bulb temperature Östersund

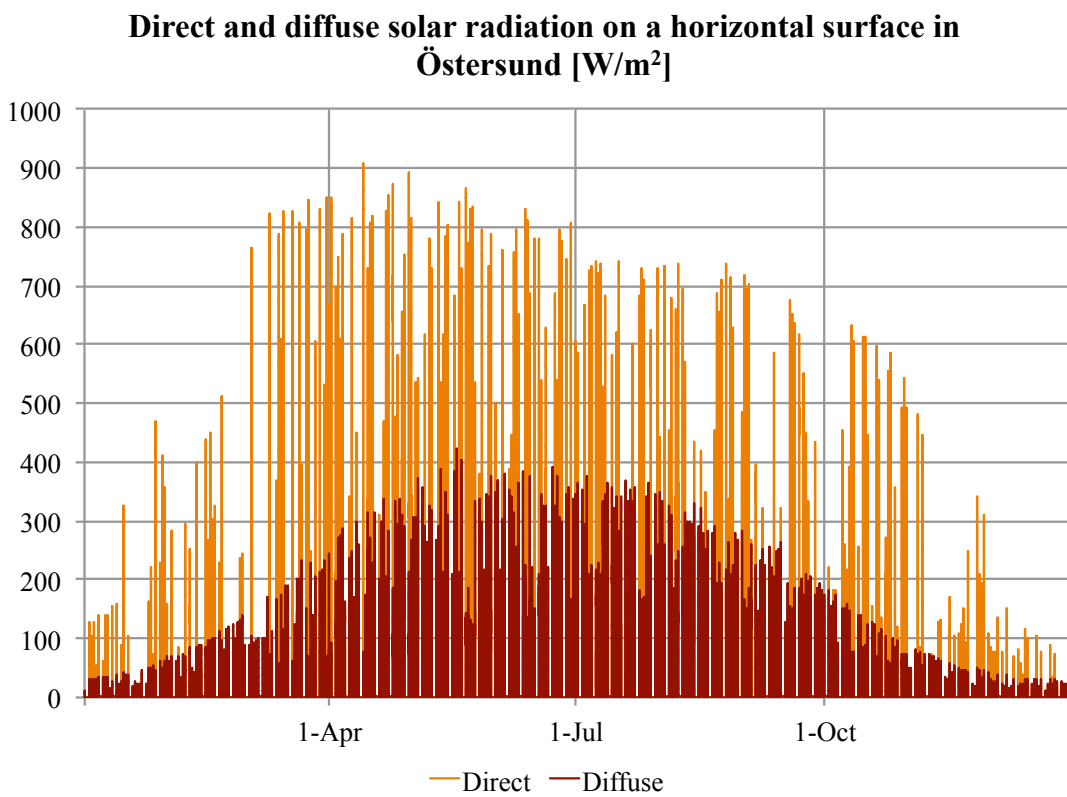


Figure 13-3: Direct and diffuse solar radiation Östersund

13.4.2 Fornebu climate data

Fornebu is located at a latitude of 59.88 ° north and longitude of 10.62 ° east at 11 meters above sea level. Fornebu is a peninsular area located in a suburban municipality bordering western parts of Oslo and has typical coastal climate for the southern parts of Norway. Annual average dry bulb temperatures and direct- and diffuse radiation on a horizontal plate can be seen in Figure 13-4 and Figure 13-5 respectively. The amount of incoming solar radiation is greater in Fornebu than in Östersund and the dry bulb temperatures are slightly higher throughout the year in Fornebu.

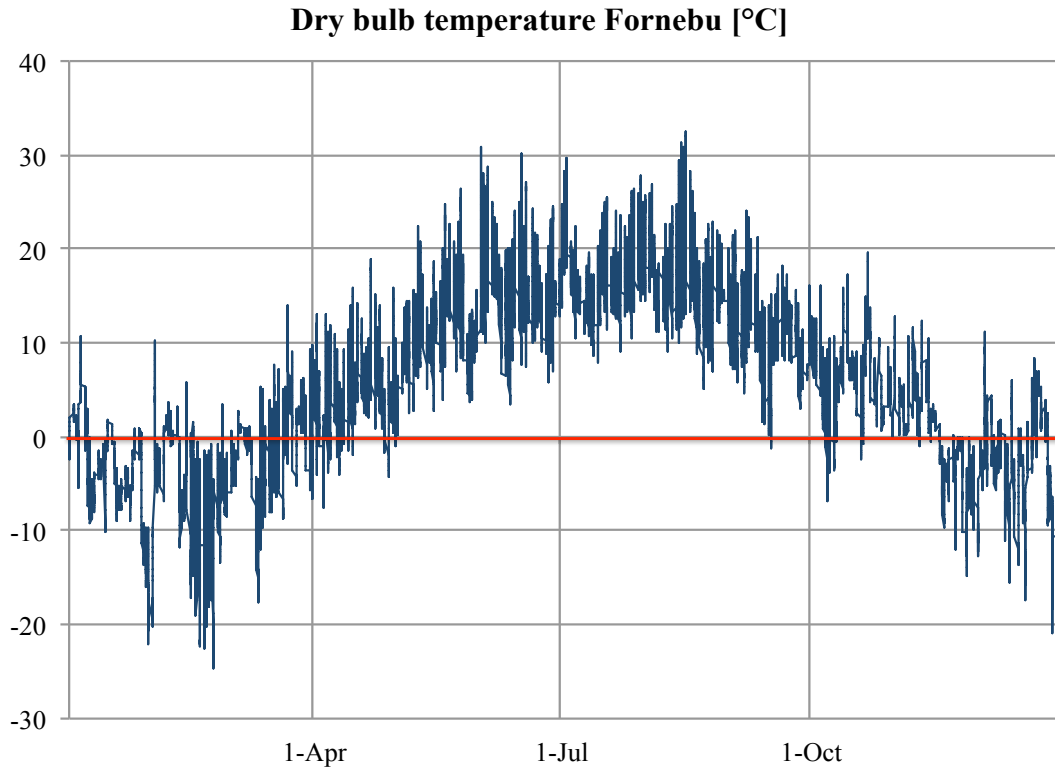


Figure 13-4: Dry bulb temperature Fornebu

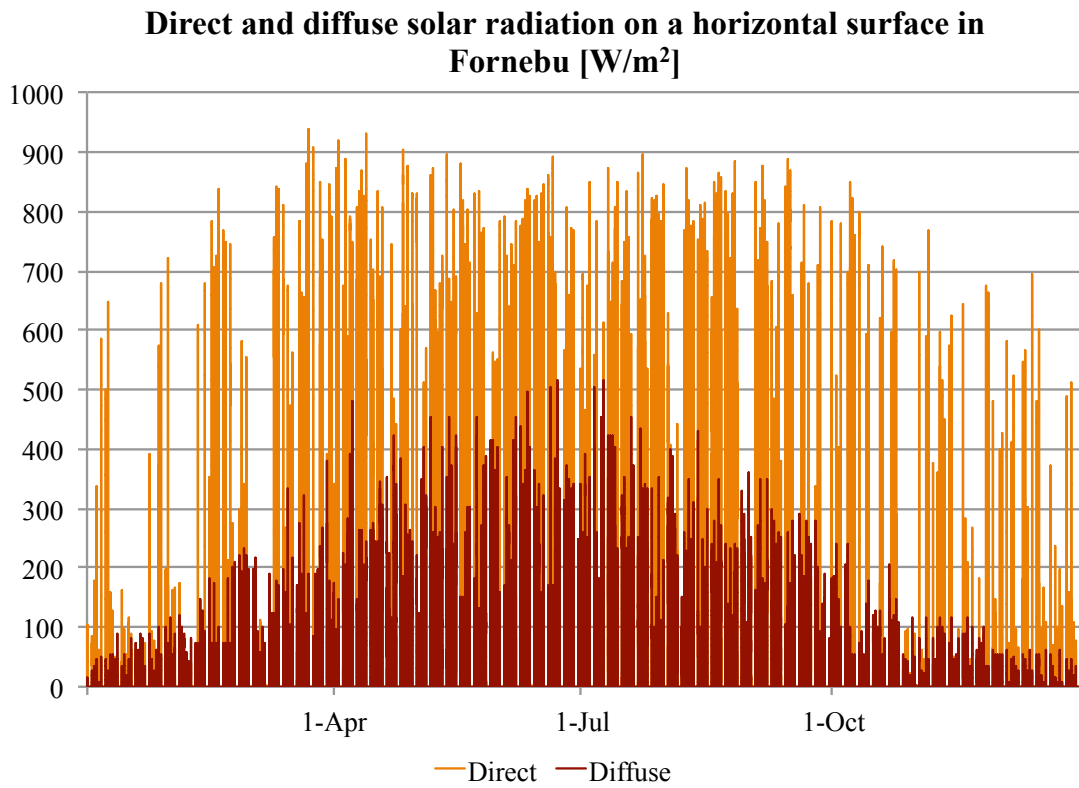


Figure 13-5: Direct and diffuse solar radiation Fornebu

14 Results and discussion

Different aspects have been looked at with regard to the solar heating system and the potential for seasonal heat storage in the different simulations. The collector area and slope have been studied, along with available thermal mass and point of heat injection. The building structure, materials and constructions used are presented in Chapter 4. Inputs for the plants and systems network are given in Section 13.1. The tables below summarize the Case simulations that will be presented in this chapter for Östersund and Fornebu respectively.

Table 14-1: Simulations with Östersund climate data

Case	Collector area [m ²]	Collector tilt [°from horizontal]	Concrete slab construction	Point of heat injection	Time period
1	-	-	Heavy mix	-	Jan-01 to Dec-31
2	-	-	Massive	-	Jan-01 to Dec-31
3a	2	70	Massive	Hydronic floor	Jan-01 to Dec-31
3b	4	70	Massive	Hydronic floor	Jan-01 to Dec-31
3c	2	90	Massive	Hydronic floor	Jan-01 to Dec-31
4	2	70	Massive	0_intzone	Jan-01 to Apr-30
				Hydronic floor	May-01 to Dec-31
5	2	70	Massive	0_intzone	Nov-01 to Apr-30
				Hydronic floor	May-01 to Oct-31
6	2	70	Massive	1_intzone	Jan-01 to Apr-30
				Hydronic floor	May-01 to Dec-31
7a	2	70	Heavy mix	1_intzone	Jan-01 to Apr-30
				Hydronic floor	May-01 to Dec-31
7b	4	70	Heavy mix	1_intzone	Jan-01 to Apr-30
				Hydronic floor	May-01 to Dec-31

Table 14-2: Simulations with Fornebu climate data

Case	Collector area [m ²]	Collector tilt [°from horizontal]	Concrete slab construction	Point of heat injection	Time period
8	-	-	Massive	-	Jan-01 to Dec-31
9	2	70	Massive	1_intzone	Jan-01 to Apr-30
				Hydronic floor	May-01 to Dec-31
10	4	70	Heavy mix	1_intzone	Jan-01 to Apr-30
				Hydronic floor	May-01 to Dec-31

The main goal is to obtain frost proof conditions within the internal zones, as this is where the sanitary installations are deemed installed. These zones together with the basement zone will therefore be emphasized when presenting the results. Results will be evaluated against SINTEF's minimum recommendation of 10 °C inside leisure homes.

Section 14.3 will present the operation of the solar heating system. Delivered energy from the solar heating systems for Östersund and Fornebu are shown in section 14.4, and energy balances for the concrete slab and the basement zone will be presented in section 14.5.

In version 11.11 of ESP-r the x-axis can only be presented in terms of hours and not weeks or months. Table 14-3 shows the dates equivalent to the hours shown on the x-axis in the temperature graphs.

Table 14-3: Time axis dates

Hour	Day number	Date
0	1	1-Jan
840	35	4-Feb
1680	70	11-Mar
2520	105	15-Apr
3360	140	20-May
4200	175	24-Juni
5040	210	29-Jul
5880	245	2-Sep
6720	280	7-Oct
7560	315	11-Nov
8400	350	16-Dec

14.1 Case simulations with Östersund climate data

14.1.1 Case 1

In the first simulation the concrete slab has the thermal properties of the material *heavy mix concrete*. The simulation is presented to get a comparison to the cases with *massive concrete* thermal properties. The zone dry bulb temperatures with the given ground conditions and with no heat injection are shown in Figure 14-1.

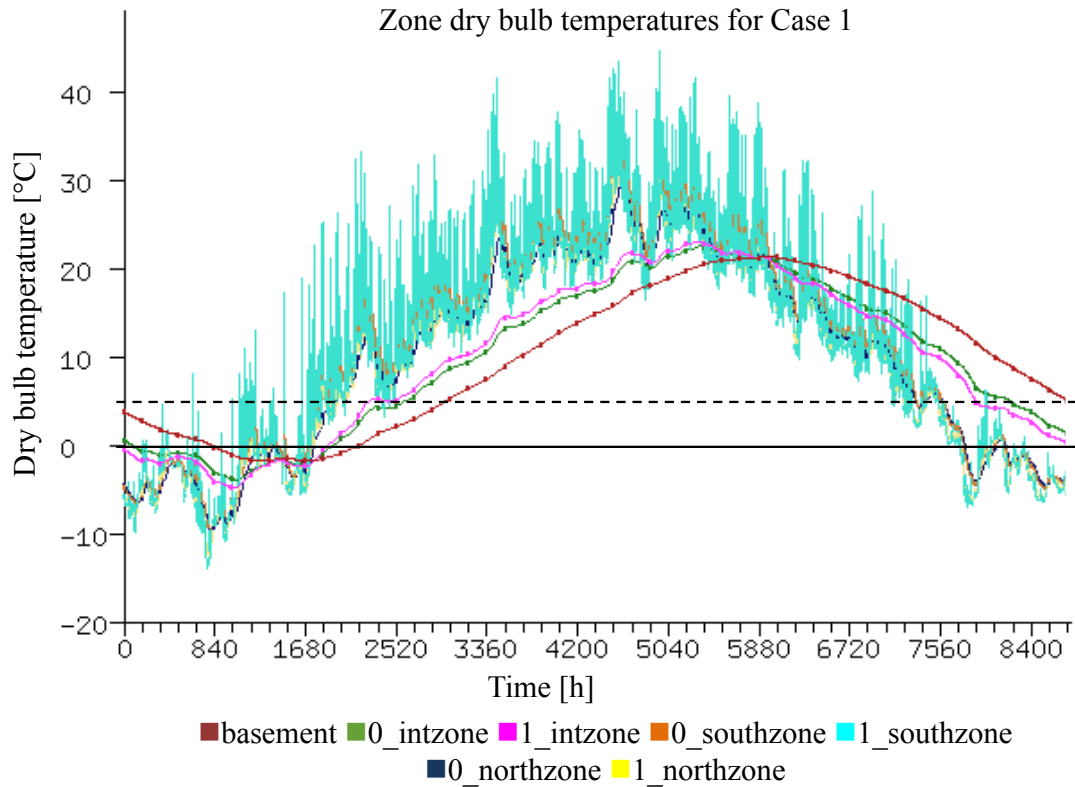


Figure 14-1: Dry bulb temperatures for Case 1

The temperatures in the basement and the well-insulated internal zones do not vary as frequently over the year as that of the outer zones. The outer zones are more affected by ambient temperature as these have surfaces adjacent to ambient air. 1_southzone has the most sudden temperatures variations. This is because this zone has a large window facing south and is therefore more affected by passive solar heat and ambient temperatures than the surrounding zones. With the given ground conditions, and no heat injection, frost proof conditions throughout the year are not obtained for any of the zones. The minimum and maximum temperatures occurring in the internal zones and the basement can be seen in Table 14-4 for Case 1. The percentage of hours in a year where the temperature falls below 0 °C is also shown.

Table 14-4: Peak values for Case 1

	Maximum		Minimum		% of hours below 0°C
	value [°C]	date	value [°C]	date	
basement	21.42	7-Sep	-1.56	14-Mar	15%
0_intzone	22.61	11-Aug	-3.76	13-Feb	21%
1_intzone	23.16	10-Aug	-4.6	13-Feb	22%

14.1.2 Case 2

In Case 2, the concrete slab has the thermal properties of the material *massive concrete*. The concrete slab was created to imitate thermally massive ground conditions surrounding the leisure home. Figure 14-2 shows dry bulb temperatures in the different zones over a year with no heat injection for Case 2.

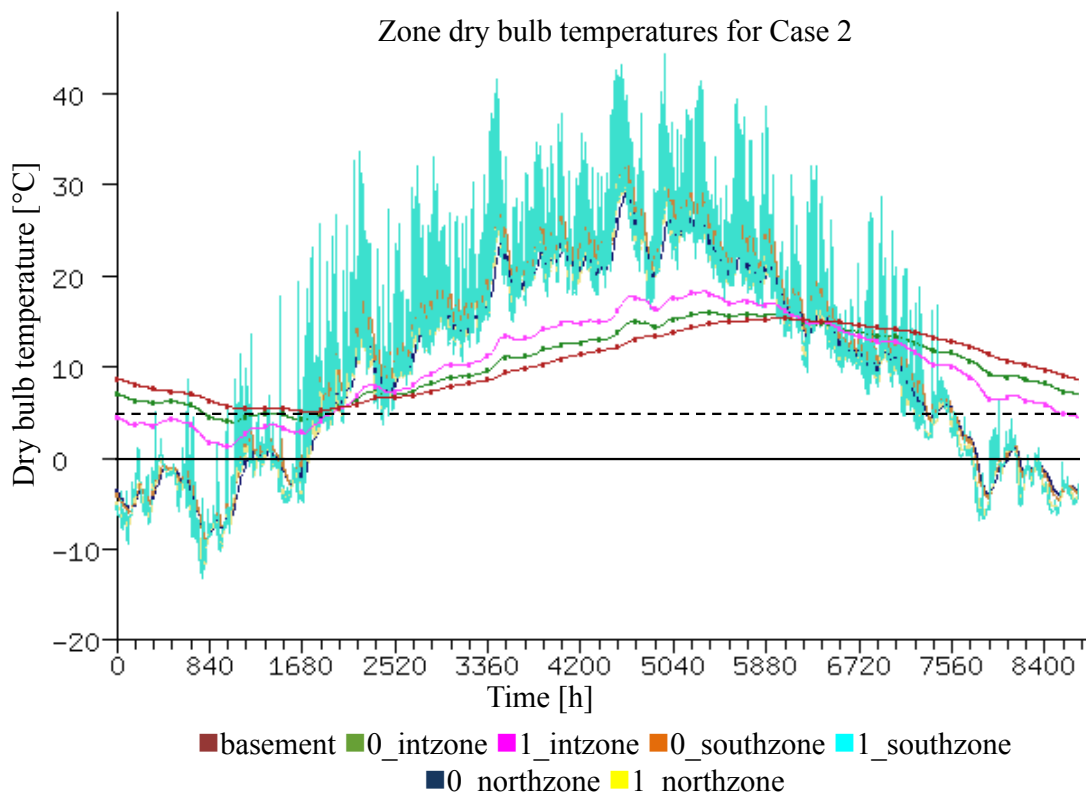


Figure 14-2: Dry bulb temperatures for Case 2

The temperatures in the internal zones and the basement are significantly higher during the winter in Case 2 than in the previous case. The temperature profiles for the outer zones however, are almost the same as for Case 1. These zones are a lot less influenced by the thermal mass in the ground, and depend more on ambient

conditions. Minimum and maximum temperatures for the internal zones and the basement are presented in Table 14-5 for Case 2. The maximum temperature in 0_intzone is 22.61 °C in Case 1, and 15.88 °C in Case 2, both occurring on August 11th. The concrete slab in Case 2 has a larger storage capacity because of the high thermal resistance. Less heat from the slab is released to the leisure home during the summer, and more is stored below ground level and available for extraction during the winter.

Table 14-5: Peak values for Case 2

	Maximum		Minimum		% of hours	
	value [°C]	date	value [°C]	date	below 5°C	below 0°C
basement	22.5	7-Sep	0.02	19-Feb	32%	0%
0_intzone	15.88	11-Aug	4.61	13-Feb	3%	0%
1_intzone	18.24	10-Aug	1.75	11-Feb	25%	0%

The table shows that the basement and the internal zones are frost proof throughout the year with the given ground conditions. However with minimum temperatures ranging from approximately 0-5 °C, there is still a risk that frost could occur on extremely cold days. In addition, the minimum temperatures are significantly lower than SINTEF's recommendation of minimum 10 °C.

14.1.3 Case 3

The potential for raising the minimum temperatures by using an active solar heating system has been evaluated. In Case 3, heat from the solar heating system is injected into the concrete slab in the ground floor of 0_intzone. The hydronic floor component is placed in a layer in the concrete slab, 0.15 m from the zone. This means that there are 1.35 m of *massive concrete* below the layer of heat injection representing thermal mass surrounding the leisure home.

Case 3a: Collector area of 2 m² placed at a 70 ° angle from the horizontal

In Case 3a the simulation is done with a collector slope of 70 ° and a collector area of 2 m². Dry bulb temperatures for the internal zones and the basement are shown in Figure 14-3. Table 14-6 shows peak values for Case 3a.

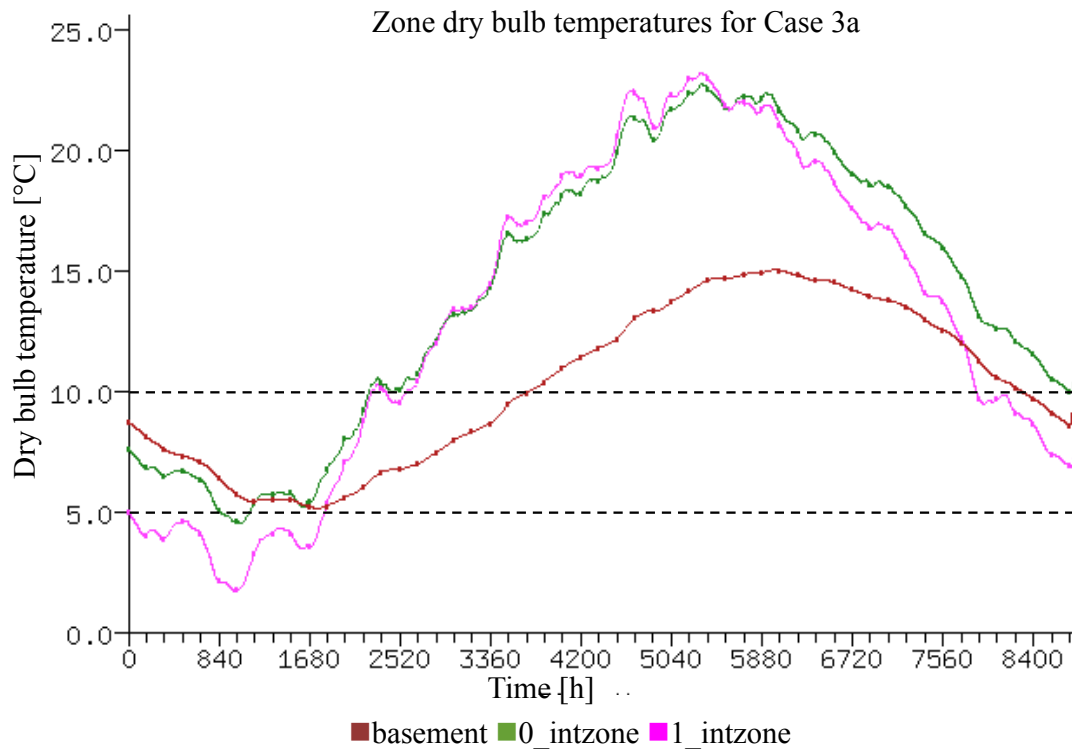


Figure 14-3: Dry bulb temperatures for Case 3a

Table 14-6: Peak values for Case 3a

	Maximum		Minimum		% of hours	
	value [°C]	date	value [°C]	date	below 10°C	below 5°C
basement	15.08	7-Sep	5.2	15-Mar	48%	0%
0_intzone	22.78	11-Aug	4.59	13-Feb	26%	3%
1_intzone	23.26	10-Aug	1.78	11-Feb	38%	21%

Table 14-6 shows the percentage of hours in a year when the temperatures fall below 5 and 10 °C for the different zones. The three zones are, as for Case 2, above 0 °C throughout the year. However the potential to further increase the temperatures should be considered, as both the internal zones fall below 5 °C. Compared to Case 2, the minimum temperatures in 0_intzone and 1_intzone are almost the same as for Case 3a, all occurring in February. The heat contribution from the hydronic floor to the concrete slab in February seems to have almost no effect on the temperature inside the internal ground floor zone. The reason for this may be a combination of the lack of incoming solar radiation in February, and the high thermal resistance in the ground

impeding heat transfer through the floor. Case 4 will investigate the effect of injecting heat directly to zone air in 0_intzone instead of to the hydronic floor for selected months.

Case 3b: Collector area of 4 m² placed at a 70 ° angle from the horizontal

A simulation was run with the same model as for Case 3a, but with a collector area of 4 m² to see whether doubling the collector area would have an impact on the minimum temperatures. The graph below shows the dry bulb temperatures throughout the year with a collector area of 4 m².

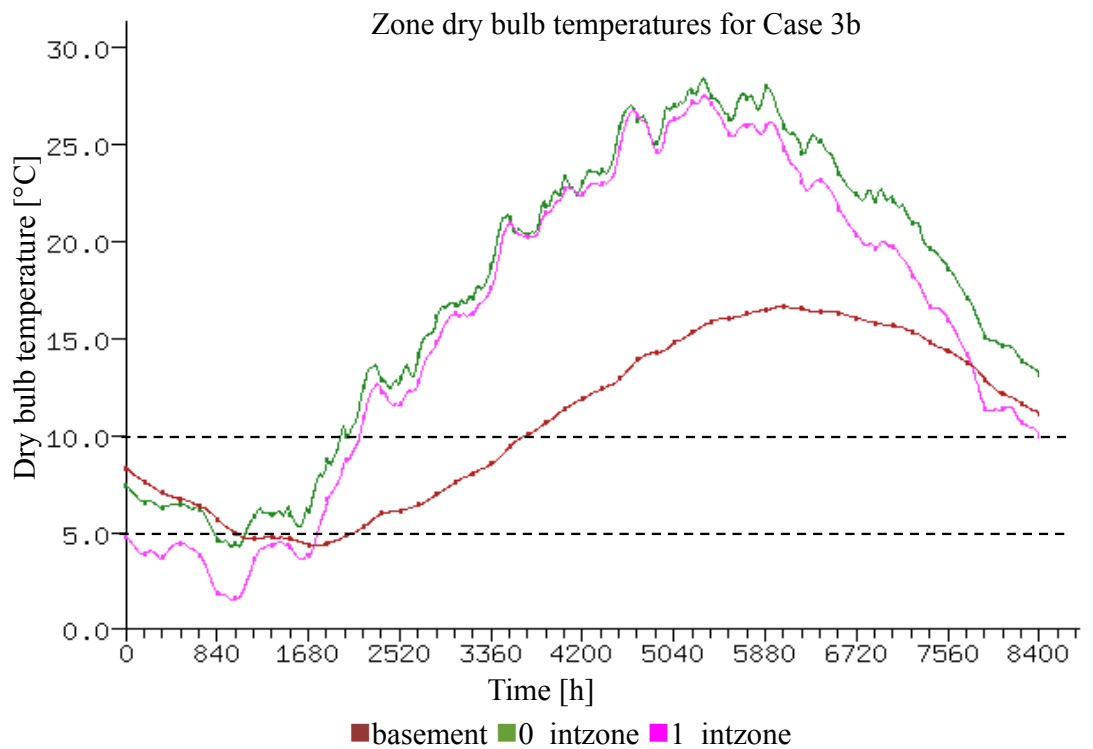


Figure 14-4: Dry bulb temperatures for Case 3b

The minimum temperatures in the internal zones and the basement for Case 3b (Table 14-7), are almost the same as for the case with a collector area of 2 m². The maximum temperatures however, are more affected by doubling the collector area and are significantly higher in Case 3b than Case 3a. More heat is collected during spring and summer, but due to limited irradiance from November to February and low ambient temperatures, it seems that the storage capacity is almost “used up” in February, even with a collector area of 4 m². In December, the temperatures are noticeably higher in Case 3b than Case 3a, but in the second week of February they are almost equal. It is

important to note here, that with only 100 start-up days, stable conditions are not obtained. This can clearly be seen in Figure 14-4 because the temperature in the last day of December is significantly higher than in the first day of January. The same applies for Case 3a, but the temperature difference between December 31st and January 1st is larger in Case 3b, than 3a. With more start-up days, the minimum temperatures for both cases would most likely be higher and it is possible that Case 3b would experience higher minimum temperatures than Case 3a as a result of more solar energy collected during the summer. Because the maximum number of start-up days in ESP-r is 100, and doubling the collector area does not seem to affect the minimum temperatures with the given number of start-up days, most of the simulations will use a collector area of 2 m². The main goal is to maintain frost proof conditions throughout the year, not to achieve very high zone temperatures in the summer.

Table 14-7: Peak values for Case 3b

	Maximum		Minimum		% of hours below 5°C
	value [°C]	date	value [°C]	date	
basement	16.66	9-Sep	4.33	15-Mar	0%
0_intzone	28.47	10-Aug	4.26	13-Feb	3%
1_intzone	27.54	10-Aug	1.51	11-Feb	20%

Case 3c: Collector area of 2 m² placed at a 90 ° angle from the horizontal

In Case 3c, the solar collector is placed at a 90 ° angle from the horizontal. This is done to investigate if a steeper incline will lead to a larger heat contribution in Östersund during winter months when the sun is set lower on the horizon.

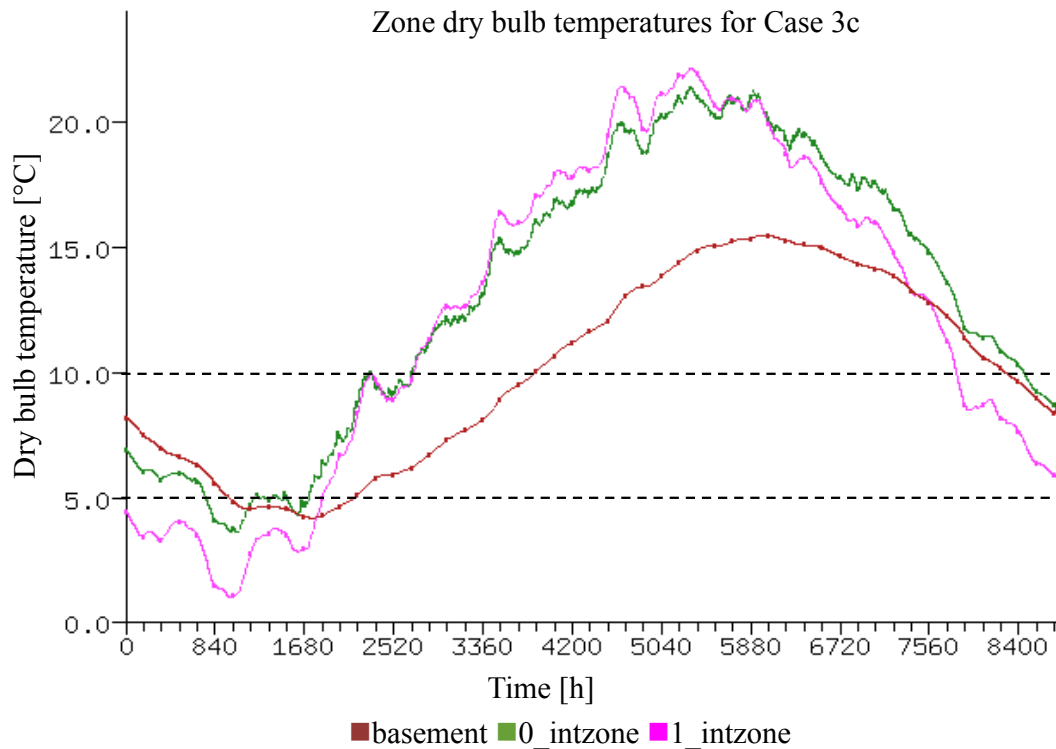


Figure 14-5: Dry bulb temperatures for Case 3c

Figure 14-5 shows that the minimum temperatures occurring in February are actually lower with a collector placed at 90 ° from the horizontal than at 70 °. The figure shows that throughout the winter months the temperatures are lower in Case 3c than in Case 3a. Because the sun is set higher on the horizon during the summer, more irradiance is collected with a collector placed at 70 ° than at 90 ° in the summer. This suggests that the minimum temperatures occurring in February are more affected by seasonal heat storage than by incoming radiation in the course of the month. A collector placed at 70 ° will be used in the rest of the cases.

14.1.4 Case 4

In Case 4, heat collected during the first four months will be injected directly to the internal ground floor zone. The solar heating system is a water-based heating system and a simplification is made in order to inject heat directly to zone air. Monthly average values of the heat contribution from the hydronic floor component from January 1st to April 30th for Case 3a have been calculated. The solar heating system is switched off during this period, and the calculated average equivalent amount of electrical heat is injected directly to zone air of 0_intzone as explained in Section 12.1. Four control loops were created, one for each month. The average heat input per day

was calculated based on monthly delivered energy from the hydronic floor divided by the number of supply hours from the hydronic floor per month. The supply hours are daily average values based on the hours per day when there exists a heat contribution from the hydronic floor to the concrete slab. The supply hours are related to the number of solar hours, but the solar heating system is not operating during all solar hours, as the pump is switched off whenever the difference between the solar collector temperature and the hydronic floor temperature is less than 5 °C. The electrical power inputs to the zone air heating control loop are presented in Table 14-8. The calculations resulting in Table 14-8 can be seen in Appendix B.3.

Table 14-8: Power input and time of heat injection from Jan-01 to Apr-30

	Monthly delivered energy from hydronic floor [Wh/month]	Supply hours from hydronic floor [h]	Average power input during supply hours [W]	Time period for heat injection per day
Jan	3408	31	110	1230-1330
Feb	15960	112	143	1100-1500
Mar	47880	186	257	1000-1600
Apr	60096	240	250	0830-1630

The annual dry bulb temperatures for the internal zones and the basement zone with this design solution are shown in Figure 14-6.

Zone dry bulb temperatures for Case 4

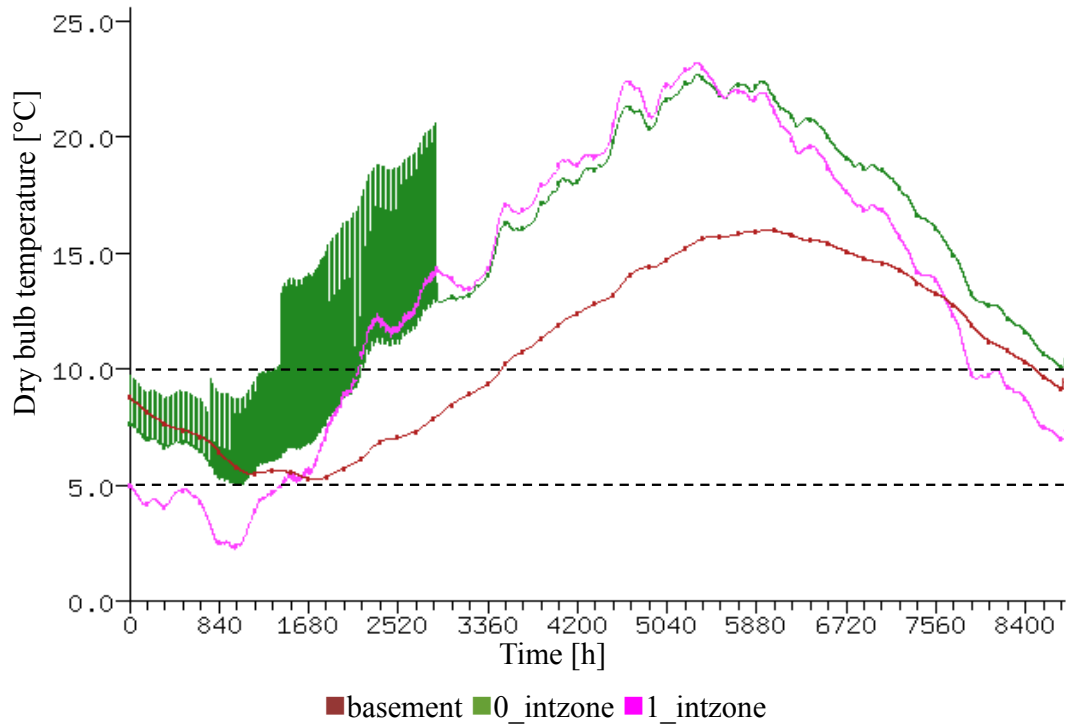


Figure 14-6: Dry bulb temperatures for Case 4

The temperature distribution from January to April in 0_intzone has larger variance in daily temperatures in this case compared to Case 3, since the heat is injected directly to the zone air. The average zone air temperatures for the first four months are higher in Case 4 than in Case 3. Figure 14-7 shows zone dry bulb temperatures based on average values per day instead of average values per hour as seen in Figure 14-6.

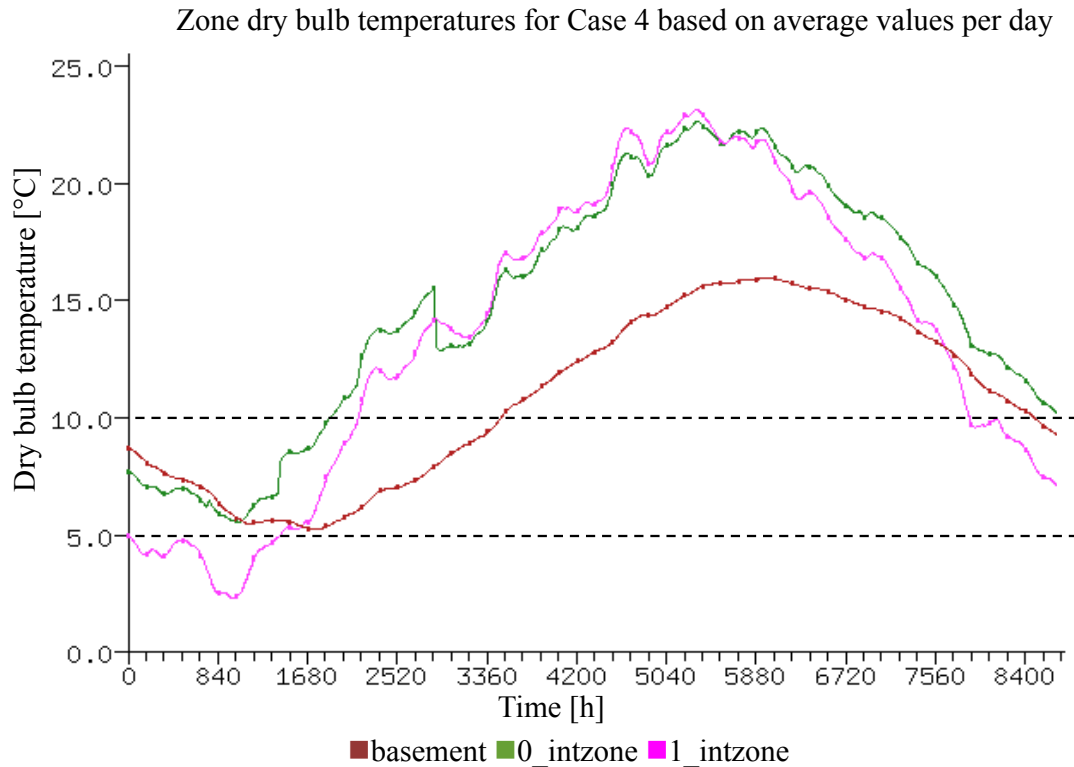


Figure 14-7: Dry bulb temperatures for Case 4, based on daily averages

Figure 14-7 shows that the daily average temperatures are higher from January to the end of April when available heat during this period is injected to zone air rather than to the hydronic floor, as in Case 3. This indicates that when solar irradiance is limited, it may be advantageous to inject heat directly to the room rather than through floor heating in order to utilize a small heating amount that would otherwise be “lost” in a large thermal mass. Table 14-9 shows peak values for Case 4. Here, both the basement zone and the internal ground floor zone hold temperatures above 5 °C throughout the year. The temperature in the internal first floor zone is below 5 °C during 16 % of a year, equivalent to approximately 58 days out of 365 days.

Table 14-9: Peak values for Case 4

	Maximum		Minimum		% of hours	
	value [°C]	date	value [°C]	date	below 10°C	below 5°C
basement	16.01	7-Sep	5.25	14-Mar	43%	0%
0_intzone	22.69	11-Aug	4.99	13-Feb	22%	0%
1_intzone	23.19	10-Aug	2.29	10-Feb	35%	16%

All the minimum temperatures are slightly higher in Case 4 than in Case 3, making Case 4 the best solution so far.

14.1.5 Case 5

Case 4 showed that injecting heat directly to zone air instead of via the floor is potentially a better solution to raise the minimum temperatures when the heat input is very limited. Case 5 is similar to Case 4, except the heat is in this case injected to zone air for a longer time period. Six control loops for each month from November 1st to April 30th are defined in Case 5. The control loop from January 1st to April 30th is the same as for Case 4. The additional control loop from November to December is shown in the table below. The calculation sheet is shown in Appendix B.3.

Table 14-10: Power input and time of heat injection from Nov-01 to Dec-31

	Monthly delivered energy from hydronic floor [Wh/month]	Supply hours from hydronic floor [h]	Average power input during supply hours [W]	Time period for heat injection per day
Nov	3384	150	23	0930-1430
Dec	144	31	5	1230-1330

The electrical power input is only 23 W in November and 5 W in December during the given time periods, supplying only 115 Wh and 5 Wh per day respectively. Figure 14-8 shows the zone dry bulb temperatures for Case 5.

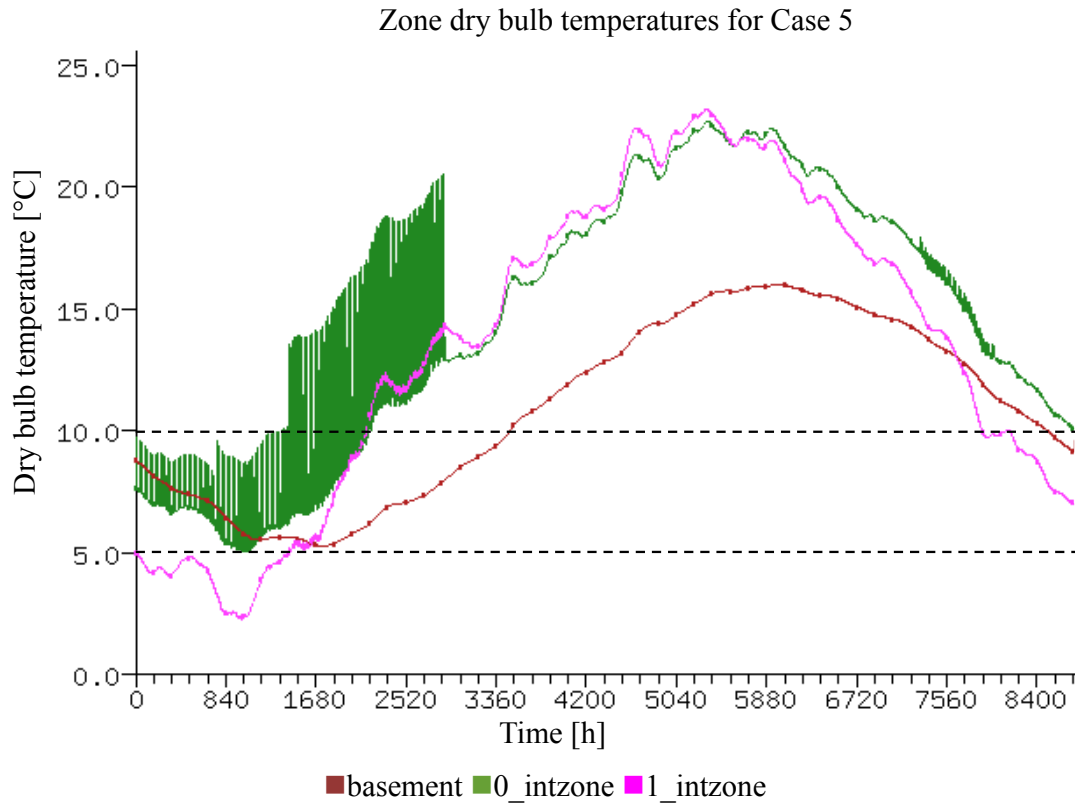


Figure 14-8: Dry bulb temperatures for Case 5

As expected, due to the limited delivered electrical heat supply in November and December, the graph is almost identical to Case 4 shown in Figure 14-6. The minimum and maximum temperatures (Table 14-11) are almost the same as for Case 4. This suggests that the zone temperatures in November and December are more a result of heat collected during the summer and late autumn, and less of heat collected during the two months. Hence, the zone temperatures during the last two months seem to be a consequence of seasonal heat storage in the concrete slab. Because injecting heat to zone air from November to December has almost no effect on the minimum temperatures, Case 5 will not be further pursued and Case 4 will still be used.

Table 14-11: Peak values for Case 5

	Maximum		Minimum		% of hours	
	value [°C]	date	value [°C]	date	below 10°C	below 5°C
basement	16.01	7-Sep	5.27	14-Mar	43%	0%
0_intzone	22.69	11-Aug	4.98	13-Feb	24%	0%
1_intzone	23.19	10-Aug	2.29	10-Feb	34%	16%

14.1.6 Case 6

Case 6 is based on the same principle as Case 4, except the heat injected to zone air from January 1st to April 30th is now injected to 1_intzone. The resulting dry bulb temperatures, based on average values per day, are shown in Figure 14-9.

Zone dry bulb temperatures for Case 6, based on average values per day

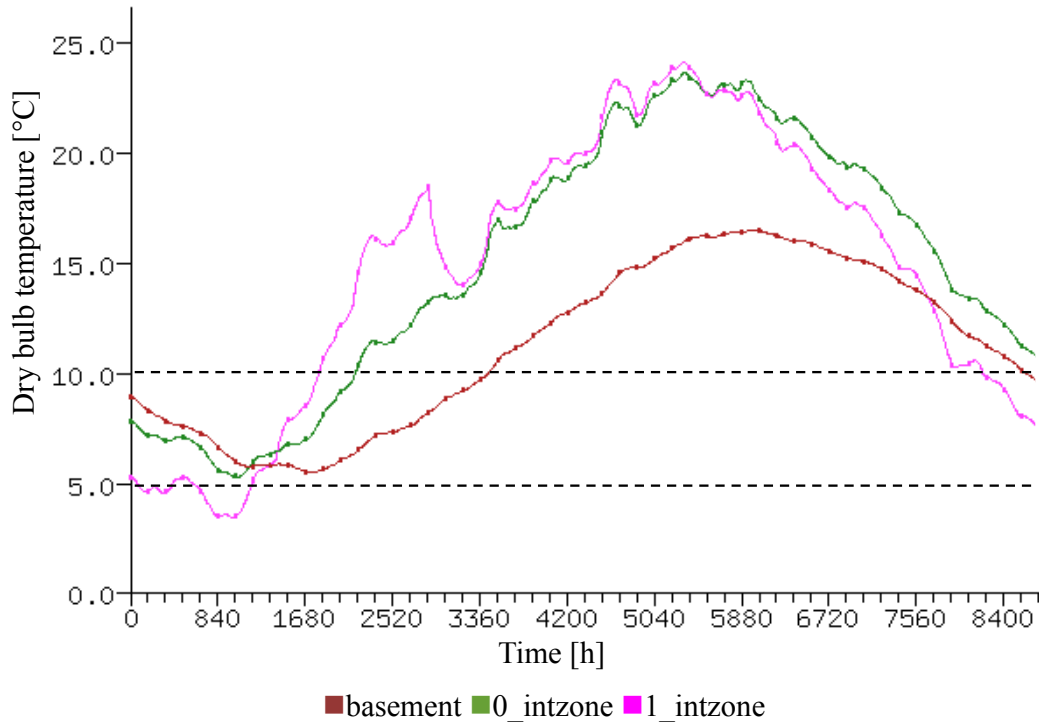


Figure 14-9: Dry bulb temperatures for Case 6, based on daily averages

Injecting heat to the internal first floor zone has a positive effect on the minimum temperatures. Compared to Case 4 where heat was injected to 0_intzone, the minimum temperatures for all zones are slightly higher in Case 6. Even 0_intzone has a higher minimum temperature when heat is injected to the floor above than directly to 0_intzone. This indicates that warming up the top floor reduces the heat loss from the bottom floor to the top. The maximum temperatures are also higher in Case 6.

Table 14-12: Peak values for Case 6

	Maximum		Minimum		% of hours	
	value [°C]	date	value [°C]	date	below 10°C	below 5°C
basement	16.52	7-Sep	5.52	15-Mar	41%	0%
0_intzone	23.72	11-Aug	5.29	13-Feb	25%	0%
1_intzone	24.19	10-Aug	3.10	11-Feb	27%	10%

Case 6 turns out with the best results out of the cases tested, maintaining frost proof conditions throughout the year in Östersund. The minimum temperature 3.10 °C and occurs in 1_intzone on February 11th. The minimum temperatures do not meet the recommendations from SINTEF of minimum 10 °C, but a safety margin of 3 °C is achieved and this might still be acceptable for a well-insulated zone. 0_intzone never falls below 5 °C and there is little risk that frost would occur in this zone.

14.1.7 Case 7

Case 7 presents simulation results for Östersund with “normal” thermal properties in the ground. The concrete slab now has the thermal properties of the *heavy mix concrete* construction. Case 7a has a collector area of 2 m² while Case 7b has a collector area of 4 m².

Case 7a: Collector area of 2 m²

The model from Case 6 is simulated with “normal” thermal properties in the concrete slab.

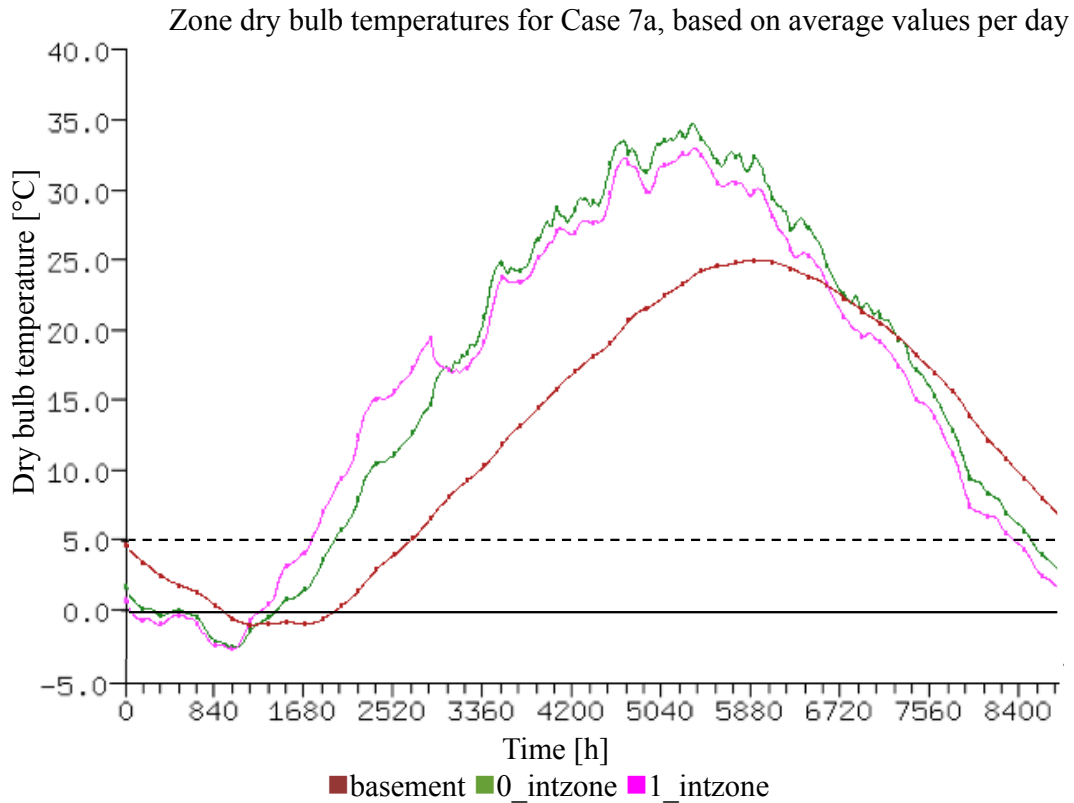


Figure 14-10: Dry bulb temperatures for Case 7a, based on daily averages

Figure 14-10 shows that the dry bulb temperatures fall below 0 °C at some point for all three zones with the given ground conditions. This shows that the heat storage capacity is much larger for Case 6 than for Case 7a as expected, resulting in more heat loss to the basement and surroundings. The temperatures during the summer are noticeably higher in Case 7a than in Case 6. Again, this is an indication that less heat is stored within the concrete slab, and more is released in all directions. Minimum and maximum temperatures are presented in Table 14-13.

Table 14-13: Peak values for Case 7a

	Maximum		Minimum		% of hours below 0°C
	value [°C]	date	value [°C]	date	
basement	24.27	7-Sep	-1.14	19-Feb	13%
0_intzone	33.80	11-Aug	-2.73	13-Feb	14%
1_intzone	32.03	10-Aug	-2.84	11-Feb	14%

Changing the thermal properties of the slab from *massive-* to *heavy mix concrete* lowers the minimum temperatures in the basement, 0_intzone and 1_intzone by 6.66 °C, 8.02 °C and 5.94 °C respectively. In Östersund, where there is limited radiation and very low ambient temperatures in the winter, it seems that the thermal properties of the building foundation and surroundings have a greater impact on the minimum zone temperatures than the heat supplied by the solar heating system during the winter. To maintain frost proof conditions within the internal zones in Östersund using only a solar heating system for heating, careful planning and analysis of the surrounding ground and building foundation is essential. A weakness in this model is that the number of start-up days is set to 100 days. Ideally, this number should be much higher, achieving more stable conditions in the ground. The temperature in the 24th hour of the 31st of December should be almost identical to the temperature of the 1st hour of the 1st of January. In Figure 14-10 it is clear that the temperatures at the end of December are slightly higher than the temperatures in the beginning of January. Table 14-14 shows the temperatures for the last hour of the 31st of December and the first hour of the 1st of January.

Table 14-14: Zone dry bulb temperatures 31-Dec and 1-Jan

	31-Dec, hour 24 [°C]	01-Jan, hour 1 [°C]	Difference [°C]
basement	6.29	4.38	1.91
0_intzone	2.49	1.27	1.22
1_intzone	1.21	0.17	1.04

With enough start-up days to have achieved stable conditions in the ground with several previous years of heating, the difference should ideally be 0 °C for all zones. However, the difference ranges from only approximately 1-2 °C for the zones, which means that the minimum temperatures in February, would most likely still be below 0 °C even with a couple of years of start-up days.

With the occurrence of extremely cold winters in Östersund and limited irradiance, a small solar heating system will most likely not cover the demand of maintaining frost proof conditions inside a building placed on arbitrary soil. The location of the building is therefore an important aspect when trying to fulfill frost proof conditions.

Placing the cabin on dense soil with high specific heat capacity, in combination with thermally resistant materials in the ground floor may be sufficient to lift the minimum temperatures to above 0 °C in combination with an active solar heating system, as presented in Case 6.

Case 7b: Collector area of 4 m²

Another simulation was run with “normal” thermal properties in the ground, but this time with a collector area of 4 m². Figure 14-11 shows the dry bulb temperatures for Case 7b.

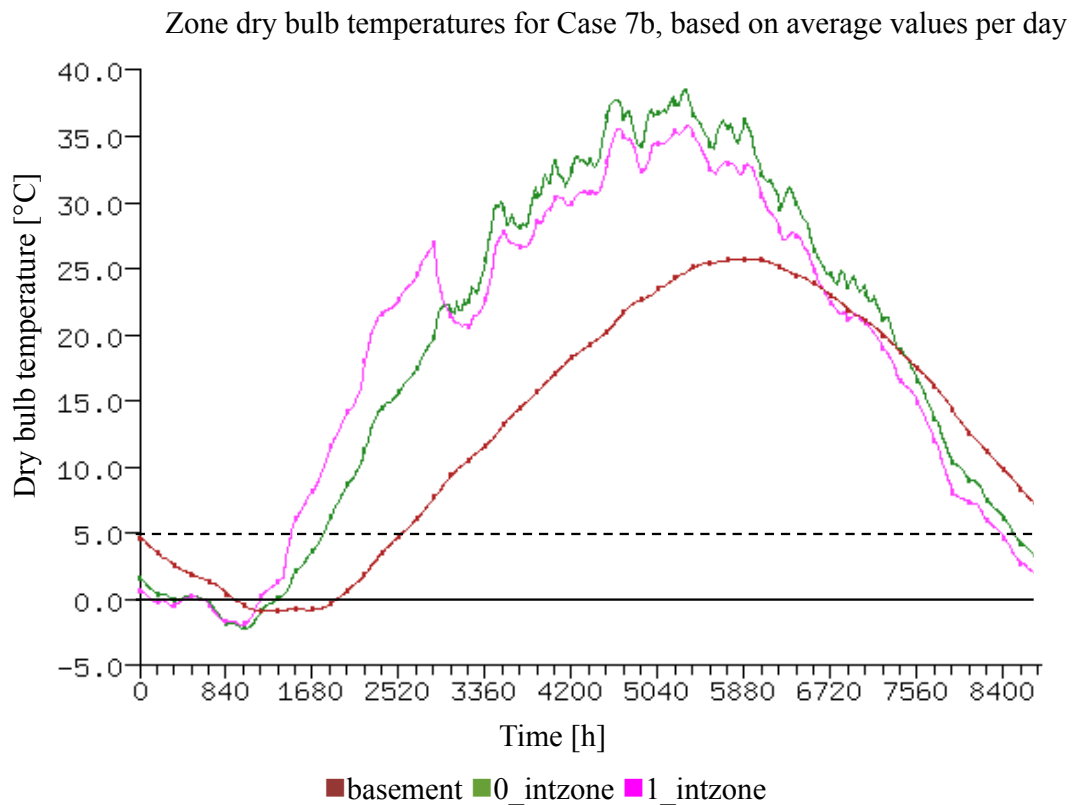


Figure 14-11: Dry bulb temperatures for Case 7b, based on daily averages

With a collector area twice the size of that used in Case 7a, the minimum temperatures still fall below 0 °C for all zones. They are slightly higher in Case 7b, but by less than 1 °C for all zones. The maximum temperatures are extremely high in Case 7b, up to almost 40 °C in 0_intzone on August 9th. If the leisure home is being used during the summer, this temperature is almost 20 °C above what is considered a comfortable indoor temperature. The peak values for Case 7b are shown in the table below.

Table 14-15: Peak values for Case 7b

	Maximum		Minimum		% of hours below 0°C
	value [°C]	date	value [°C]	date	
basement	25.76	7-Sep	-0.89	19-Feb	11%
0_intzone	39.51	9-Aug	-2.16	11-Feb	9%
1_intzone	35.92	11-Aug	-2.44	11-Feb	11%

14.2 Case simulations with Fornebu Climate data

14.2.1 Case 8

Case 8 is simulated with the Fornebu climate file with no heat injection and *massive concrete* in the slab (Figure 14-12). Compared to Case 2, which is simulated with the Östersund climate file, the temperatures in Case 8 are higher throughout the year. Peak values for dry bulb temperatures when simulating with Fornebu climate data and no heating system are presented in Table 14-16.

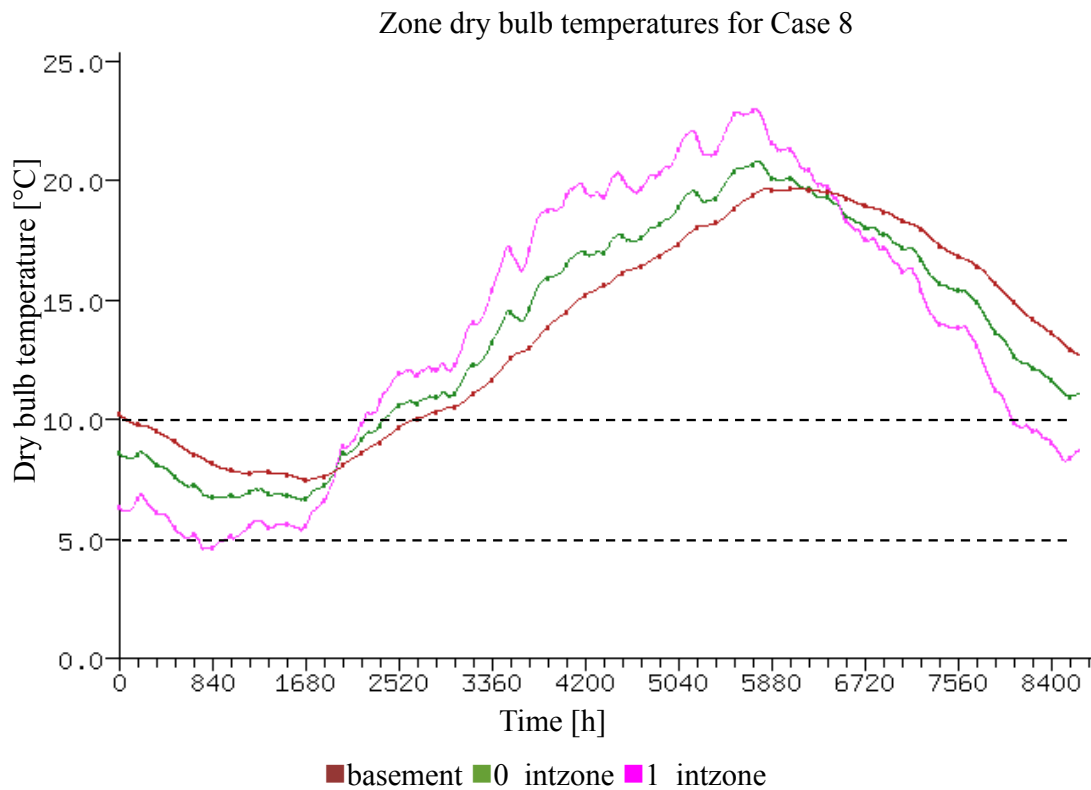


Figure 14-12: Dry bulb temperatures for Case 8

Table 14-16: Peak values for Case 8

	Maximum		Minimum		% of hours	
	value [°C]	date	value [°C]	date	below 10°C	below 5°C
basement	19.66	12-Sep	7.48	12-Mar	29%	0%
0_intzone	20.80	28-Aug	6.63	10-Mar	27%	0%
1_intzone	22.99	28-Aug	4.60	1-Feb	33%	3%

With the dense thermal mass in the concrete slab, the minimum temperatures are all above 4 °C all year with no heat supply. Fornebu has more hours of sunshine during the critical winter months than Östersund, in addition to higher average ambient temperatures. Both Case 2 and Case 8, simulated with *massive concrete* in the ground in both Östersund and Fornebu, obtain frost proof conditions throughout the year with no heat supply.

14.2.2 Case 9

Case 9 has electrical heat injection to 1_intzone from January 1st to April 30th and heat supplied by the hydronic floor the rest of the year as in Case 6. Case 9 is simulated with Fornebu climate data. Figure 14-13 shows that the temperatures in the internal zones are in general higher than when simulating with Östersund climate data. However, the minimum temperature in the basement is lower in Case 9 than in Case 6. This could be a result of more frequent temperature variations in Fornebu during the first trimester. Although the average ambient temperatures are higher in Fornebu than in Östersund, the ambient temperature falls below -20 °C more days in Fornebu than in Östersund in the first trimester.

Zone dry bulb temperatures for Case 9, based on average values per day

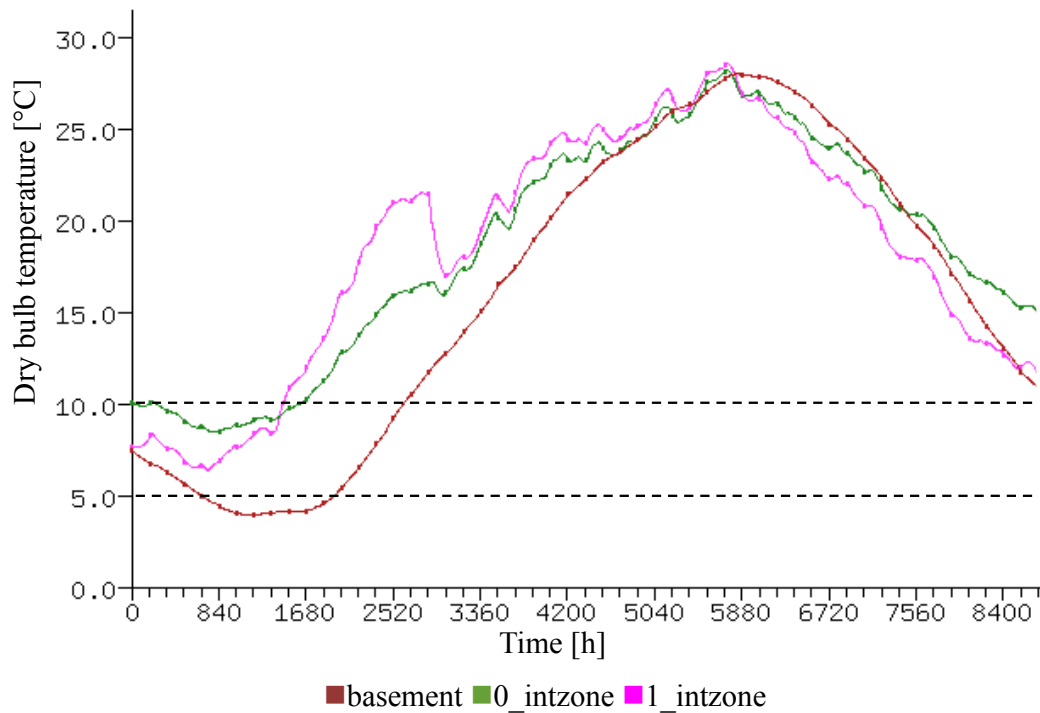


Figure 14-13: Dry bulb temperatures for Case 9, based on daily averages

The two internal zones and the basement are above 5 °C all year. 0_intzone has a minimum temperature of 8.49 °C which almost meets the recommendations from SINTEF. Again, for a well-insulated internal zone, an acceptable limit could possibly be below that of SINTEF's recommendation. In addition, increasing the number of startup days would most likely increase the minimum temperatures. Peak values are shown in the table below for Case 9.

Table 14-17: Peak values for Case 9

	Maximum		Minimum		% of hours	
	value [°C]	date	value [°C]	date	below 10°C	below 5°C
basement	28.04	1-Sep	7.99	18-Feb	41%	0%
0_intzone	28.28	28-Aug	8.49	2-Feb	16%	0%
1_intzone	28.61	28-Aug	6.12	1-Feb	17%	0%

14.2.3 Case 10

The last simulation has the same heating solution as Case 6 and Case 9, but with a solar collector area of 4 m² and “normal” thermal properties in the concrete slab. Fornebu receives more irradiance during the winter than Östersund, and a collector area of 4 m² is chosen here because it is likely that doubling the collector area will have a bigger impact in Fornebu than in Östersund.

Zone dry bulb temperatures for Case 10, based on average values per day

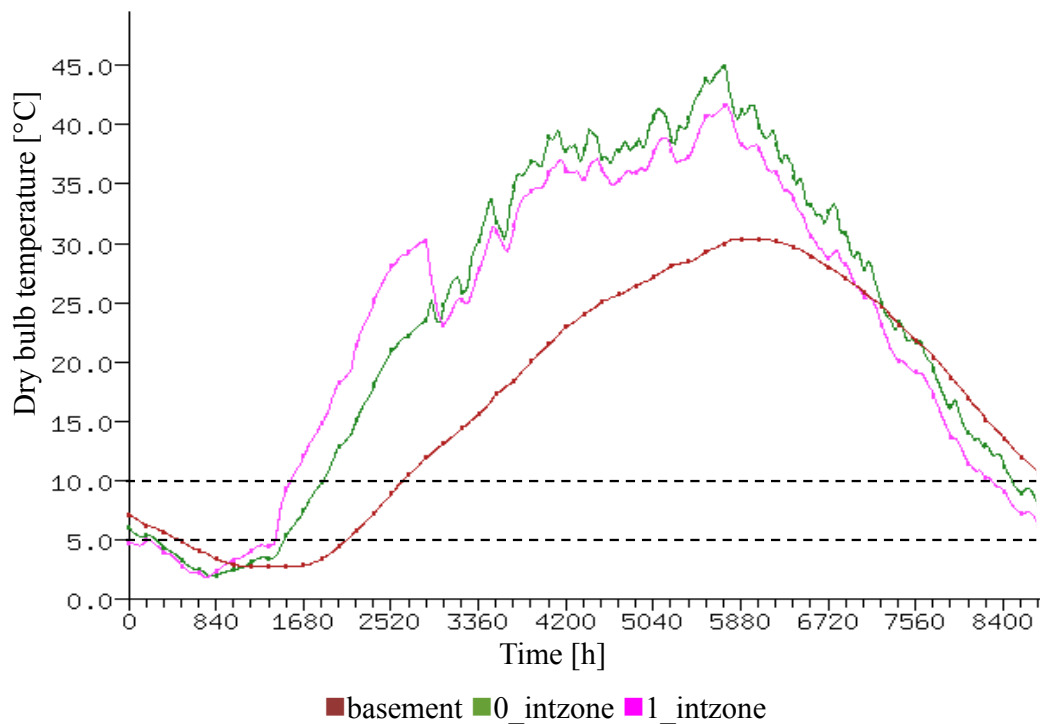


Figure 14-14: Dry bulb temperatures for Case 10, based on daily averages

The zone dry bulb temperatures are above 0 °C throughout the year in the internal zones and the basement. However, the minimum temperatures in the internal zones are below 2 °C, which is 8 °C lower than the recommendation from SINTEF. Heat

transfer occurs at a much higher rate through the slab when it holds the properties of *heavy mix concrete* than of *massive concrete*, and hence more heat is “lost” out of the control volume. The peak values are shown in the table below for Case 10.

Table 14-18: Peak values for Case 10

	Maximum		Minimum		% of hours	
	value [°C]	date	value [°C]	date	below 10°C	below 5°C
basement	30.40	10-Sep	2.76	19-Feb	30%	18%
0_intzone	45.84	26-Aug	1.97	2-Feb	24%	14%
1_intzone	41.82	28-Aug	1.36	31-Jan	23%	15%

The site ground thermal properties have a big impact on the minimum temperatures in the internal zones. In Fornebu, the internal zones are above 0 °C throughout the year with *heavy mix concrete* in the slab while in Östersund, more thermal mass is required to maintain frost proof conditions. The importance of careful analysis of the site ground conditions increases with colder and less sunny climate, when trying to maintain frost proof conditions. This shows the importance of carefully studying climatic conditions and site ground conditions in the design process. This is especially true for a leisure home placed in Scandinavian climate, experiencing great variations in solar radiation and ambient temperatures.

14.3 Solar heating system

Figure 14-15 is presented to illustrate the operation of the solar heating system. The graph is shown for one week in May for Case 6. The pump is switched off whenever the temperature difference between the solar collector and the hydronic floor is 5 °C or less.

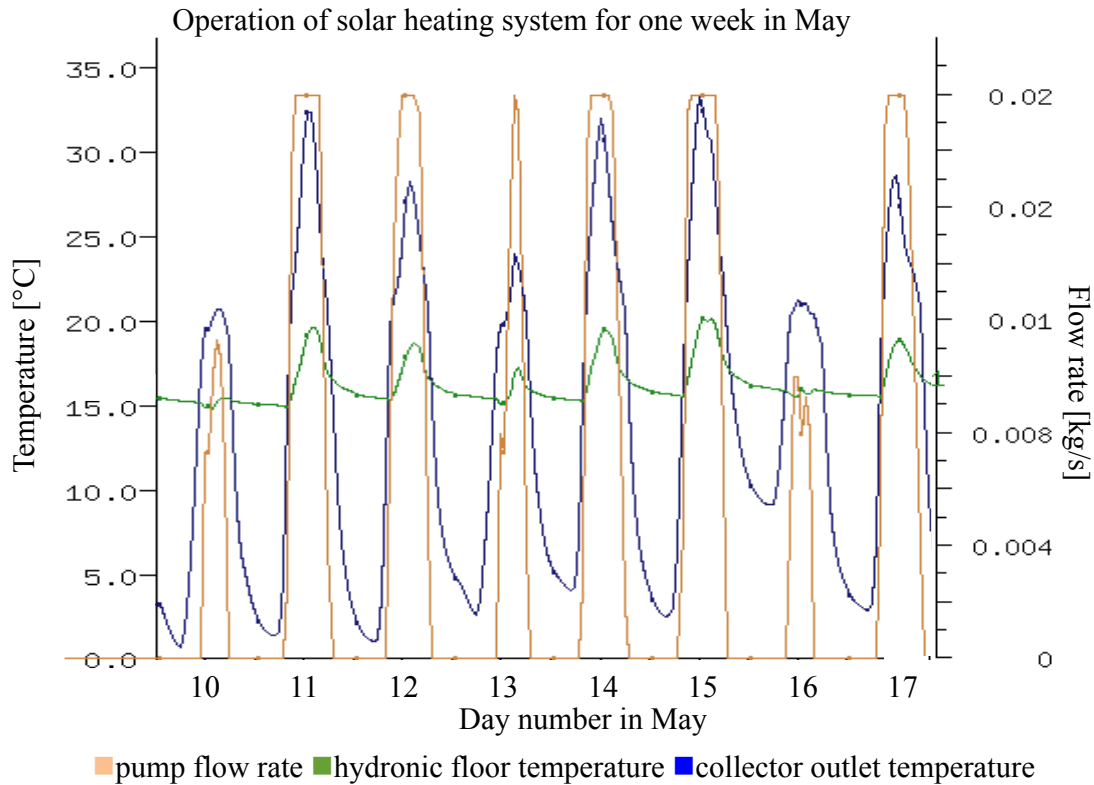


Figure 14-15: Operation of solar heating system

The hydronic floor receives a heat pulse whenever the system is in operation. This is clear from the figure, as the hydronic floor temperature (green graph), is increasing each day in the time period where the solar collector is making a heat contribution. Figure 14-16 shows the temperature distribution in the hydronic floor component throughout the year. Because the solar heating system is switched off from January 1st to April 30th, the temperature variations during this period are not as frequent as during the rest of the year. In the first trimester, it is the zone air of the first floor that is subject to the most frequent temperature variations as this is where heat is injected during this period. In the last two months of the year, the temperatures vary less frequently than from May to October. This is due to limited irradiance in short time periods during the two last months. The hydronic floor in Case 6, holds a temperature above 6 °C throughout the year.

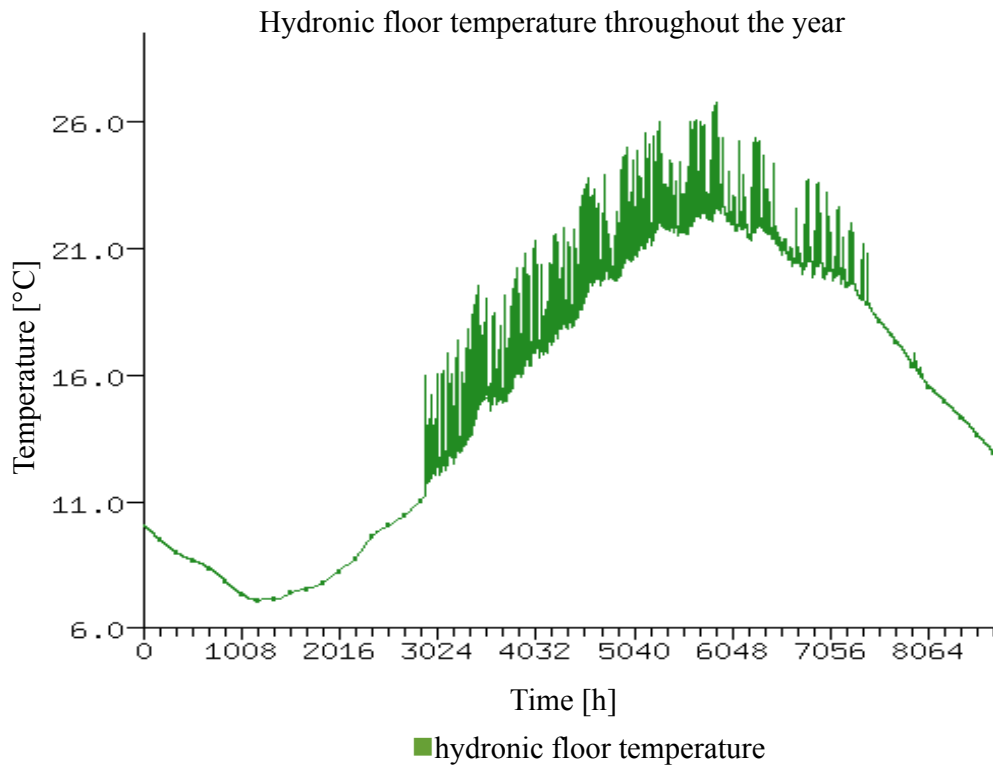


Figure 14-16: Hydronic floor temperature

14.4 Delivered energy to concrete slab from hydronic floor

The heat contribution from the hydronic floor to the concrete slab was calculated based on average values per month for Östersund and Fornebu. The calculations are based on a collector area of 2 m² and collector slope of 70 °. The resulting values and the distribution are presented in Table 13-19 and Figure 13-18 respectively.

Table 14-19: Delivered energy from hydronic floor

Delivered energy from hydronic floor to concrete slab [kWh]		
Month	Östersund	Fornebu
Jan	3.41	3.26
Feb	15.96	16.22
Mar	47.88	53.50
Apr	60.10	59.71
May	76.20	77.47
Jun	69.26	84.65
Jul	75.98	78.70
Aug	62.52	75.96
Sep	39.62	49.85
Oct	27.26	27.22
Nov	3.38	13.58
Dec	0.14	6.96
Sum	481.73	547.08

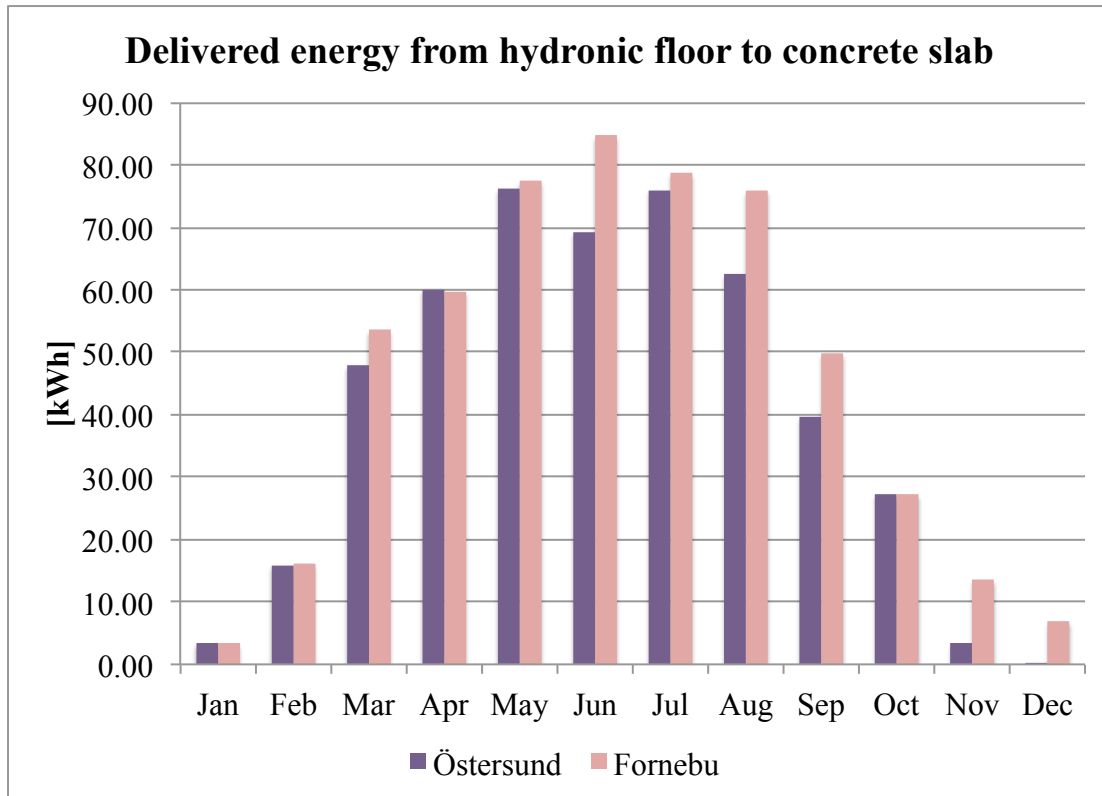


Figure 14-17: Delivered energy from hydronic floor to concrete slab

As seen in the figure above, the hydronic floor component annually supplies more heat if the leisure home is placed in Fornebu than in Östersund. Especially in November and December, there is a significant difference in delivered energy. Östersund is located further north, and will therefore receive less irradiance during the winter months. The annual delivered energy from the hydronic floor to the concrete slab is 482 kWh in Östersund, and 547 kWh in Fornebu.

14.5 Heat transfer

The potential for seasonal heat storage in the ground has been analyzed using climate data from Östersund. The concrete slab, together with the BASESIMP configuration in the basement, is modeled to represent thermal mass surrounding the building. An energy balance for the concrete slab will be presented to investigate whether heat collected during the summer is stored within the concrete block and released to the building during colder periods. An energy balance for the basement zone will also be presented to get an approximation of heat loss to surrounding ground outside the leisure home. The heat transfer is calculated one-dimensionally through all constructions in the model. The following equation is used in the energy balance equations:

$$\sum Q = Q_{in} - Q_{out} - Q_{stored} = 0 \quad (14-1)$$

where Q_{in} represents heat flux into the control volume, Q_{out} is heat flux out of the control volume and Q_{stored} is heat stored within the control volume. The heat fluxes are calculated using the following equation:

$$Q = U_{ij} * A_{ij} * \Delta T_{ij} \quad (14-2)$$

where U_{ij} is the U-value of the construction element between points i and j . A_{ij} is the surface area of the construction element between the two points, and ΔT_{ij} is the temperature difference between point i and point j .

14.5.1 Energy balance for the concrete slab

The heat input to the concrete slab is from the solar heating system. Heat loss from the concrete slab is to the internal ground floor zone and the basement zone. The heat loss to the basement zone imitates heat loss to surrounding ground. However, there may be a reversed heat transfer from the basement/surroundings to all the ground floor zones if the temperature in the basement/surroundings is higher than that of the zones. This is shown in Section 14.5.2. The amount of heat stored in the concrete block is calculated from the energy balance equation below:

$$Q_{stored} = Q_{in,solar\ heat} - Q_{out,internal\ zone} - Q_{out,basement} \quad (14-3)$$

Figure 14-18 shows the control volume for the concrete slab illustrating the heat fluxes in and out of the system. Solar heat is injected at 0.15 m depth into the slab construction.

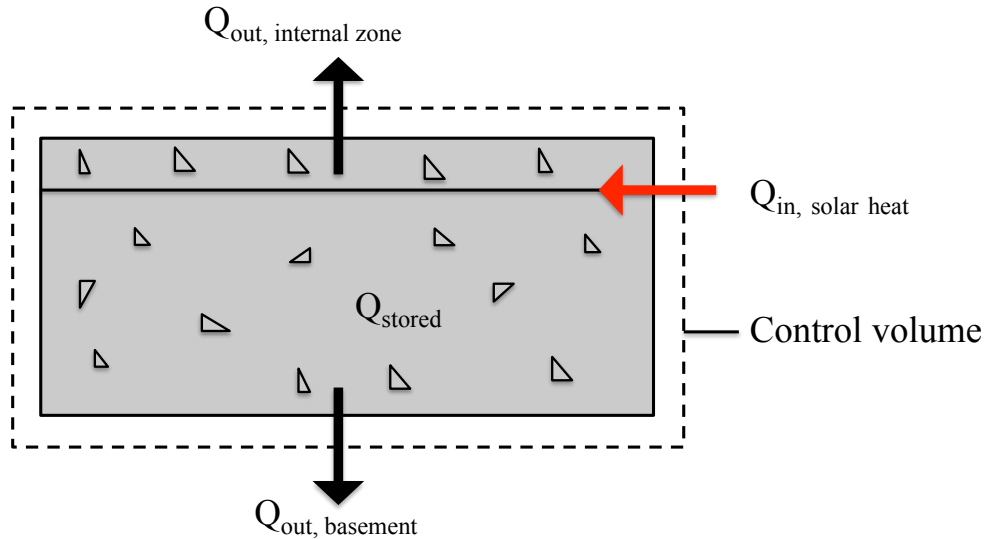


Figure 14-18: Concrete slab control volume and heat fluxes

The heat supply from the solar heating system to the concrete slab is calculated based on monthly average delivered energy from the hydronic floor in Östersund, given in Table 14-19. The heat transfer to the internal zone and the basement zone is calculated based on equation (14-3). The concrete slab temperature used to calculate ΔT between the slab and the surrounding zones is the temperature in the layer of heat injection, 0.15 m into the ground. In reality, temperature variations will occur in the different layers of the concrete slab, and the point of heat injection is chosen as the reference point for the calculations. Table 14-20 and Figure 14-19 show the resulting energy balance for the concrete slab. Note that the heat fluxes in Table 14-20 and Figure 14-19 are listed as *to* concrete slab *from* 0_intzone and basement, whereas the arrows in Figure 14-18 show heat fluxes in direction *from* the slab *to* the zones. This is done to show that the net energy transfer is zero, hence the energy is conserved. A negative heat transfer from a zone to the slab means a heat gain to the slab from the zone. If the graph were to be presented showing heat fluxes *from* slab *to* zones, the heat transfer from the hydronic floor would have to be presented in terms of heat transfer *from* slab *to* hydronic floor which is misleading as the hydronic floor is the main heat source to the control volume.

Table 14-20: Heat fluxes to and from concrete slab

	Heat transfer from hydronic floor to slab [kWh]	Reduction in stored heat within slab [kWh]	Heat transfer from 0_intzone to slab [kWh]	Heat transfer from basement to slab [kWh]
Jan	3.6	14.8	-10.6	-7.9
Feb	12.9	0.8	-6.4	-7.3
Mar	46.4	-44.9	6.7	-8.2
Apr	66.6	-76.1	17.4	-7.9
May	76.2	-72.8	7.5	-10.9
Jun	69.3	-65.0	8.2	-12.5
Jul	76.0	-68.5	8.6	-16.0
Aug	62.5	-49.4	5.7	-18.9
Sep	39.6	-19.7	-0.6	-19.3
Oct	27.3	-3.0	-6.0	-18.3
Nov	3.4	23.5	-11.4	-15.4
Dec	0.1	28.9	-14.2	-14.9

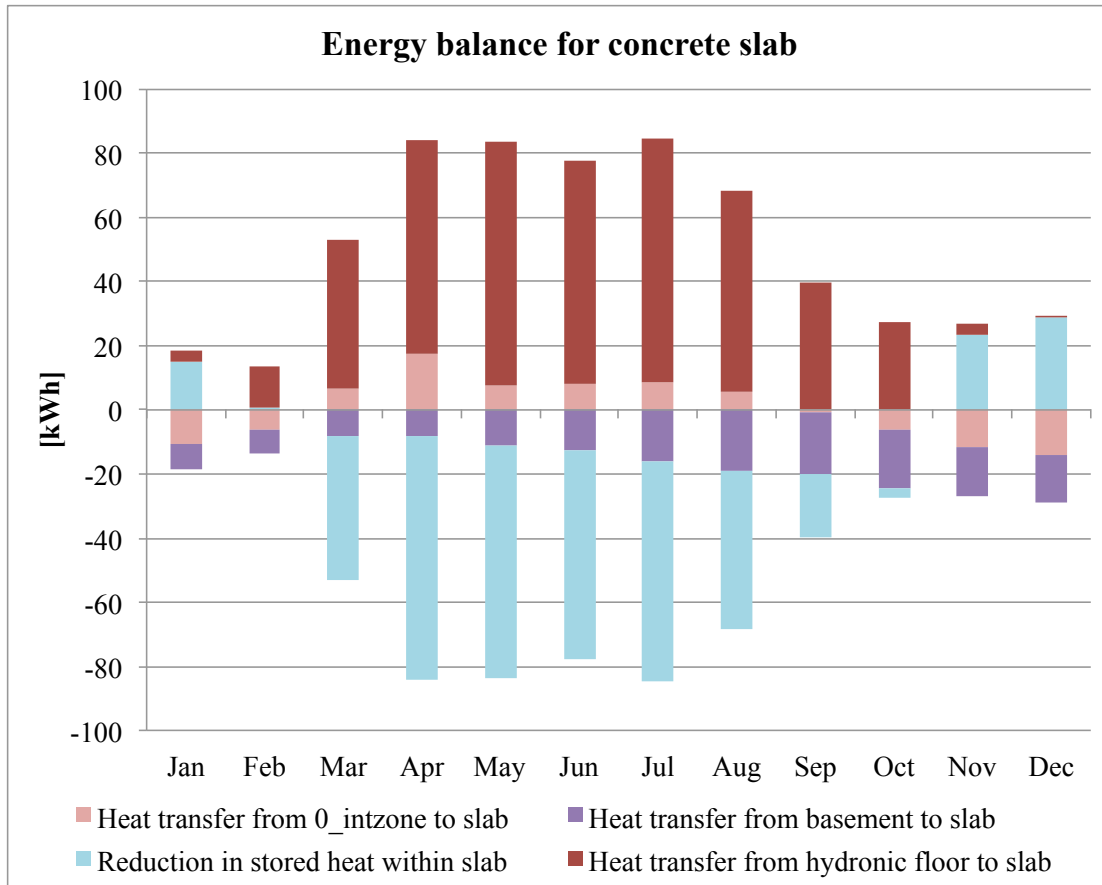


Figure 14-19: Energy balance for concrete slab

Heat transfer from the hydronic floor is positive throughout the year because the layer in the slab where heat injection occurs is always warmer than the surrounding temperatures.

From March to August, heat transfer from 0_intzone to slab is positive which means that the slab is being heated from the zone during these months. Heat transfer from 0_intzone to slab is negative between September and February, which means that there is actually a positive heat transfer from the slab to the zone during these months. The concrete slab is indeed heating 0_intzone in the fall and in the winter when the risk for frost formation is highest. This indicates that heat collected from the solar heating system during spring and summer has been stored in the concrete slab and is transferred upwards in the construction to the building in the fall and winter.

Heat transfer from the basement to the slab is negative for all months, which means that the slab is losing heat to the basement zone throughout the year. Since the basement zone, together with the slab, is created to mimic ground conditions below

the building, the heat transfer to the basement can in a sense be seen as heat loss to surrounding ground. However, the basement zone also faces the north- and south zones, which are subject to much lower temperatures than that of the internal zones. If the basement zone has a higher temperature than the north- or south zones, heat transfer from the basement/surrounding ground to the respective zones will occur. An energy balance for the basement zone will be presented in the next section to see the final heat loss to surroundings for each month.

Reduction in stored heat within the concrete slab is positive from November to February. This means that the amount of heat stored in the slab is reduced during these months, because the leisure building is being heated. Between March and October the reduction is negative, which means that the amount of stored heat is actually increasing. The stored heat in the concrete slab is increasing in the spring and summer when the heat contribution from the hydronic floor is high. During late autumn and winter, the stored heat in the slab is reduced because heat transfer occurs from the slab to the zones. The directions of the heat fluxes to and from the concrete slab for the different months are shown in Figure 14-20. The total heat gain to the heat storage in the slab is 331.4 kWh.

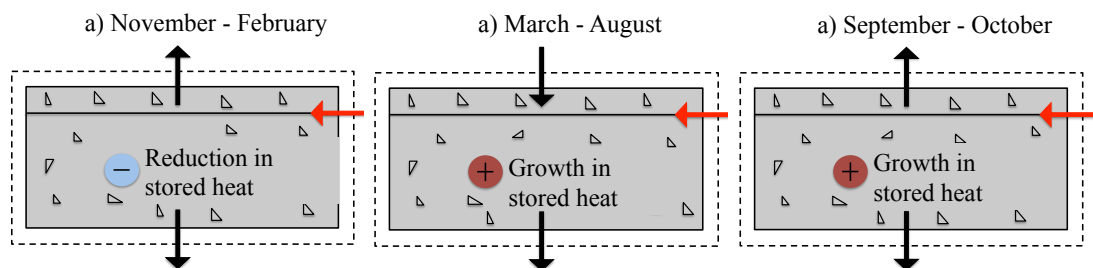


Figure 14-20: Direction of heat fluxes to and from concrete slab

14.5.2 Energy balance for the basement zone

The energy balance for the basement zone is based on heat fluxes to and from 0_southzone, 0_northzone, surrounding ground, and heat loss from the concrete slab to the basement. Heat loss to surrounding ground is calculated using equation (14-4).

$$Q_{out,surrounding\ ground} = Q_{in,slab} - Q_{out,north\ zone} - Q_{out,south\ zone} \quad (14-4)$$

Figure 14-21 shows the control volume for the basement illustrating heat fluxes in and out of the system.

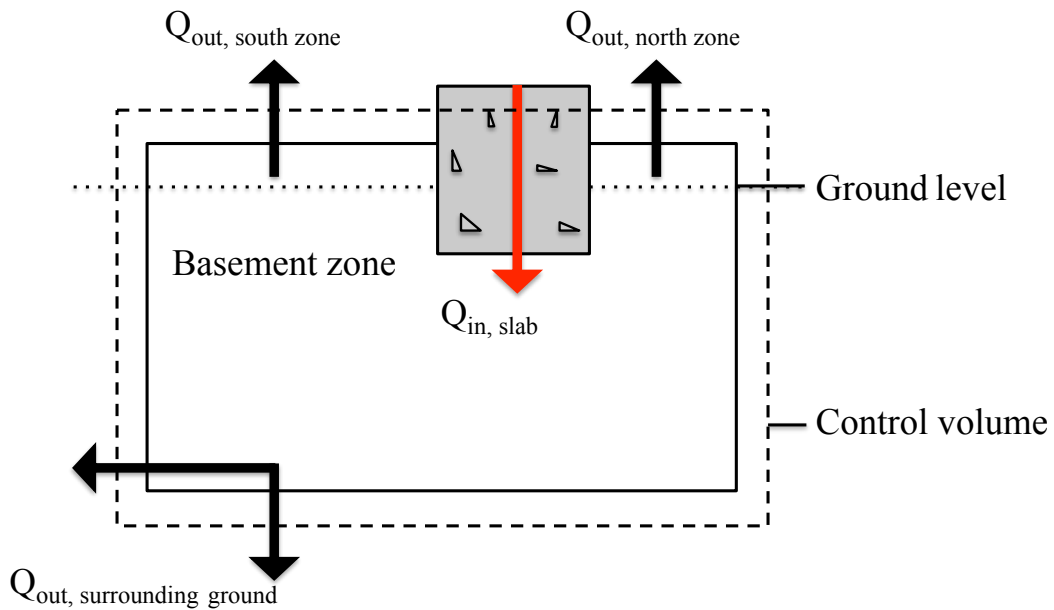


Figure 14-21: Basement control volume and heat fluxes

The main “heat source” for the basement zone is the concrete slab subject to heat injection by the solar heating system. Figure 14-22 shows the energy balance for the basement zone and the values are given in Table 13-21.

Table 14-21: Heat fluxes to and from basement zone

	Heat transfer from slab to basement [kWh]	Heat transfer from basement to 0_northzone [kWh]	Heat transfer from basement to 0_southzone [kWh]	Heat transfer from basement to ground [kWh]
Jan	7.9	26.1	24.3	-58.3
Feb	7.3	20.6	17.9	-45.8
Mar	8.2	7.1	2.7	-18.1
Apr	7.9	-8.9	-13.4	14.4
May	10.9	-18.7	-22.4	30.3
Jun	12.5	-21.9	-24.6	34.0
Jul	16.0	-24.5	-27.6	36.1
Aug	18.9	-17.5	-20.9	19.5
Sep	19.3	-1.7	-4.9	-12.6
Oct	18.3	11.6	8.2	-38.0
Nov	15.4	26.9	25.1	-67.4
Dec	14.9	30.4	29.1	-74.4

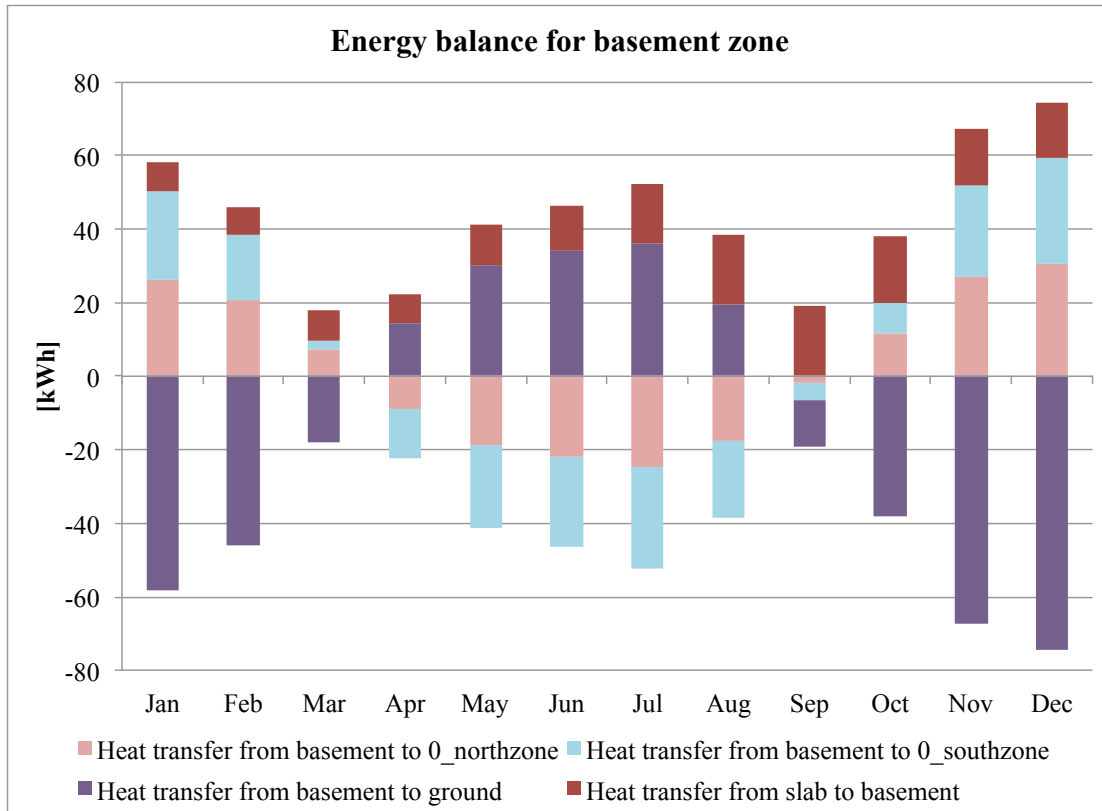


Figure 14-22: Energy balance for basement zone

Heat transfer from the concrete slab to the basement is positive throughout the year. This means that a certain amount of heat is “lost” from the concrete slab every month to the basement.

Heat transfer from the basement to 0_northzone and 0_southzone is positive from October to March. This means that there is a heat contribution from the basement to the two zones during these months. Between April and September, the heat transfer is negative, meaning heat loss from the zones to the basement. Hence, the ground is being heated from mid spring to late summer.

Heat transfer from the basement to surrounding ground is negative from September to March. This means that during this period, the ground is warmer than the air inside the basement zone, and heat transfer occurs from the ground to the zone. From April to August, the heat transfer from the basement to surrounding ground is positive which indicates heat loss out of the system. Figure 14-23 shows the direction of the heat fluxes to and from the basement zone for the different months.

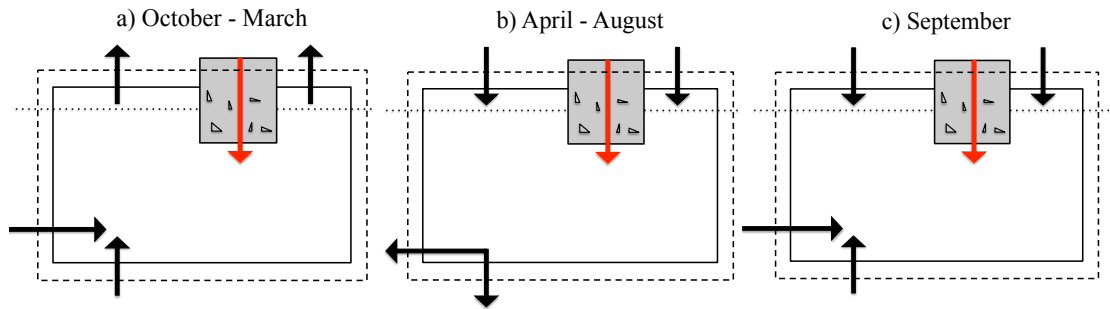


Figure 14-23: Direction of heat fluxes to and from basement zone

14.6 Cross-section temperatures in the concrete slab

The energy balances were calculated based on temperature differences. The reference temperatures used for the concrete slab were the temperatures within the layer 0.15m down in the slab where heat injection occurs. In reality, the temperatures in the concrete slab vary depending on depth. Figure 14-24 and Figure 14-25 show the temperature variations in the concrete slab for July 1st and December 1st respectively.

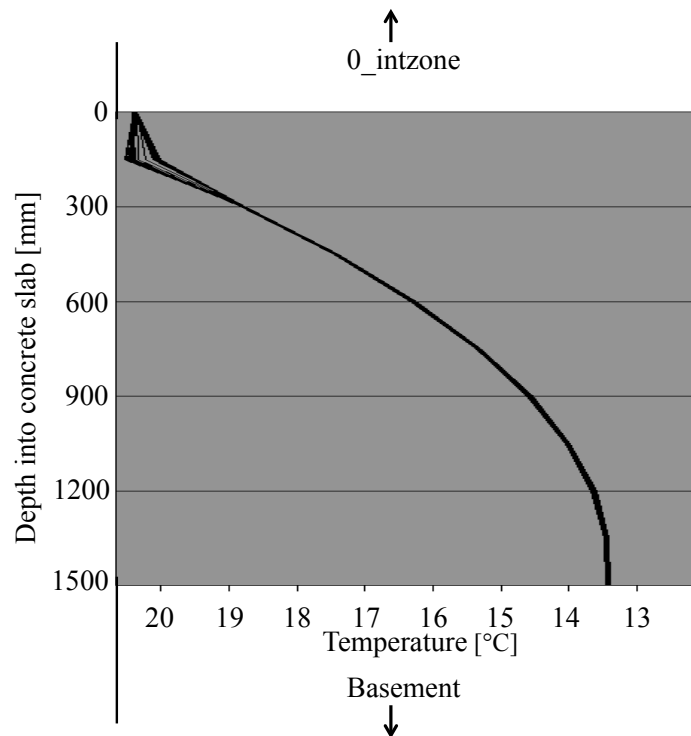


Figure 14-24: Cross section through concrete slab on July 1st

In Figure 14-24, for one day in July, the temperature in the slab varies from approximately 13.5 °C at the bottom layer adjacent to the basement zone, to approximately 20.5 °C in the top layer where heat injection occurs close to 0_intzone.

The heat pulse from the solar heating system can be seen in the center node of the layer adjacent to the internal zone. The temperature is decreasing further down in the construction for a typical summer day. Heat transfer occurs naturally from a warm element to a colder element. Whenever the temperatures in the top layers (close to 0_intzone) are warmer than further down in the construction, heat transfer will occur downwards. This is the desired effect as the concrete slab is being heated in periods when there is a large solar energy yield.

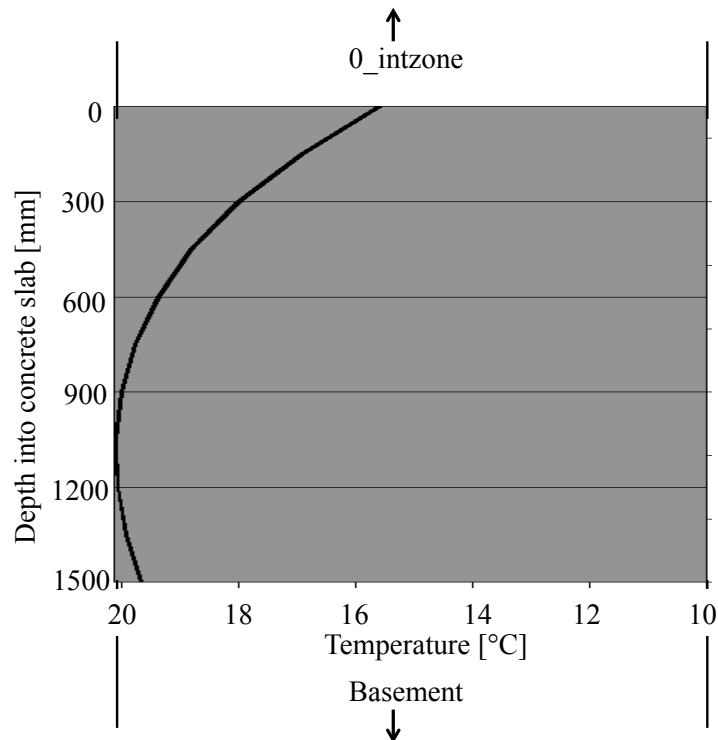


Figure 14-25: Cross section through the concrete slab on December 1st

In Figure 14-25, for one day in December, the temperature in the slab varies from approximately 20 °C in a layer closer to the basement zone, to approximately 16 °C to the layer adjacent to 0_intzone. Here, the temperature is warmer further down in the construction as a result of heat collected during the summer. The heat transfer is reversed relative to that seen for a typical summer day. In the winter case the heat transfer occurs from layers close to the bottom of the slab, to layers close to the top, which is the desired effect. When the temperatures in the top layers are decreasing as a result of low ambient temperatures and lack of irradiance, heat stored in the concrete slab works as a heat source transferring heat upwards in the slab and into the leisure home.

15 Comparison between Case 6 and Ida

Auråen's results

In Ida Auråen's master thesis, the final construction of the leisure home model was exactly the same as the one used in this report. The concrete slab was represented by five layers of *massive concrete*, and the basement zone was defined with the given BASESIMP configuration. The solar heating system however, was modeled more simplified as explained in sections 10.2 and 12.1. The chosen solution from Auråen's thesis consisted of electrical heat injection to the concrete slab from January 1st to April 30th and from September 1st to December 31st. The heating control loop was switched off between May 1st and August 31st to avoid extremely high temperatures in the leisure home during the summer. Heat injection to zone air in Case 6 is between January 1st and April 30th. Table 15-1 shows the electrical heat injection to zone air for Case 6 and the electrical heat injection to the concrete slab from Auråen's thesis from January 1st to April 30th. The number of hours per day when the control loop is active is also given for the two situations.

Table 15-1: Old and new control loop

		Control loop from Case 6		Control loop from Auråen's thesis	
Period	Month	Hours per day	Heat injection [W]	Hours per day	Heat injection [W]
1	Jan	1	110	5	260
2	Feb	4	143	7	491
3	Mar	6	257	11	550
4	Apr	8	250	13	548

In Auråen's thesis, the number of hours per day is based on a theoretical maximum number of solar hours per day. The number of hours in Case 6 is based on average time periods when there is a heat contribution from the hydronic floor to the concrete slab per day. The heat injection values from Auråen's thesis are based on a collector area of 4 m² while Case 6 uses a collector area of 2 m². Table 15-2 presents the

electrical heat injection equivalent to heat supplied by the hydronic floor if Case 6 has a collector area of 4 m².

Table 15-2: Control loop if Case 6 has a collector area of 4m²

Control loop from Case 6 with collector area of 4 m ²			
Period	Month	Hours per day	Heat injection [W]
1	Jan	1	195
2	Feb	4	210
3	Mar	6	448
4	Apr	8	460

The heat input is lower for Case 6 with a collector area of 4 m² than Auråen’s case. In addition, the number of hours per day when the heat is on differs for all months. The resulting dry bulb temperatures with Ida Auråen’s model can be seen in Figure 15-1. These temperatures are consistently higher than Case 6, as should be expected because more heat is injected during longer time periods per month.

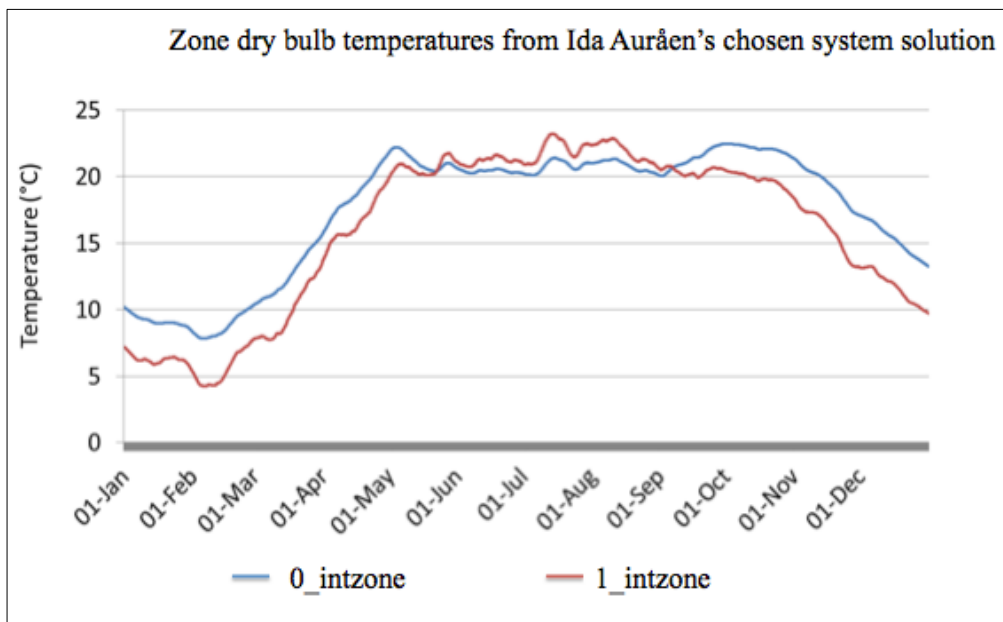


Figure 15-1: Dry bulb temperatures from Ida Auråen’s model, based on [7]

The peak values for Auråen’s case are shown in the table below. The minimum temperatures are higher in Auråen’s case than in Case 6 as expected. This is also caused by the amount of energy supplied as discussed above.

Table 15-3: Peak values for temperatures in Auråen's case

	Maximum		Minimum	
	value [°C]	date	value [°C]	date
0_intzone	22.5	30-Sep	7.8	6-Feb
1_intzone	23.2	14-Jul	4.2	6-Feb

In this thesis, the solar heating system has been built up using the necessary solar components. The results from Case 6 have thus been progressed in encompassing a real active solar heating system than the simplified case in Auråen's master where all heat is injected through electrical heating during all solar hours.

16 Conclusion

The focus on reducing energy use from the building sector has increased greatly during the last decades. New technologies are constantly sought to contribute to sustainable development with reduced consumption and emissions. This thesis has focused on energy use in leisure homes in Norway. Although the electricity consumption originating from leisure homes is small-scale compared to that of residential and industrial buildings, the demand is increasing rapidly and should be given attention. There is great potential for utilizing more renewable energy sources to reduce the electricity demand in leisure homes. While leisure homes are normally being used for short periods during the year, the electricity is often left on throughout the winter to avoid frost damages to sanitary installations and for increased comfort.

A concept for a frost proof leisure home without the use of primary energy has been developed in this report. Climate data from Östersund in Sweden, and Fornebu in Norway have been used to represent typical mountain regions and coastal regions in southern Norway. Frost proof conditions are achieved in well-insulated internal zones by using an active solar heating system and heat exchange with the ground. Heat is injected to the ground floor of the internal zone from May 1st to December 31st via a water-based floor heating component, hydronic floor, and directly to the well-insulated internal zone from January 1st to April 30th via an electric control loop.

The site ground conditions have been modeled to represent thermal mass surrounding the leisure home. The results show that with the modeled ground conditions, and by locating sanitary installations within well-insulated internal zones, it is possible to obtain temperatures that are well above 0 °C throughout the year, both in Östersund and in Fornebu.

Average ambient temperatures are lower in Östersund than in Fornebu and the results have therefore mainly been evaluated against Östersund climate data. In addition, Fornebu receives more solar radiation during the winter months than Östersund and therefore it is very likely that if frost proof conditions are obtained in Östersund for a given model, this will be obtained for the same case with Fornebu climate data.

The chosen system design for Östersund was Case 6. In Case 6 the solar heating system had a solar collector area of 2 m² placed at an angle of 70 ° from the horizontal. Heat was injected from May 1st to December 31st to a hydronic floor component embedded in the internal ground floor. From January 1st to April 30th, heat was injected to the internal first floor zone at the air point. This was done because the amount of heat supplied by the hydronic floor in the first months of the year was so limited that it did not contribute to any significant warming of the internal zones through the dense floor. The minimum temperature for Case 6 was 3.10 °C and occurred in the internal first floor zone (1_intzone) on February 11th. This temperature does not meet SINTEF's recommended value of 10 °C as minimum indoor temperature to minimize the risk for frost damages. However, because this temperature occurs within a well-insulated internal zone, barely affected by sudden changes in ambient temperatures, 3.10 °C may still be sufficient to say that frost proof conditions are obtained. The minimum temperature in the internal ground floor zone (0_intzone) for Case 6 was 5.29 °C and occurred on February 13th. To achieve a more even temperature distribution, holes could be drilled between the two zones creating buoyancy-driven airflow.

The same system solution was tested with climate data from Fornebu. The minimum temperatures in 0_intzone and 1_intzone turned out to be 8.49 °C and 6.12 °C, both higher than for the Östersund case.

The model responded to changes in different system parameters. The amount of available thermal mass had great impact on the potential for heat storage. Increasing the thermal mass showed significantly higher minimum temperatures in the winter for both locations. The effect of doubling the collector area lead to undesirably high temperatures in the summer and did not contribute to any major temperature rises in the coldest periods in February. It seemed that the storage capacity in the concrete slab was “used up” towards mid-February even with a collector area of 4 m² in Östersund. Changing the collector angle of inclination from 70 ° to 90 ° had a negative effect on the minimum temperatures although a steep angle at a high latitude would suggest more irradiance collected in the winter. This indicates that heat collected during the summer is of greater significance to the minimum temperatures in February than the limited solar energy collected in the winter months.

An active solar heating system requires a pump, and the pump needs electricity to operate. The required amount of electricity for a solar pump has not been studied in this report, but to obtain a system minimizing the use of primary energy sources, the pump could be operated using photovoltaic panels or batteries.

The storage potential in the concrete slab has been studied. With the dense thermal properties mimicking thermal mass in the ground, the results showed great potential for utilizing seasonal heat storage to raise the minimum temperatures. The net heat gain to the floor layer 0.15 m into the concrete slab throughout the year turned out to be the equivalent of 331.4 kWh. Because this number is positive it means that the stored heat in the slab has increasing over a year. If the number of start-up days had been several years, the minimum temperatures would most likely be raised as a result of the positive heat gain to the storage per year. It should be noted here that the heat fluxes are calculated one-dimensionally through each construction element. The heat gain to the slab must therefore be seen as an approximation to illustrate the effect of heat storage in thermal mass. If the number of start-up days had been equivalent to several years, the heat gain to the slab should be close to zero, having obtained stable thermal ground conditions.

An energy building performance simulation will never truly represent the real situation. It is important to note that there are weaknesses in any simulation model. The leisure home model is subject to several simplifications. It is difficult to say to what degree a model can be approximated to the real case, and it is important to recognize that there is always room for improvements and further analysis.

With the modeled leisure home and heating solution presented in this report, frost proof conditions are obtained for well-insulated internal zones. Zones adjacent to ambient conditions prove to be much more affected by sudden changes in outdoor temperatures. Locating sanitary installations within well-insulated internal zones shows that it is possible to maintain frost proof conditions throughout the year using an active solar heating system and heat exchange with thermal mass in the ground.

17 Proposals for further work

In this thesis, a significant amount of time has been spent to develop an active solar heating system in ESP-r. All heat collected from the solar heating system is utilized for heating purposes. Ideally, a system solution with a domestic hot water tank in addition to the hydronic floor would be more realistic for a leisure home. Most of the year there is no domestic hot water demand as leisure homes are normally used for short periods of the year. The potential to cover the hot water demand in periods when the leisure home is used should be considerable. An improved control system with the possibility of bypassing between a hydronic floor circuit and the tank could be established. The principle is illustrated in Figure 17-1.

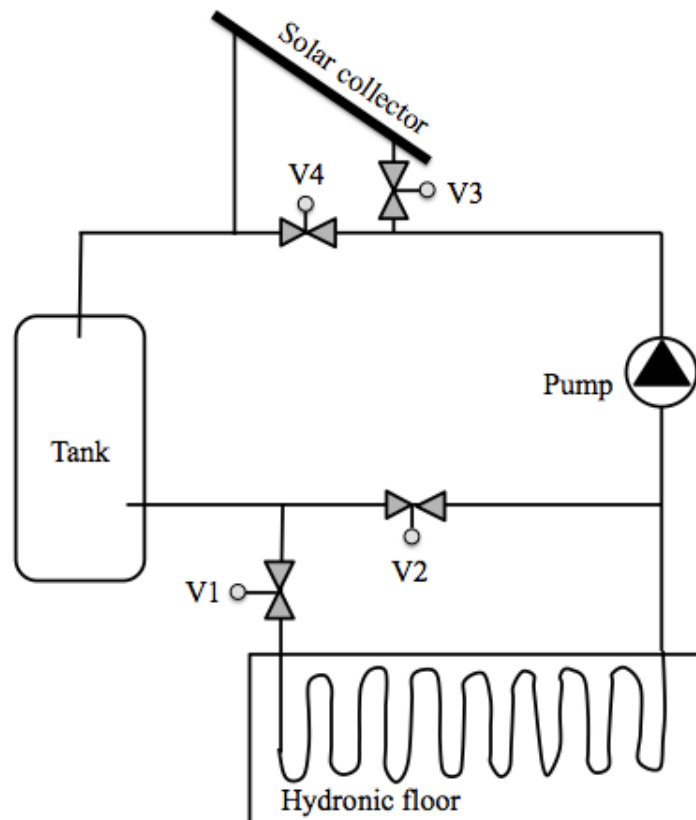


Figure 17-1: Advanced control system for the solar heating system

The solar collector supplies heat to the storage tank. If the tank is full or if the leisure home is left unused, excess heat from the tank is transferred to the hydronic floor circuit (V1) if the desired indoor temperature is too low. If the hydronic floor has provided sufficient heat, the control valve to the hydronic floor circuit (V1) closes, and a control valve leading the flow from the bottom/cold side of the tank to the solar

collector (V2) opens to recharge the tank. If the temperature in the solar collector is lower than the temperature in the tank, a control valve placed between the pump and the solar collector (V3) closes, and one leading directly from the pump to the storage tank (V4) opens. For further analysis of the possibility of a frost proof leisure home with a solar heating system and heat exchange with the ground, the plants and systems network along with the control strategy should be considered improved.

The operation of the solar heating system is based on on-off control of the pump. To improve the control system, a frequency-controlled pump could be installed. It is not realistic to use an on-off controlled pump, but it is used in this report for simulation purposes and it is assumed that changing the control strategy would have minimal or no impact on the minimum temperatures which is the main point of attention here. A frequency controlled pump would most likely contribute to a lower electricity consumption for the pump.

As mentioned, a simulated model will never truly represent a real situation. For further work there are several factors which could be of interest for further study. The BASESIMP configuration could be studied to see how this boundary condition changes over the year with respect to ground temperatures. The leisure home is planned located in Norway, where there will most likely be snow for some parts of the year. Snow is not accounted for in this report as there was no option to model this in ESP-r. Snow surrounding the leisure home would act as an insulating layer for the ground, decreasing the depth of frozen ground.

The construction of the leisure home is very simplified in the sense that it is modeled as a rectangular box with no doors and only one window. Improving the construction design could contribute to a more realistic model.

The solar heating system, built up by the plants and systems network in ESP-r requires numerous inputs. A more thorough parameter study on selected inputs could also contribute to optimizing the model. For Scandinavian climate, an evacuated tube solar collector is most likely more suitable than a flat plate collector. ESP-r does not have an option to model evacuated tube collectors, and the possibility to implement this using a different simulation tool could be considered for further work.

18 Bibliography

- [1] G. K. Pavlov and B. W. Olesen. 8 november). Seasonal Ground Solar Thermal Energy Storage - Review of Systems and Applications. Available: http://orbit.dtu.dk/fedora/objects/orbit:72783/datastreams/file_6383017/content
- [2] Statistisk Sentralbyrå. (17 september). Available: <https://http://www.ssb.no/statistikkbanken/SelectVarVal/Define.asp?MainTable=Fritidsbygg&KortNavnWeb=byggningsmasse&PLanguage=0&checked=true>
- [3] Statistisk Sentralbyrå. (18 september). Available: <https://http://www.ssb.no/statistikkbanken/selectvarval/Define.asp?subjectcode=&ProductId=&MainTable=ByggFritid&nvl=&PLanguage=0&nyTmpVar=true&CMSSubjectArea=bygg-bolig-og-eiendom&KortNavnWeb=byggeareal&StatVariant=&checked=true>
- [4] Sintef Byggforsk. (2011, 16 September). Available: <http://www.sintef.no/upload/Byggforsk/Vannskadekontoret/unng%C3%A5-vannskader-p%C3%A5-hytta.pdf>
- [5] Lovdata. (2010, 24 October). *FOR 2010-03-26 nr 489: Forskrift om tekniske krav til byggverk (Byggteknisk forskrift)*. Available: <http://www.lovdata.no/cgi-wifi/ldles?doc=/sf/sf/sf-20100326-0489.html - 14-2>
- [6] Energy Systems Research Unit. (4 october). *ESP-r Overview*. Available: http://www.esru.strath.ac.uk/Programs/ESP-r_overview.htm
- [7] I. K. Auråen, "Modeling of heat exchange with the ground and analyses of energy use for a frost proof leisure building with active solar heating," Master of Science, Department of Energy and Process Engineering, Norwegian University of Science and Technology, Norway, 2013.
- [8] RETScreen. (2001-2004, 20 september). Available: http://www.retscreen.net/download.php/ang/120/0/textbook_swh.pdf
- [9] Norges Vassdrag og Energidirektorat. (2009, 25 september). *Solenergi*. Available: <http://www.nve.no/no/Energi1/Fornybar-energi/Solenergi/>
- [10] Sintef Byggforsk and KanEnergi AS. (2011, 15 september). Available: <http://www.solenergi.no/wp-content/uploads/2010/01/Enova-mulighetsstudie-2011.pdf>
- [11] The German Solar Energy Society, *Planning and Installing Solar Thermal Systems: A guide for installers, architects and engineers*, 1 ed. London: James & James, 2005.
- [12] GRID Arendal. (2008, 14 september). Available: http://www.grida.no/graphicslib/detail/natural-resource-solar-power-potential_b1d5
- [13] Norsk Solenergiforening. (12 september). Available: <http://www.solenergi.no/om-solenergi/>
- [14] I. Andresen and Sintef Byggforsk, "Planlegging av solvarmeanlegg for lavenergiboliger og passivhus. En introduksjon," 2008.
- [15] BLUE MARBLE SOLAR. (2013, 8 october). *Solutions - Solar Hot Water*. Available: <http://www.bluemarblesolar.com/solutions.php>
- [16] B. Ramlow and B. Nusz, *Solar Water Heating*. Gabriola Island, BC, Canada: New Society Publishers, 2006.
- [17] Adam Solar Resources. (8 october). *Solar Thermal - Flat Plates*. Available: <http://www.adamsolarresources.com/solarthermal.html - solarthermal>

- [18] icon SOLAR. (2009, 3 october). *About Icon Solar*. Available: <http://www.iconsolar.com.au/aboutus.html>
- [19] D. F. Mahjouri. (12 November). *Vacuum Tube Liquid-Vapor (Heat-Pipe) Collectors*. Available: <http://www.thermomax.com/Downloads/Vacuum Tube Paper.pdf>
- [20] Pratts Plumbing. (7 november). *Vacuum Tube Technology*. Available: http://www.pratts.co.nz/solar_sub2.htm
- [21] The Encyclopedia of Alternative Energy and Sustainable Living. (12 November). *evacuated tube collector*. Available: http://www.daviddarling.info/encyclopedia/E/AE_evacuated_tube_collector.html
- [22] Alternative Energy Tutorials. (2013, 6 December). *Evacuated Tube Collector*. Available: <http://www.alternative-energy-tutorials.com/solar-hot-water/evacuated-tube-collector.html>
- [23] INTELLIGENT ENERGY SOLUTIONS. (2008, 12 November). *Solar Collectors - Heat Pipe vs Direct Flow*. Available: <http://www.intelligentenergysolutions.com/journal/2008/03/solar-collectors-heat-pipe-vs-direct-flow/>
- [24] OSO HOTWATER. (2013, 11 November). *OSO Ecoline Sun - RI SD - Providing free solar heated hot water with electric booster*. Available: <http://www.osohotwater.com/domestic-products/ecoline-sun.html>
- [25] OSO HOTWATER. (2013, 12 November). *Ecoline Twin Coil - RI TC - Combining high- and low temperature energy sources*. Available: <http://www.osohotwater.com/domestic-products/ecoline-twin-coil.html>
- [26] netgreen heat. (2012, 29 October). *Solar Heating System*. Available: http://www.netgreensolar.com/netgreen_heat_promo/body/netgreen_system.html
- [27] Sustainable Sources. (2013, 26 september). *Passive Solar Design*. Available: <http://passivesolar.sustainablesources.com/-heat>
- [28] The Engineering Toolbox. (6 December). *Propylene Glycol based Heat-Transfer Fluids*. Available: http://www.engineeringtoolbox.com/propylene-glycol-d_363.html
- [29] New4old and ITW. (3 oktober). *Integration of solar thermal collectors*. Available: http://new4old.eu/guidelines/C6_Part1_H5.html
- [30] SOLAR ENERGY USA. (2011, 3 october). *Solar Thermal*. Available: <http://solarenergy-usa.com/solar-energy-products/solar-thermal/>
- [31] Radiant Floor Company. (2009, 3 oktober). *Heating Water With Solar Energy*. Available: <http://www.radiantcompany.com/system/solar.shtml>
- [32] Regional Energy and Environment Agency and Climasol. (3 october). *Solar assisted cooling at the University Hospital in Freiburg*. Available: http://www.raee.org/climatisationsolaire/gb/pop/pop_or/frei_un_hos.htm
- [33] I. H. T. icax. (2007, 29 October). *Solar Roofing*. Available: http://www.icax.co.uk/image_Solar_Roofing.html
- [34] winkler SOLAR. (29 October). *The new module collector MetroSol*. Available: <http://www.winklersolar.com/271.html>
- [35] I. Beausoleil-Morrison, CANMET Energy Technology Centre, Natural Resources Canada, and G. Mitalas, "BASESIMP: a residential-foundation heat-loss algorithm for incorporating into whole-building energy-analysis programs," p. 8, 1997.

- [36] CloudForge. (11 october). *Basesimp Foundation Model*. Available: <http://espr.trac.cvsdude.com/esp-r/wiki/BASESIMP.bsm>
- [37] D. Thevenard, K. Haddad, and J. Purdy. (2004, 7 october). *Development of a new solar collector model in ESP-r*. Available: http://www.esru.strath.ac.uk/Documents/04/solar_collector.pdf
- [38] J. W. Hand. (17 october). *THE ESP-r COOKBOOK - Strategies for Deploying Virtual Representations of the Built Environment*. Available: http://www.esru.strath.ac.uk/Documents/ESP-r_cookbook_july_2011.pdf
- [39] DJURS SOLVARME. (1999, 18 November). *Datablad for solfanger - effektivitet*. Available: <http://djurssolvarme.dk/wordpress/wp-content/uploads/2011/03/Datablad-DS-4.pdf>
- [40] JRC - European Commision. (2013, 09 December). *Photovoltaic Geographical Information System - Interactive Maps*. Available: <http://re.jrc.ec.europa.eu/pvgis/apps4/pvest.php>
- [41] European Solar Thermal Industry Federation (ESTIF), "The Spanish Technical Building Code - English translation of the solar thermal sections of the code," ed, 2006.
- [42] A. S. Børset, "Utvikling av konsept for en nullutslipp fritidsbolig med en isolert frostfri indre sone og soloppvarmet vannmagasin," Master of Science, Institutt for energi og prosessteknikk, NTNU, 2009.
- [43] T. Wigenstad, "Prosjektveileder - Forenklet anlegg for vannbåren oppvarming av boliger," 2009.
- [44] GoogleMaps. (2013, 21 October). Available: <https://maps.google.com>

Appendix

Appendix A

Detailed description of the leisure home model in ESP-r

Appendix B

Energy calculations in Excel

Appendix C

Zone dry bulb temperature graphs

Appendix D

Challenges with ESP-r

Appendix A

Detailed description of the leisure home model in ESP-r

A.1 Appendix comment

To allow for a replication of the simulation, the description of the model is restored as in ESP-r.

A.2 Location and climate

A.2.1 Östersund climate data

The model is located at latitude 63.18 with a longitude difference of 14.64 from the local time meridian. The year used in simulations is 2013 and weekends occur on Saturday and Sunday. The site exposure is typical city center and the ground reflectance is 0.20.

The climate is: OSTERSUND/FROSON - SWE

Calculated ground temp at 0.5m depth

-1.9597 -5.0454 -5.8853 -5.1568 -0.99080 3.6750 8.0648 11.243 12.171
10.678 7.0813 2.5468

Calculated ground temp at 1.0m depth

-0.86512 -3.9428 -5.0408 -4.6372 -1.2336 2.8999 6.9788 10.134 11.347
10.349 7.3528 3.3290

Calculated ground temp at 2.0m depth

0.81430 -2.0766 -3.4534 -3.5032 -1.3041 1.8879 5.3212 8.2645 9.7855
9.5010 7.4716 4.3546

Calculated ground temp at 4.0m depth

2.6250 0.38079 -0.99802 -1.4214 -0.60971 1.2485 3.5568 5.8234 7.3466
7.7115 6.8402 5.0151

A.2.1 Fornebu climate data

The model is located at latitude 59.90 with a longitude difference of -4.10 from the local time meridian. The year used in simulations is 2013 and weekends occur on Saturday and Sunday. The site exposure is typical city centre and the ground reflectance is 0.20.

The climate is: DRY Oslo

Calculated ground temp at 0.5m depth

0.53527 -2.9246 -3.8664 -3.0496 1.6217 6.8534 11.776 15.340 16.380
14.706 10.673 5.5883

Calculated ground temp at 1.0m depth

1.7626 -1.6884 -2.9196 -2.4670 1.3494 5.9843 10.558 14.096 15.456
14.337 10.977 6.4655

Calculated ground temp at 2.0m depth

3.6457 0.40417 -1.1396 -1.1954 1.2704 4.8495 8.6993 12.000 13.705
13.386 11.110 7.6154

Calculated ground temp at 4.0m depth

5.6760 3.1596 1.6136 1.1389 2.0490 4.1325 6.7208 9.2624 10.970 11.379
10.402 8.3560

A.3 Controls

The model includes ideal controls as follows:

Zones control includes 2 functions.

A.3.1 Zone control function 1

The sensor for function 1 senses dry bulb temperature in basement.
The actuator for function 1 is within 0_intground in basement.
There have been 1 day types defined.

Day type 1 is valid Tue-01-Jan to Tue-31-Dec, 2013 with 1 periods.

Per	Start	Sens.	Act.	Control law	Data
1	0.00	dbtemp	flux	flux zone/plant	0.0 0.0 3.0 0.0 0.0 0.0 0.0

OnOff std mode 1.0 on setpt 5.00C off setpt 1.00C output @ hi 0.000
output @ lo 0.000 sensor lag 0.0s actuator lag 0.0s.

A.3.2 Zone control function 2

The sensor for function 2 senses dry bulb temperature in lint_zone.
The actuator for function 2 is the air point in lint_zone.
There have been 5 day types defined.

Day type 1 is valid Tue-01-Jan to Thu-31-Jan, 2013 with 3 periods.

Per	Start	Sens.	Act.	Control law	Data
1	0.00	dbtemp	flux	free float	
2	13.00	dbtemp	flux	basic contr.	110.0 110.0 0.0 0.0 100.0 100.0
0.0					
3	14.00	dbtemp	flux	free float	

basic control:

max heating capacity 110.0W
min heating capacity 110.0W
max cooling capacity 0.0W
min cooling capacity 0.0W.
Heating setpoint 100.00C
cooling setpoint 100.00C.

Day type 2 is valid Fri-01-Feb to Thu-28-Feb, 2013 with 3 periods.

Per	Start	Sens.	Act.	Control law	Data
1	0.00	dbtemp	flux	free float	
2	12.00	dbtemp	flux	basic contr.	143.0 143.0 0.0 0.0 100.0 100.0
0.0					
3	15.30	dbtemp	flux	free float	

basic control:

max heating capacity 143.0W
min heating capacity 143.0W
max cooling capacity 0.0W
min cooling capacity 0.0W.
Heating setpoint 100.00C
cooling setpoint 100.00C.

Day type 3 is valid Fri-01-Mar to Sun-31-Mar, 2013 with 3 periods.

Per	Start	Sens.	Act.	Control law	Data
1	0.00	dbtemp	flux	free float	
2	11.00	dbtemp	flux	basic contr.	257.0 257.0 0.0 0.0 100.0 100.0
0.0					
3	17.00	dbtemp	flux	free float	

basic control:

max heating capacity 257.0W
min heating capacity 257.0W
max cooling capacity 0.0W
min cooling capacity 0.0W.
Heating setpoint 100.00C
cooling setpoint 100.00C.

Day type 4 is valid Mon-01-Apr to Tue-30-Apr, 2013 with 3 periods.

Per	Start	Sens.	Act.	Control law	Data
1	0.00	dbtemp	flux	free float	
2	10.00	dbtemp	flux	basic contr.	250.0 250.0 0.0 0.0 100.0 100.0 0.0
3	18.00	dbtemp	flux	free float	

basic control:

max heating capacity 250.0W
min heating capacity 250.0W
max cooling capacity 0.0W
min cooling capacity 0.0W.
Heating setpoint 100.00C
cooling setpoint 100.00C.

Day type 5 is valid Wed-01-May to Tue-31-Dec, 2013 with 1 periods.

Per	Start	Sens.	Act.	Control law	Data
1	0.00	dbtemp	flux	free float	

A.3.3 Control loop linkages to zones

Zone to control loop linkages:

zone (1) 0north_zone << control 0
zone (2) 0south_zone << control 0
zone (3) 0int_zone << control 0
zone (4) 1north_zone << control 0
zone (5) 1south_zone << control 0
zone (6) 1int_zone << control 2
zone (7) basement << control 1

A.3.4 Plant control function

Plant control includes 1 loops.

The sensor for function 1 sen var diff bet compt 1:sol_coll @ node 1
and compt 3:hyd_floor @ node 1

The actuator for function 1 is plant component 2:pump @ node 1

There have been 2 day types defined.

Day type 1 is valid Tue-01-Jan to Tue-30-Apr, 2013 with 1 periods.

Per	Start	Sens.	Act.	Control law	Data
1	0.00	drybulb	flux	period off	

Day type 2 is valid Wed-01-May to Tue-31-Dec, 2013 with 1 periods.

Per	Start	Sens.	Act.	Control law	Data
1	0.00	delt T	flow	On-Off control	1.0 5.0 1.0 0.0 0.0 0.0 0.0

OnOff std mode 1.0 on setpt 5.00C off setpt 1.00C output @ hi 0.000
output @ lo 0.000 sensor lag 0.0s actuator lag 0.0s.

A.4 Plant network

The model includes a plant network.

A.4.1 Plant components

The plant network contains 3 components from plantc.db1

Component: sol_coll (1) code 1, db reference 84

No Control data

Modified parameters for solar_coll

Collector area (m2)	:	2.0000
Type of efficiency equ. (1=North-American,2=Europe)	:	2.0000
Constant coef. of efficiency equ. (-)	:	0.62000
Linear coef. of efficiency equ. (W/m2/C)	:	3.8700
Quadratic coef. of efficiency equ. (W/m2/C2)	:	0.11000E-01
Collector test flow rate (kg/s)	:	0.20000E-01
Heat capacitance of fluid used for test (J/kg/C)	:	3600.0
Inc. angle correction (=1 Fit,=2 Interpolation)	:	2.0000
Inc. angle equation linear term coef. (-)	:	0.20000
Inc. angle equation quadratic term coef. (-)	:	0.0000
Number of data pairs for inc angle correction (-)	:	5.0000
1st inc. angle correction data pair angle (Deg)	:	0.0000
1st inc. angle correction data pair factor (-)	:	1.0000
2nd inc. angle correction data pair angle (Deg)	:	30.000
2nd inc. angle correction data pair factor (-)	:	0.99400
3rd inc. angle correction data pair angle (Deg)	:	45.000
3rd inc. angle correction data pair factor	:	0.96400
4th inc. angle correction data pair angle (Deg)	:	60.000
4th inc. angle correction data pair factor (-)	:	0.82800
5th inc. angle correction data pair angle (Deg)	:	70.000
5th inc. angle correction data pair factor (-)	:	0.74000
6th inc. angle correction data pair angle (Deg)	:	0.0000
6th inc. angle correction data pair factor (-)	:	1.0000
7th inc. angle correction data pair angle (Deg)	:	0.0000
7th inc. angle correction data pair factor (-)	:	1.0000
8th inc. angle correction data pair angle (Deg)	:	0.0000
8th inc. angle correction data pair factor (-)	:	1.0000
9th inc. angle correction data pair angle (Deg)	:	0.0000
9th inc. angle correction data pair factor (-)	:	1.0000
10th inc. angle correction data pair angle (Deg)	:	0.0000
10th inc. angle correction data pair factor (-)	:	1.0000
Collector slope (deg. from horizontal)	:	70.000
Collector azimuth (deg., N=0, E=90)	:	180.00
Mass fraction of propylene glycol (%)	:	50.000
Mass of collector (kg)	:	50.000
Collector average capacitance (J/kg-C)	:	847.00

Component: pump (2) code 2, db reference 15

Control data: 0.000

Modified parameters for pump

Component total mass (kg)	:	5.0000
Mass weighted average specific heat (J/kgK)	:	2250.0
UA modulus from wall to environment (W/K)	:	0.0000
Rated total absorbed power (W)	:	25.000
Rated volume flow rate (m ³ /s)	:	0.20000E-04
Overall efficiency (-)	:	0.0400

Component: hyd_floor (3) code 3, db reference 63

No Control data

Modified parameters for hydro_floor

Number of circuits (integer)	:	1.0000
Inside diameter of pipe (m)	:	0.17000E-01

```

Outside diameter of pipe (m) : 0.20000E-01
Pipe spacing (m) : 0.20000
Thermal conductivity of pipe material (W/mK) : 0.38000
Volumetric specific heat of pipe material - rho*Cp : 0.32000E+07
Served zone number (integer) : 3.0000
Zone surface number (integer) : 6.0000
Injection node number (integer) : 10.000

```

A.4.2 Plant connections

```

Nb of plant component connections: 3
Con|receiving|node |type |send. |node |details
 1 |sol_coll |node 1|from component|pump |node 1|1.00 0.00 0.00
 2 |hyd_floor|node 1|from component|sol_coll |node 1|1.00 0.00 0.00
 3 |pump |node 1|from component|hyd_floor|node 1|1.00 0.00 0.00

```

A.4.3 Plant containments

```

No of component containments: 2
Component|Containment descr.| Type
1 sol_coll |outside air | 0 details: 0.00 0.00 0.00
2 hyd_floor|zone: basement | 3 details: 7.00 8.00 3.00

```

A.5 Construction details

A.5.1 Construction details: roof

Multi-layer constructions used:

Details of opaque construction: roof and overall thickness 0.810

Layer	Matr db	Thick (mm)	Conduc- tivity	Density	Specif heat	IR emis	Solr abs	Diffu resis	R m^2K/W
Ext	234	300.0	0.049	110	1	0.90	0.13	10	6.12
snow: snow									
	2	64	160.0	0.140	419	2720	0.90	0.65	12
fir: Fir (20%mc)									
Int	205	350.0	0.030	30	837	0.90	0.50	90	11.67
Polyurethane foam bd: Polyurethane foam board									

ISO 6946 U values (horiz/upward/downward heat flow)= 0.052 0.052
0.052 (partition) 0.052
Total area of roof is 64.00

A.5.2 Construction details: 0_ext_wall

Details of opaque construction: 0ext_wall and overall thickness 0.500

Layer	Matr db	Thick (mm)	Conduc- tivity	Density	Specif heat	IR emis	Solr abs	Diffu resis	R m^2K/W
Ext	32	200.0	1.400	2100.	653.	0.90	0.65	19.	0.14
Heavy mix concrete : Heavy mix concrete									
Int	211	300.0	0.040	250.	840.	0.90	0.30	4.	7.50
Glasswool : Glasswool									

ISO 6946 U values (horiz/upward/downward heat flow)= 0.128 0.128
 0.127 (partition) 0.127
 Total area of 0ext_wall is 64.00

A.5.3 Construction details: 1ext_wall

Details of opaque construction: 1ext_wall and overall thickness
 0.150

Layer	Matr	Thick	Conduc-	Density	Specif	IR	Solr	Diffu	R
	db	(mm)	tivity		heat	emis	abs	resis	m^2K/W
1	64	150.0	0.140	419.	2720.	0.90	0.65	12.	1.07
Fir (20% mc) : Fir (20% mc)									

ISO 6946 U values (horiz/upward/downward heat flow)= 0.806 0.825
 0.780 (partition) 0.751
 Total area of 1ext_wall is 102.40

A.5.4 Construction details: int_wall

Details of opaque construction: int_wall and overall thickness
 0.350

Layer	Matr	Thick	Conduc-	Density	Specif	IR	Solr	Diffu	R
	db	(mm)	tivity		heat	emis	abs	resis	m^2K/W
Ext	205	250.0	0.030	30.	837.	0.90	0.50	90.	8.33
Polyurethane foam board : Polyurethane foam									
Int	32	100.0	1.400	2100.	653.	0.90	0.65	19.	0.07
Heavy mix concrete : Heavy mix concrete									

ISO 6946 U values (horiz/upward/downward heat flow)= 0.117 0.117
 0.116 (partition) 0.115
 Total area of int_wall is 60.00

A.5.5 Construction details: part_wall

Details of transparent construction: part_wall with DCF7671_06nb
 optics and overall thickness 0.024

Layer	Matr	Thick	Conduc-	Density	Specif	IR	Solr	Diffu	R
	db	(mm)	tivity		heat	emis	abs	resis	m^2K/W
Ext	242	6.0	0.760	2710.	837.	0.83	0.05	19200	0.01
Plate glass : Glass with placeholder single									
2	0	12.0	0.000	0.	0.	0.99	0.99	1.	0.17
air 0.17 0.17 0.17									
Int	242	6.0	0.760	2710.	837.	0.83	0.05	19200	0.01
Plate glass : Glass with placeholder single									

ISO 6946 U values (horiz/upward/downward heat flow)= 2.811 3.069
 2.527 (partition) 2.243

Clear float 76/71, 6mm, no blind: with id of: DCF7671_06nb
 with 3 layers [including air gaps] and visible trn: 0.76
 Direct transmission @ 0, 40, 55, 70, 80 deg
 0.611 0.583 0.534 0.384 0.170
 Layer| absorption @ 0, 40, 55, 70, 80 deg

```

1 0.157 0.172 0.185 0.201 0.202
2 0.001 0.002 0.003 0.004 0.005
3 0.117 0.124 0.127 0.112 0.077
Total area of part_wall is      66.00

```

A.5.6 Construction details: part_floor

Details of opaque construction: part_floor and overall thickness 0.150

Layer	Matr	Thick	Conduc-	Density	Specif	IR	Solr	Diffu	R
	db	(mm)	tivity		heat	emis	abs	resis	m^2K/W
1	32	150.0	1.400	2100.	653.	0.90	0.65	19.	0.11
Heavy mix concrete : Heavy mix concrete									

```

ISO 6946 U values (horiz/upward/downward heat flow)= 3.608 4.046
3.153 (partition) 2.724
Total area of part_floor is      128.00

```

A.5.7 Construction details: floor

Details of opaque construction: floor and overall thickness 0.600

Layer	Matr	Thick	Conduc-	Density	Specif	IR	Solr	Diffu	R
	db	(mm)	tivity		heat	emis	abs	resis	m^2K/W
Ext	65	100.0	0.140	600.	1210.	0.91	0.65	14.	0.71
Flooring : Flooring									
2	214	250.0	0.030	25.	1000.	0.90	0.30	67.	8.33
EPS : EPS									
Int	32	250.0	1.400	2100.	653.	0.90	0.65	19.	0.18
Heavy mix concrete : Heavy mix concrete									

```

ISO 6946 U values (horiz/upward/downward heat flow)= 0.106 0.107
0.106 (partition) 0.105
Total area of floor is      57.75

```

A.5.8 Construction details: window

Details of transparent construction: window with DAG6349_06nb optics and overall thickness 0.028

Layer	Matr	Thick	Conduc-	Density	Specif	IR	Solr	Diffu	R
	db	(mm)	tivity		heat	emis	abs	resis	m^2K/W
Ext	242	6.0	0.760	2710.	837.	0.83	0.05	19200	0.01
Plate glass : Glass with placeholder single									
2	0	16.0	0.000	0.	0.	0.99	0.99	1.	0.17
air 0.17 0.17 0.17									
Int	242	6.0	0.760	2710.	837.	0.83	0.05	19200	0.01
Plate glass : Glass with placeholder single									

```

ISO 6946 U values (horiz/upward/downward heat flow)= 2.811 3.069
2.527 (partition) 2.243

```

Antisun green 63/49, 6mm, no blind: with id of: DAG6349_06nb with 3 layers [including air gaps] and visible trn: 0.63

Direct transmission @ 0, 40, 55, 70, 80 deg
 0.381 0.353 0.316 0.221 0.096
 Layer| absorption @ 0, 40, 55, 70, 80 deg
 1 0.502 0.527 0.539 0.522 0.432
 2 0.001 0.002 0.003 0.004 0.005
 3 0.047 0.046 0.044 0.036 0.023
 Total area of window is 25.60

A.5.9 Construction details: base_floor

Details of opaque construction: base_floor and overall thickness
 0.100

Layer	Matr db	Thick (mm)	Conduc- tivity	Density	Specif heat	IR emis	Solr abs	Diffu resis	R m^2K/W
1	32	100.0	1.400	2100.	653.	0.90	0.65	19.	0.07

Heavy mix concrete : Heavy mix concrete

ISO 6946 U values (horiz/upward/downward heat flow)= 4.142 4.730
 3.553 (partition) 3.017
 Total area of base_floor is 32.00

A.5.10 Construction details: base_wall

Details of opaque construction: base_wall and overall thickness
 0.300

Layer	Matr db	Thick (mm)	Conduc- tivity	Density	Specif heat	IR emis	Solr abs	Diffu resis	R m^2K/W
Ext	211	100.0	0.040	250.	840.	0.90	0.30	4.	2.50
Glasswool : Glasswool									
Int	32	200.0	1.400	2100.	653.	0.90	0.65	19.	0.14
Heavy mix concrete : Heavy mix concrete									

ISO 6946 U values (horiz/upward/downward heat flow)= 0.356 0.359
 0.351 (partition) 0.344
 Total area of base_wall is 32.00

A.5.11 Construction details: Heavymix_floor

Details of opaque construction: Heavymix_floor and overall thickness
 1.500

Layer	Matr db	Thick (mm)	Conduc- tivity	Density	Specif heat	IR emis	Solr abs	Diffu resis	R m^2K/W
Ext	32	300.0	1.400	2100.	653.	0.90	0.65	19.	0.21
Heavy mix concrete : Heavy mix concrete									
2	32	300.0	1.400	2100.	653.	0.90	0.65	19.	0.21
Heavy mix concrete : Heavy mix concrete									
3	32	300.0	1.400	2100.	653.	0.90	0.65	19.	0.21
Heavy mix concrete : Heavy mix concrete									
4	32	300.0	1.400	2100.	653.	0.90	0.65	19.	0.21
Heavy mix concrete : Heavy mix concrete									
Int	32	300.0	1.400	2100.	653.	0.90	0.65	19.	0.21

Heavy mix concrete : Heavy mix concrete

ISO 6946 U values (horiz/upward/downward heat flow)= 0.806 0.825
 0.780 (partition) 0.751
 Total area of Heavymix is 12.50

A.5.12 Construction details: Massive_floor

Details of opaque construction: Massive_floor and overall thickness
 1.500

Layer	Matr db	Thick (mm)	Conduc- tivity	Density	Specif heat	IR emis	Solr abs	Diffu resis	R m^2K/W
Ext	50	300.0	1.400	9000.	1524.	0.90	0.65	19.	0.21
Massive concrete : Massive concrete (copy of Heavy mix concrete)									
2	50	300.0	1.400	9000.	1524.	0.90	0.65	19.	0.21
Massive concrete : Massive concrete (copy of Heavy mix concrete)									
3	50	300.0	1.400	9000.	1524.	0.90	0.65	19.	0.21
Massive concrete : Massive concrete (copy of Heavy mix concrete)									
4	50	300.0	1.400	9000.	1524.	0.90	0.65	19.	0.21
Massive concrete : Massive concrete (copy of Heavy mix concrete)									
Int	50	300.0	1.400	9000.	1524.	0.90	0.65	19.	0.21
Massive concrete : Massive concrete (copy of Heavy mix concrete)									

ISO 6946 U values (horiz/upward/downward heat flow)= 0.806 0.825
 0.780 (partition) 0.751
 Total area of Heavymix is 12.50

A.6 Zone geometry

ID	Zone Name	Volume m^3	Surface			
			No.	Opaque	Transp	~Floor
1	0north_zone	59.5	10	108.5	11.0	29.8
2	0south_zone	56.0	8	91.0	11.0	28.0
3	0int_zone	12.5	6	32.5	0.0	6.3
4	1north_zone	119.0	10	157.5	22.0	29.8
5	1south_zone	112.0	9	100.4	47.6	28.0
6	1int_zone	25.0	6	52.5	0.0	6.3
7	basement	128.0	8	192.0	0.0	64.0
	all	512.	57	734.	92.	192.

A.6.1 Geometry details for 0_northzone

Zone 0_northzone (1) is composed of 10 surfaces and 16 vertices.
 It encloses a volume of 59.5m^3 of space, with a total surface
 area of 120.m^2 & approx floor area of 29.8m^2

There is 34.000m2 of exposed surface area, 34.000m2 of which is vertical.
 Outside walls are 114.29 % of floor area & avg U of 0.128 & UA of 4.3518

A summary of the surfaces in 0_northzone(1) follows:

Sur environment	Area m^2	Azim other side deg	Elev side deg	surface name	geometry optical locat	construction use	name
1 < external	9.00	90.	0.	0_E_wall	OPAQUE VERT	-	0ext_wall
2 < external	16.0	0.	0.	0_N_wall	OPAQUE VERT	-	0ext_wall
3 < external	9.00	270.	0.	0_W_wall	OPAQUE VERT	-	0ext_wall
4 < 0_N_part:1_northzone	29.8	0.	90.	0_N_part	OPAQUE CEIL	-	part_floor
5 < 0_N_ground:basement	29.8	0.	-90.	0_N_ground	OPAQUE FLOR	-	floor
6 < 0_W_intwall:0_intzone	5.00	90.	0.	0_W_intwall	OPAQUE VERT	-	int_wall
7 < 0_N_intwall:0_intzone	5.00	180.	0.	0_N_intwall	OPAQUE VERT	-	int_wall
8 < 0_E_intwall:0_intzone	5.00	270.	0.	0_E_intwall	OPAQUE VERT	-	int_wall
9 < part_wall_W:0_southzone	9.00	180.	0.	part_wall_W	DCF7671_ VERT	-	part_wall
10 < part_wall_E:0_southzone	2.00	180.	0.	part_wall_E	DCF7671_ VERT	-	part_wall

All surfaces will receive diffuse insolation (if shading not calculated).

Air schedule notes:

In this room nothing happen in terms of infiltration, ventilation from other zones or internal gains.

A.6.2 Geometry details for 0_southzone

Zone 0_southzone (2) is composed of 8 surfaces and 12 vertices. It encloses a volume of 56.0m^3 of space, with a total surface area of 102.m^2 & approx floor area of 28.0m^2
 There is 30.000m2 of exposed surface area, 30.000m2 of which is vertical.
 Outside walls are 107.14 % of floor area & avg U of 0.128 & UA of 3.8398

A summary of the surfaces in 0south_zone(2) follows:

Sur environment	Area m^2	Azim other deg	Elev side deg	surface name	geometry optical locat use	construction name
1 < external	16.0	180.	0.	0_S_wall	OPAQUE VERT -	0ext_wall
2 < external	7.00	90.	0.	0_E_wall	OPAQUE VERT -	0ext_wall
3 < external	7.00	270.	0.	0_W_wall	OPAQUE VERT -	0ext_wall
4 < S_floorslab:1_southzone	28.0	0.	90.	S_floorslab	OPAQUE CEIL -	part_floor
5 < S_groundfloo:basement	28.0	0.	-90.	S_groundfloo	OPAQUE FLOR -	floor
6 < 0_S_intwall:0_intzone	5.00	0.	0.	0_S_int_mid	OPAQUE VERT -	int_wall
7 < part_wall_W:0_northzone	9.00	0.	0.	part_wall_W	DCF7671_ VERT -	part_wall
8 < part_wall_E:0_northzone	2.00	0.	0.	part_wall_E	DCF7671_ VERT -	part_wall

All surfaces will receive diffuse insolation (if shading not calculated).

Uses same operations as zone 0_northzone

A.6.3 Geometry details for 0_intzone

Zone 0_intzone (3) is composed of 6 surfaces and 8 vertices. It encloses a volume of 12.5m³ of space, with a total surface area of 32.5m² & approx floor area of 6.25m²

A summary of the surfaces in 0int_zone(3) follows:

Sur environment	Area m^2	Azim other deg	Elev side deg	surface name	geometry optical locat use	construction name
1 < 0_S_int_mid:0_southzone	5.00	180.	0.	0_S_intwall	OPAQUE VERT -	int_wall_inv
2 < 0_E_intwall:0north_zone	5.00	90.	0.	0_E_intwall	OPAQUE VERT -	int_wall_inv
3 < 0_N_intwall:0north_zone	5.00	0.	0.	0_N_intwall	OPAQUE VERT -	int_wall_inv
4 < 0_W_intwall:0north_zone	5.00	270.	0.	0_W_intwall	OPAQUE VERT -	int_wall_inv
5 < 0_intpart:1int_zone	6.25	0.	90.	0_intpart	OPAQUE CEIL -	part_floor
6 < 0_intground:basement	6.25	0.	-90.	0_intground	OPAQUE FLOR -	test_CONC

All surfaces will receive diffuse insolation (if shading not calculated).

Uses same operations as zone 0north_zone

A.6.4 Geometry details for 1_northzone

Zone 1north_zone (4) is composed of 10 surfaces and 16 vertices. It encloses a volume of 119.m³ of space, with a total surface area of 180.m² & approx floor area of 29.8m²

There is 97.750m² of exposed surface area, 68.000m² of which is vertical.

Outside walls are 228.57 % of floor area & avg U of 0.806 & UA of 54.776

Flat roof is 100.00 % of floor area & avg U of 0.052 & UA of 1.5599

A summary of the surfaces in 1north_zone(4) follows:

Sur	Area	Azim	Elev	surface	geometry	construction
environment	other	side				
m ²	deg	deg	name	optical	locat	use name
1	18.0	90.	0.	1_E_wall	OPAQUE	VERT - 1ext_wall
<	external					
2	32.0	0.	0.	1_N_wall	OPAQUE	VERT - 1ext_wall
<	external					
3	18.0	270.	0.	1_W_wall	OPAQUE	VERT - 1ext_wall
<	external					
4	29.8	0.	90.	N_roof	OPAQUE	CEIL - roof
<	external					
5	10.0	270.	0.	1_E_intwall	OPAQUE	VERT - int_wall_inv
<	1_E_intwall:	lint_zone				
6	10.0	180.	0.	1_N_intwall	OPAQUE	VERT - int_wall_inv
<	1_N_intwall:	lint_zone				
7	10.0	90.	0.	1_W_intwall	OPAQUE	VERT - int_wall_inv
<	1_W_intwall:	lint_zone				
8	29.8	0.	-90.	0_N_part	OPAQUE	FLOR - part_floor
<	0_N_part:	0north_zone				
9	18.0	180.	0.	partition_W	DCF7671_	VERT - part_wall
<	1part_wall_W:	1south_zone				
10	4.00	180.	0.	partition_E	DCF7671_	VERT - part_wall
<	1part_wall_E:	1south_zone				

All surfaces will receive diffuse insolation (if shading not calculated).

Uses same operations as zone 0north_zone

A.6.5 Geometry details for 1_southzone

Zone 1south_zone (5) is composed of 9 surfaces and 16 vertices. It encloses a volume of 112.m^3 of space, with a total surface area of 148.m^2 & approx floor area of 28.0m^2 There is 88.000m2 of exposed surface area, 60.000m2 of which is vertical. Outside walls are 122.86 % of floor area & avg U of 0.806 & UA of 27.710 Flat roof is 100.00 % of floor area & avg U of 0.052 & UA of 1.4681 Glazing is 91.428 % of floor & 42.667 % facade with avg U of 2.811 & UA of 71.953

A summary of the surfaces in 1south_zone(5) follows:

Sur	Area	Azim	Elev	surface	geometry	construction		
environment	other	side						
	m^2	deg	deg	name	optical	locat	use	name
1	6.40	180.	0.	1_S_wall	OPAQUE	VERT -		1ext_wall
< external								
2	14.0	90.	0.	1_E_wall	OPAQUE	VERT -		1ext_wall
< external								
3	14.0	270.	0.	1_W_wall	OPAQUE	VERT -		1ext_wall
< external								
4	28.0	0.	90.	1_S_roof	OPAQUE	CEIL -		roof
< external								
5	10.0	0.	0.	1_middlewall	OPAQUE	VERT -		int_wall_inv
< 1_middlewall:1int_zone								
6	28.0	0.	-90.	S_floorslab	OPAQUE	FLOR -		part_floor
< S_floorslab:0south_zone								
7	25.6	180.	0.	window	DAG6349_	VERT	C-WIN	window
< external								
8	18.0	0.	0.	1part_wall_W	DCF7671_	VERT -		part_wall
< partition_W:1north_zone								
9	4.00	0.	0.	1part_wall_E	DCF7671_	VERT -		part_wall
< partition_E:1north_zone								

All surfaces will receive diffuse insolation (if shading not calculated).

Uses same operations as zone 0north_zone

A.6.6 Geometry details for 1_intzone

Zone 1int_zone (6) is composed of 6 surfaces and 8 vertices. It encloses a volume of 25.0m^3 of space, with a total surface area of 52.5m^2 & approx floor area of 6.25m^2 There is 6.2500m2 of exposed surface area. Flat roof is 100.00 % of floor area & avg U of 0.052 & UA of 0.32771

A summary of the surfaces in 1int_zone(6) follows:

Sur environment	Area m^2	Azim other deg	Elev side deg	surface name	geometry optical	locat use	construction name
1 < 1_E_intwall:1north_zone	10.0	90.	0.	1_E_intwall	OPAQUE	VERT -	int_wall
2 < 1_N_intwall:1north_zone	10.0	0.	0.	1_N_intwall	OPAQUE	VERT -	int_wall
3 < 1_W_intwall:1north_zone	10.0	270.	0.	1_W_intwall	OPAQUE	VERT -	int_wall
4 < external	6.25	0.	90.	1_introof	OPAQUE	CEIL -	roof
5 < 0_intpart:0int_zone	6.25	0.	-90.	0_intpart	OPAQUE	FLOR -	part_floor
6 < 1_middlewall:1south_zone	10.0	180.	0.	1_middlewall	OPAQUE	VERT -	int_wall

All surfaces will receive diffuse insolation (if shading not calculated).

Uses same operations as zone 0north_zone

A.6.7 Geometry details for basement

Zone basement (7) is composed of 8 surfaces and 14 vertices. It encloses a volume of 128.m^3 of space, with a total surface area of 192.m^2 & approx floor area of 64.0m^2

A summary of the surfaces in basement(7) follows:

Sur environment	Area m^2	Azim other deg	Elev side deg	surface name	geometry optical	locat use	construction name
1 < BASESIMP config type 24	16.0	180.	0.	S_wall_base	OPAQUE	VERT -	base_wall
2 < BASESIMP config type 24	16.0	90.	0.	E_wall_base	OPAQUE	VERT -	base_wall
3 < BASESIMP config type 24	16.0	0.	0.	N_wall_base	OPAQUE	VERT -	base_wall
4 < BASESIMP config type 24	16.0	270.	0.	W_wall_base	OPAQUE	VERT -	base_wall
5 < BASESIMP config type 24	64.0	0.	-90.	base_ground	OPAQUE	FLOR -	base_floor
6 < 0_N_ground:0north_zone	29.8	0.	90.	0_N_ground	OPAQUE	CEIL -	floor_inv
7 < S_groundfloo:0south_zone	28.0	0.	90.	S_groundfloo	OPAQUE	CEIL -	floor_inv

```
8 6.25      0. 90. 0_intground OPAQUE CEIL - test_CONC_in
||< 0_intground:0int_zone
```

All surfaces will receive diffuse insolation (if shading not calculated).

Uses same operations as zone 0north_zone

Appendix B

Energy calculations in Excel

**B.1: Calculated average temperatures 0.15m into the concrete slab
Östersund**

Day	Jan	Feb	Mar	Apr	May	Jun
1	10.9	8.9	7.5	8.3	10.3	13.9
2	10.8	8.8	7.5	8.3	10.5	13.9
3	10.7	8.7	7.5	8.4	10.6	14.0
4	10.6	8.6	7.5	8.5	10.8	14.0
5	10.6	8.6	7.5	8.5	10.9	14.1
6	10.5	8.5	7.6	8.6	11.0	14.1
7	10.4	8.4	7.6	8.7	11.1	14.2
8	10.3	8.4	7.6	8.8	11.2	14.3
9	10.2	8.3	7.6	8.9	11.3	14.4
10	10.2	8.2	7.6	9.0	11.4	14.6
11	10.1	8.1	7.6	9.0	11.5	14.7
12	10.0	8.1	7.6	9.1	11.6	14.8
13	10.0	8.0	7.6	9.2	11.7	14.9
14	9.9	7.9	7.6	9.2	11.7	15.1
15	9.8	7.9	7.6	9.3	11.9	15.2
16	9.7	7.8	7.7	9.3	12.0	15.2
17	9.7	7.8	7.7	9.4	12.0	15.4
18	9.6	7.7	7.7	9.4	12.1	15.5
19	9.5	7.7	7.7	9.5	12.2	15.6
20	9.5	7.7	7.7	9.5	12.3	15.7
21	9.4	7.6	7.8	9.6	12.5	15.7
22	9.4	7.6	7.8	9.7	12.6	15.8
23	9.3	7.6	7.9	9.7	12.8	15.8
24	9.3	7.6	7.9	9.8	13.0	15.9
25	9.2	7.6	7.9	9.8	13.2	16.0
26	9.2	7.6	8.0	9.9	13.4	16.1
27	9.1	7.5	8.0	10.0	13.5	16.3
28	9.1	7.5	8.1	10.0	13.6	16.4
29	9.0		8.1	10.1	13.7	16.5
30	9.0		8.2	10.2	13.7	16.6
31	8.9		8.2		13.8	
Sum	304	225	240	278	374	454
Days in month	31	28	31	30	31	30
Average temp [°C]	9.81	8.02	7.74	9.25	12.06	15.14

Day	Jul	Aug	Sep	Oct	Nov	Dec
1	16.6	19.6	21.3	21.0	19.7	16.7
2	16.7	19.7	21.4	20.9	19.6	16.6
3	16.8	19.8	21.5	20.8	19.5	16.5
4	16.8	19.9	21.6	20.7	19.4	16.4
5	16.9	20.0	21.6	20.7	19.3	16.3
6	17.0	20.1	21.7	20.6	19.2	16.2
7	17.1	20.1	21.6	20.5	19.2	16.1
8	17.3	20.2	21.5	20.5	19.1	16.0
9	17.5	20.4	21.5	20.4	19.0	16.0
10	17.7	20.5	21.5	20.3	18.9	15.9
11	17.9	20.6	21.4	20.3	18.8	15.8
12	18.0	20.6	21.4	20.4	18.7	15.7
13	18.1	20.6	21.4	20.4	18.6	15.6
14	18.2	20.6	21.3	20.3	18.5	15.5
15	18.3	20.7	21.3	20.3	18.4	15.4
16	18.4	20.7	21.3	20.3	18.3	15.3
17	18.4	20.7	21.2	20.3	18.2	15.2
18	18.5	20.7	21.1	20.3	18.1	15.1
19	18.6	20.7	21.2	20.2	18.0	15.1
20	18.6	20.7	21.2	20.2	17.9	15.0
21	18.6	20.7	21.3	20.2	17.8	14.9
22	18.6	20.8	21.3	20.1	17.7	14.8
23	18.7	20.9	21.3	20.1	17.6	14.7
24	18.7	21.0	21.3	20.0	17.5	14.6
25	18.9	21.1	21.3	20.0	17.4	14.5
26	19.0	21.2	21.2	20.0	17.3	14.4
27	19.2	21.2	21.2	19.9	17.2	14.3
28	19.2	21.3	21.2	19.9	17.0	14.2
29	19.3	21.3	21.1	19.8	16.9	14.1
30	19.4	21.3	21.0	19.8	16.8	14.0
31	19.5	21.3		19.7		14.9
Sum	563	639	640	629	550	475
Days in month	31	31	30	31	30	31
Average temp [°C]	18.15	20.60	21.34	20.28	18.32	15.34

B.2 Calculated average temperatures and temperature differences Östersund

	Average internal air temperature [°C]					
	0_intzone	0_northzone	0_southzone	1_intzone	basement	Concrete slab
Jan	6.97	-3.41	-3.3	4.42	7.71	9.81
Feb	6.13	-3.86	-3.09	3.4	5.87	8.02
Mar	9.53	2.51	4.3	6.94	5.54	7.74
Apr	14.04	11.01	13.35	12.3	7.07	9.25
May	14.06	17.15	19.31	14.65	9.16	12.06
Jun	17.41	21.33	23.23	18.17	11.7	15.14
Jul	20.43	24.32	26.39	21.13	13.87	18.15
Aug	22.13	23.04	25.02	22.34	15.56	20.60
Sep	21.17	16.8	18.32	20.3	16.03	21.34
Oct	18.68	10.47	11.7	16.96	15.41	20.28
Nov	15.17	2.24	2.33	12.47	14.07	18.32
Dec	11.55	-1.59	-1.8	8.55	11.37	15.34

	Temperature differences [°C]				
	$\Delta T(\text{groundfloor} - 0_intzone)$	$\Delta T(\text{groundfloor} - \text{basement})$	$\Delta T(\text{basement} - 0_southzone)$	$\Delta T(\text{basement} - 0_northzone)$	$\Delta T(\text{basement} - \text{groundfloor})$
Jan	2.84	2.10	11.01	11.12	-2.10
Feb	1.89	2.15	8.96	9.73	-2.15
Mar	-1.79	2.20	1.24	3.03	-2.20
Apr	-4.79	2.18	-6.28	-3.94	-2.18
May	-2.00	2.90	-10.15	-7.99	-2.90
Jun	-2.27	3.44	-11.53	-9.63	-3.44
Jul	-2.28	4.28	-12.52	-10.45	-4.28
Aug	-1.53	5.04	-9.46	-7.48	-5.04
Sep	0.17	5.31	-2.29	-0.77	-5.31
Oct	1.60	4.87	3.71	4.94	-4.87
Nov	3.15	4.25	11.74	11.83	-4.25
Dec	3.79	3.97	13.17	12.96	-3.97

**B.3 Calculated average delivered energy from hydronic floor from
Jan-01 to Dec-31 Östersund**

Day	JANUARY	FEBRUARY	MARCH	APRIL	MAY	JUNE
	Wh/day	Wh/day	Wh/day	Wh/day	Wh/day	Wh/day
1	0	0	0	2016	3072	1368
2	0	240	0	3024	1920	2256
3	0	0	2112	2448	2136	864
4	0	0	0	2304	2568	2856
5	0	0	0	2112	1608	1560
6	48	480	552	2712	2664	1896
7	0	576	0	72	936	2688
8	168	360	0	648	2760	3240
9	168	336	1176	2328	2712	3432
10	0	288	3096	0	744	2448
11	0	960	0	1728	3264	1248
12	120	240	1728	912	2352	3240
13	0	480	3192	3672	1248	3528
14	48	1176	2328	168	2904	2520
15	528	864	3144	2184	3624	720
16	0	1344	888	2136	720	3624
17	48	984	936	2472	2472	3504
18	0	960	3672	1560	1920	2280
19	0	912	288	600	3432	936
20	0	1464	1296	1608	2496	2760
21	0	792	2352	3336	3696	648
22	0	480	1440	2232	3888	1728
23	0	456	3000	3216	4032	2736
24	0	312	3648	1704	4056	2448
25	264	0	888	2160	2568	3096
26	0	600	48	1392	2568	3216
27	864	1008	1896	2088	3024	2400
28	144	648	2760	2256	720	1608
29	600		864	3264	1128	3072
30	240		2544	3744	2520	1344
31	168		4032		2448	0
Monthly delivered energy [Wh/month]	3408	15960	47880	60096	76200	69264
Hours of sunshine per month	31	112	186	240	310	330
Supply power [W]	110	143	257	250	246	210

Day	JULY	AUG	SEP	OCT	NOV	DEC
	Wh/day	Wh/day	Wh/day	Wh/day	Wh/day	Wh/day
1	2712	2352	3096	600	0	0
2	2712	1656	3096	672	0	0
3	1032	3312	3072	168	0	0
4	2904	2496	960	552	1104	144
5	1968	2976	2208	672	0	0
6	3504	624	0	0	1056	0
7	3624	3096	456	1200	48	0
8	3672	3000	1464	456	0	0
9	3624	2928	192	432	0	0
10	3624	2088	1176	1056	0	0
11	2472	1344	192	2136	0	0
12	2928	1440	2304	2112	0	0
13	2208	1440	912	216	0	0
14	2304	2016	1392	168	0	0
15	1008	1296	1176	1968	0	0
16	1944	1800	0	1992	24	0
17	3000	816	216	1032	0	0
18	1680	2088	2544	600	0	0
19	960	1056	2544	288	0	0
20	960	1368	2304	1872	0	0
21	1416	1824	2352	1008	0	0
22	1968	3144	312	264	0	0
23	1824	2688	1728	480	0	0
24	3312	2784	1128	1488	0	0
25	3600	2712	960	1488	0	0
26	3648	1344	360	168	336	0
27	1968	2472	1776	888	240	0
28	1848	2400	552	48	168	0
29	2976	912	696	1128	408	0
30	1584	1104	456	1224	0	0
31	3000	1944	0	888	0	0
Monthly delivered energy [Wh/month]	75984	62520	39624	27264	3384	144
Hours of sunshine per month	341	248	210	217	150	31
Supply power [W]	223	252	189	126	23	5

B.3 Calculated inputs for energy balance Östersund

	Jan	Feb	Mar	Apr	May	Jun	Jul	Aug	Sep	Oct	Nov	Dec
$\Delta T(\text{basement-0_southzone})$	11.01	8.96	1.24	-6.28	-10	-11.5	-12.5	-9.46	-2.29	3.71	11.74	13.17
$\Delta T(\text{basement-0_northzone})$	11.12	9.73	3.03	-3.94	-8	-9.63	-10.5	-7.48	-0.77	4.94	11.83	12.96
$\Delta T(\text{basement-intfloor})$	-2.10	-2.15	-2.20	-2.18	-2.90	-3.44	-4.28	-5.04	-5.31	-4.87	-4.25	-3.97
surface area southfloor [m2]	28	28	28	28	28	28	28	28	28	28	28	28
surface area northfloor [m2]	29.75	29.75	29.75	29.75	29.8	29.75	29.75	29.75	29.75	29.75	29.75	29.75
surface area ground [m2]	64	64	64	64	64	64	64	64	64	64	64	64
surface area intfloor [m2]	6.25	6.25	6.25	6.25	6.25	6.25	6.25	6.25	6.25	6.25	6.25	6.25
U-value partition floor [W/m2K]	0.106	0.106	0.106	0.106	0.11	0.106	0.106	0.106	0.106	0.106	0.106	0.106
U-value groundfloor [W/m2K]	4.142	4.142	4.142	4.142	4.14	4.142	4.142	4.142	4.142	4.142	4.142	4.142
U-value intfloor [W/m2K]	0.806	0.806	0.806	0.806	0.81	0.806	0.806	0.806	0.806	0.806	0.806	0.806
Days in month	31	28	31	30	31	30	31	31	30	31	30	31

B.4 Energy balance basement zone and concrete slab

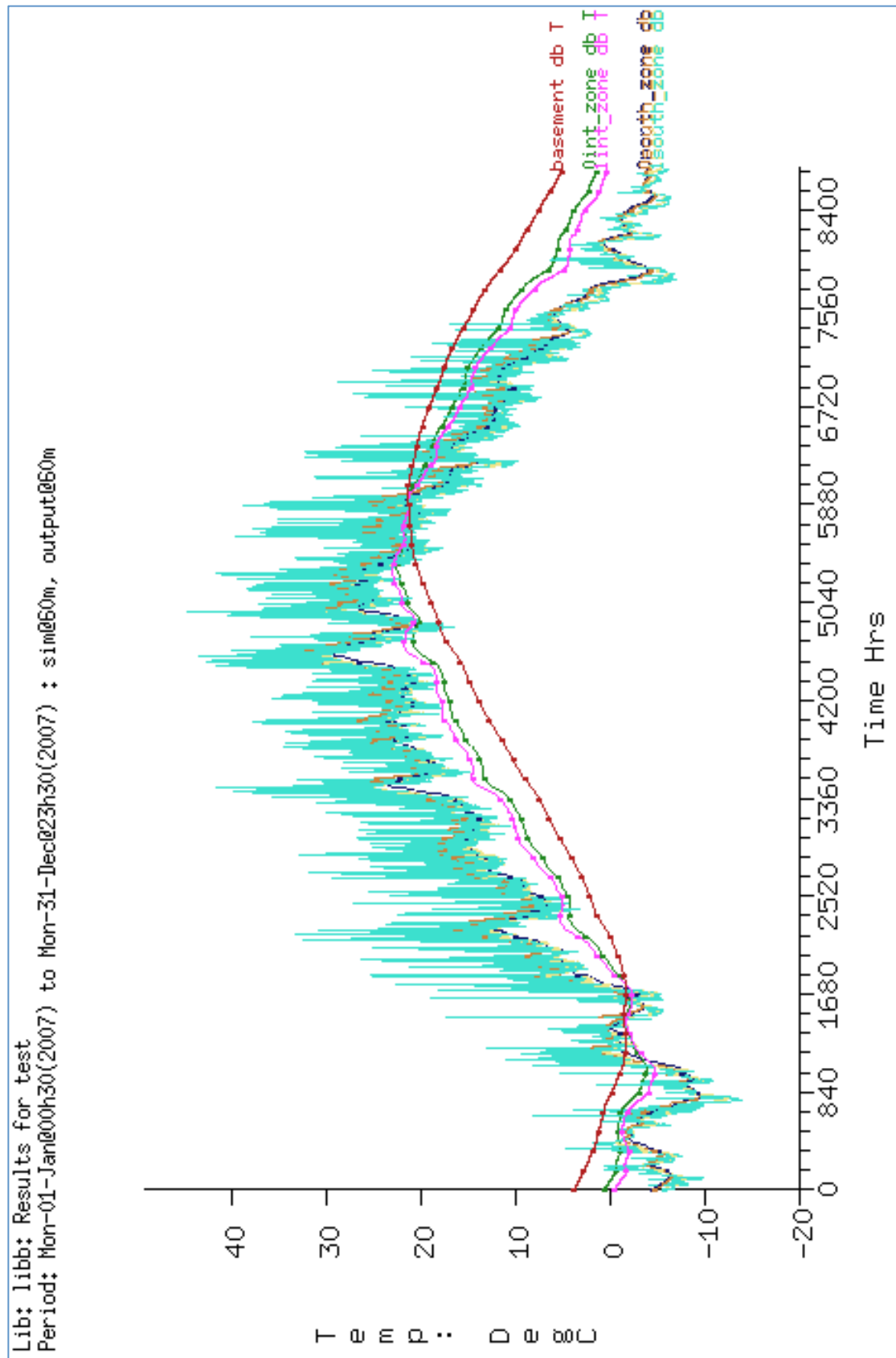
	Heat transfer from slab to basement [kWh]	Heat transfer from basement to 0_northzone [kWh]	Heat transfer from basement to 0_southzone [kWh]	Heat transfer from basement to ground [kWh]
Jan	7.9	26.1	24.3	-58.3
Feb	7.3	20.6	17.9	-45.8
Mar	8.2	7.1	2.7	-18.1
Apr	7.9	-8.9	-13.4	14.4
May	10.9	-18.7	-22.4	30.3
Jun	12.5	-21.9	-24.6	34.0
Jul	16.0	-24.5	-27.6	36.1
Aug	18.9	-17.5	-20.9	19.5
Sep	19.3	-1.7	-4.9	-12.6
Oct	18.3	11.6	8.2	-38.0
Nov	15.4	26.9	25.1	-67.4
Dec	14.9	30.4	29.1	-74.4

	Heat transfer from hydronic floor to slab [kWh]	Reduction in stored heat within slab [kWh]	Heat transfer from 0_intzone to slab [kWh]	Heat transfer from basement to slab [kWh]
Jan	3.6	14.8	-10.6	-7.9
Feb	12.9	0.8	-6.4	-7.3
Mar	46.4	-44.9	6.7	-8.2
Apr	66.6	-76.1	17.4	-7.9
May	76.2	-72.8	7.5	-10.9
Jun	69.3	-65.0	8.2	-12.5
Jul	76.0	-68.5	8.6	-16.0
Aug	62.5	-49.4	5.7	-18.9
Sep	39.6	-19.7	-0.6	-19.3
Oct	27.3	-3.0	-6.0	-18.3
Nov	3.4	23.5	-11.4	-15.4
Dec	0.1	28.9	-14.2	-14.9

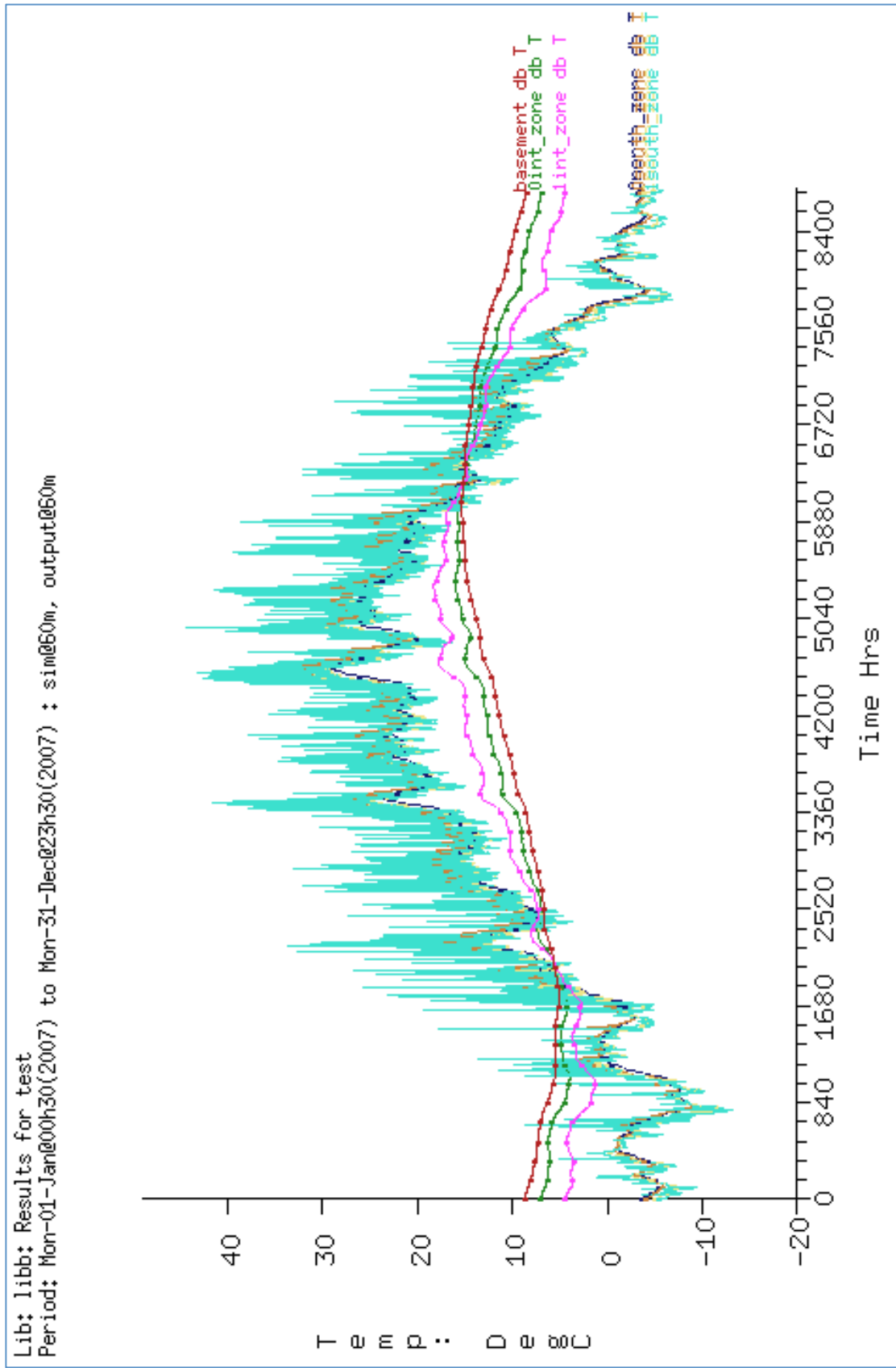
Appendix C

Zone dry bulb temperature graphs

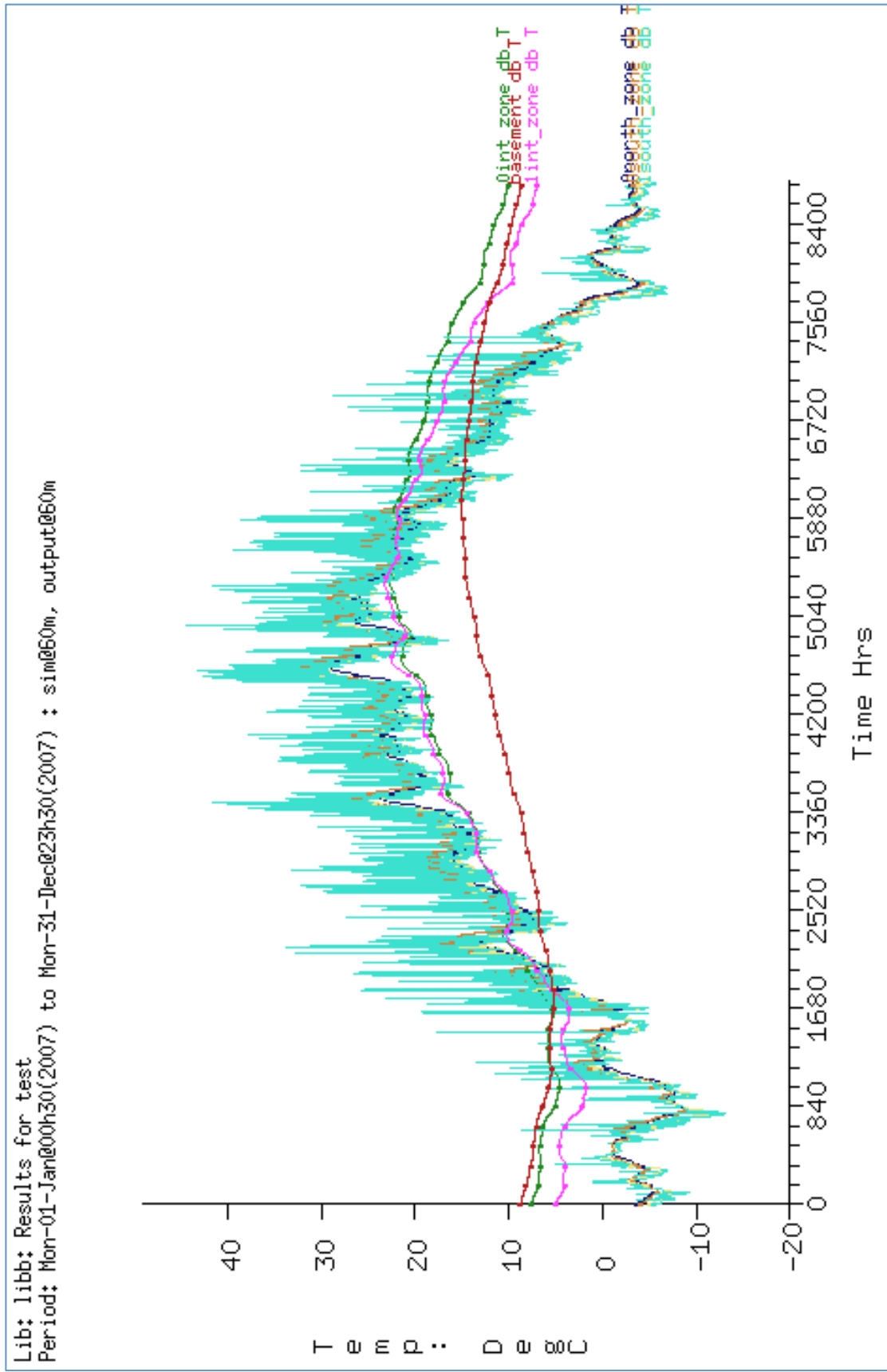
C.1 Case 1



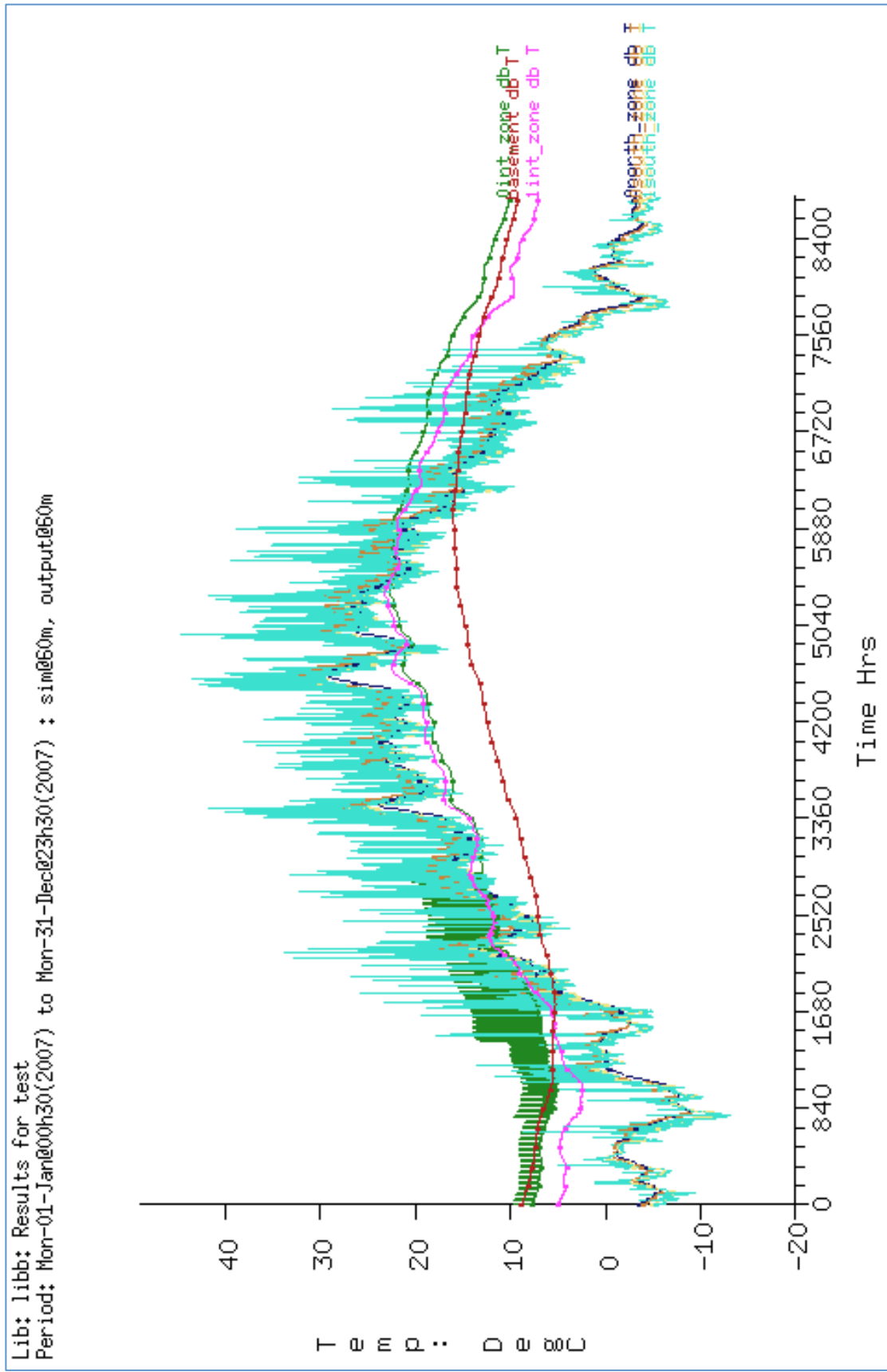
C.2 Case 2



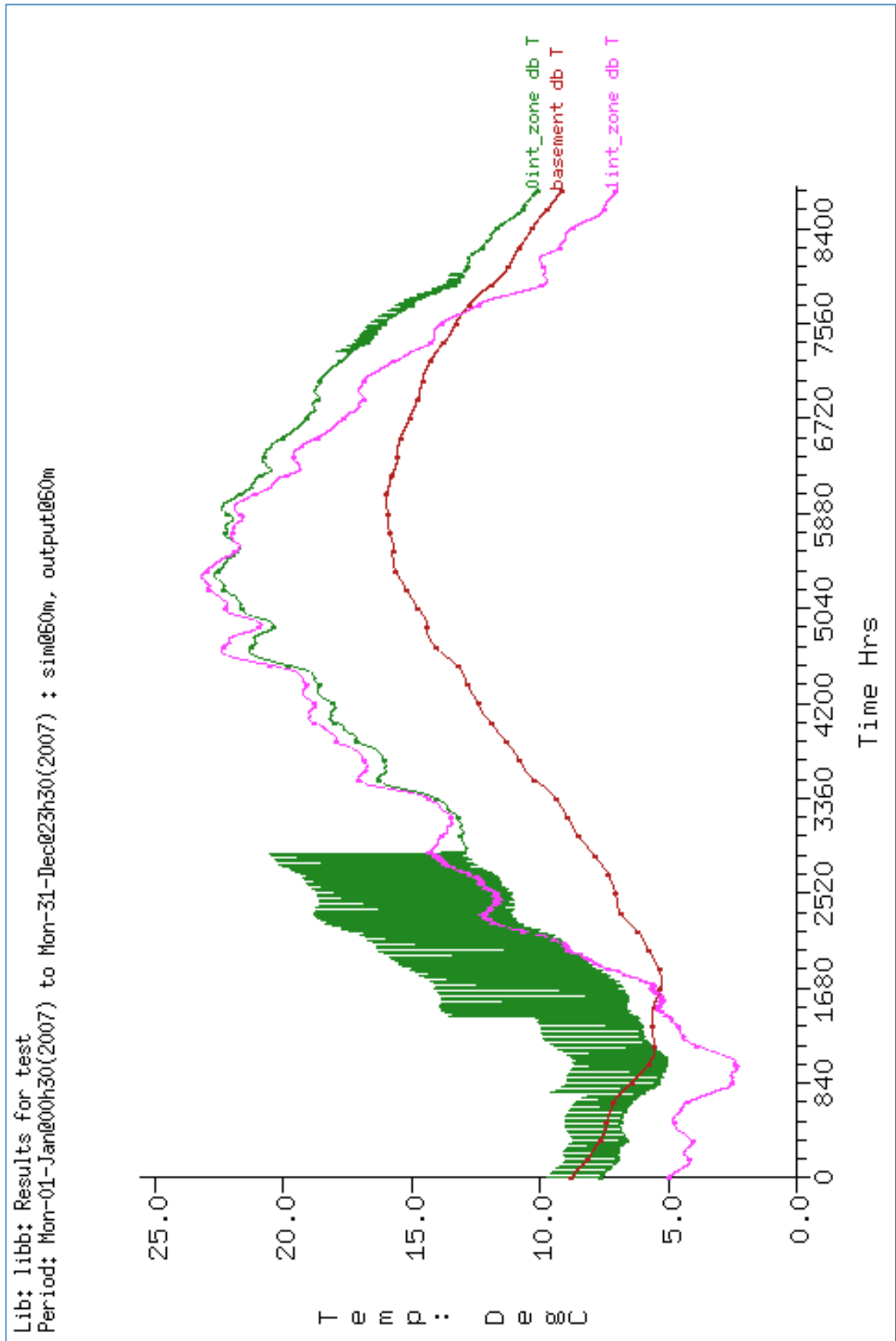
C.3 Case 3a



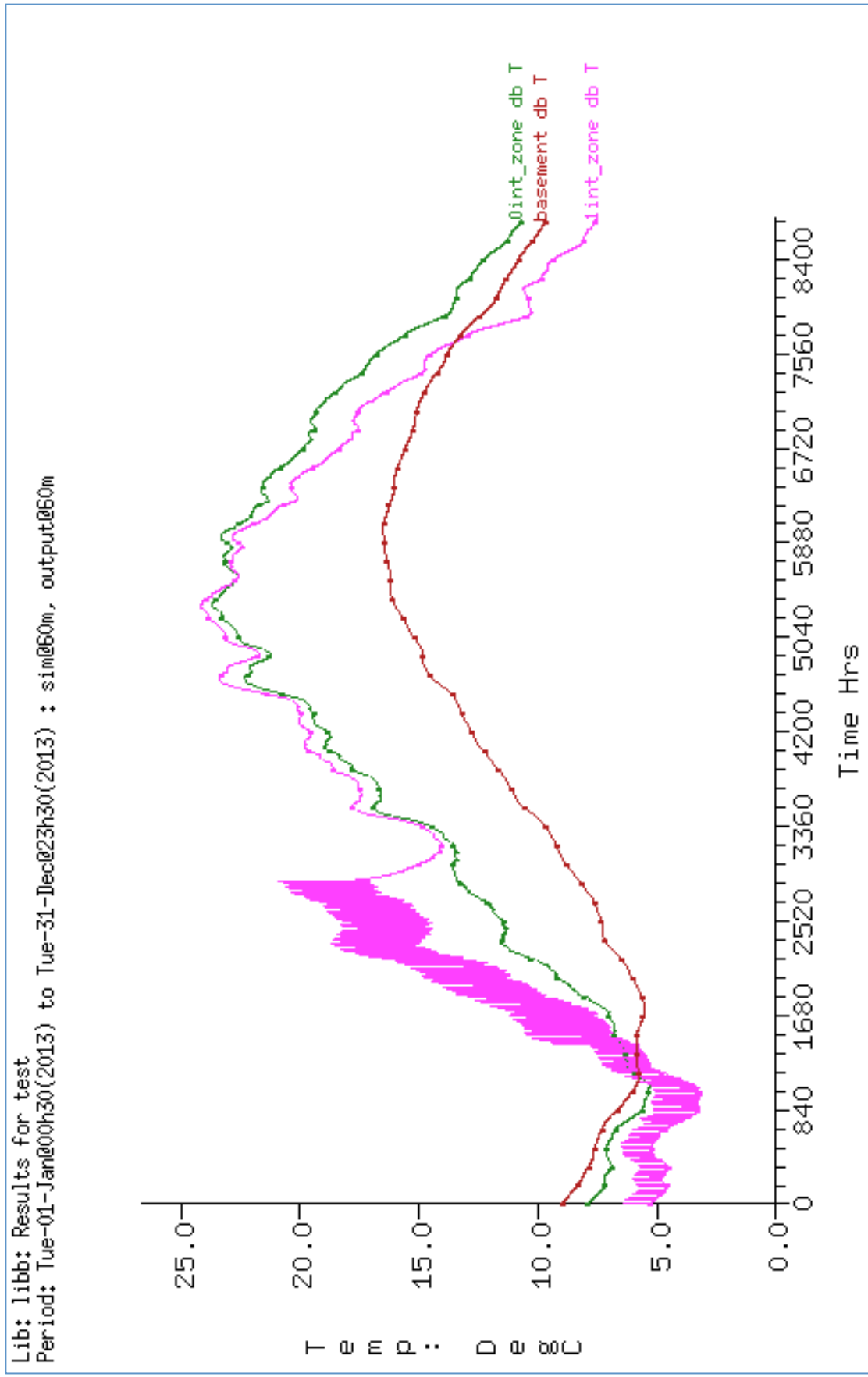
C.4 Case 4



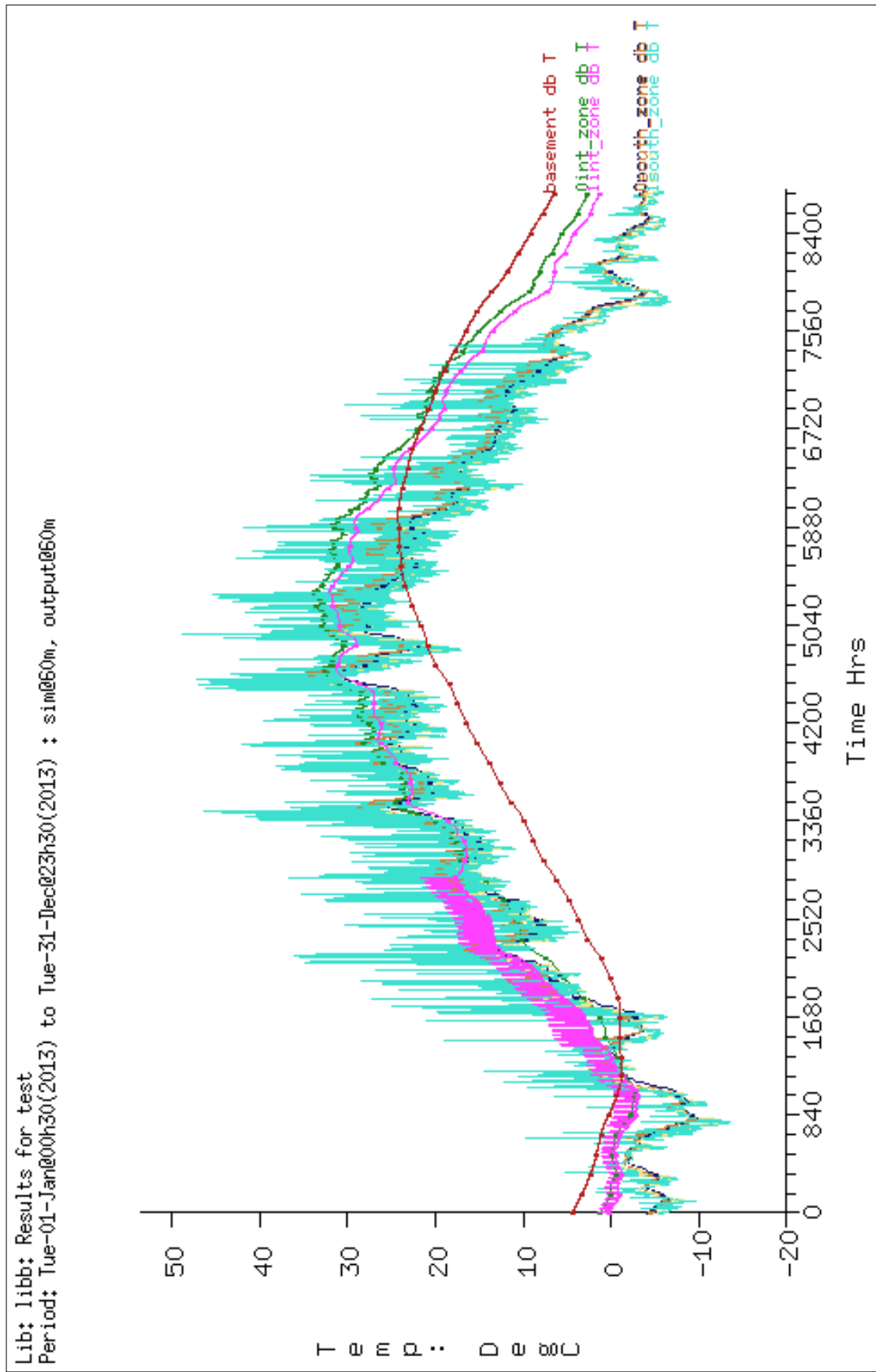
C.5 Case 5



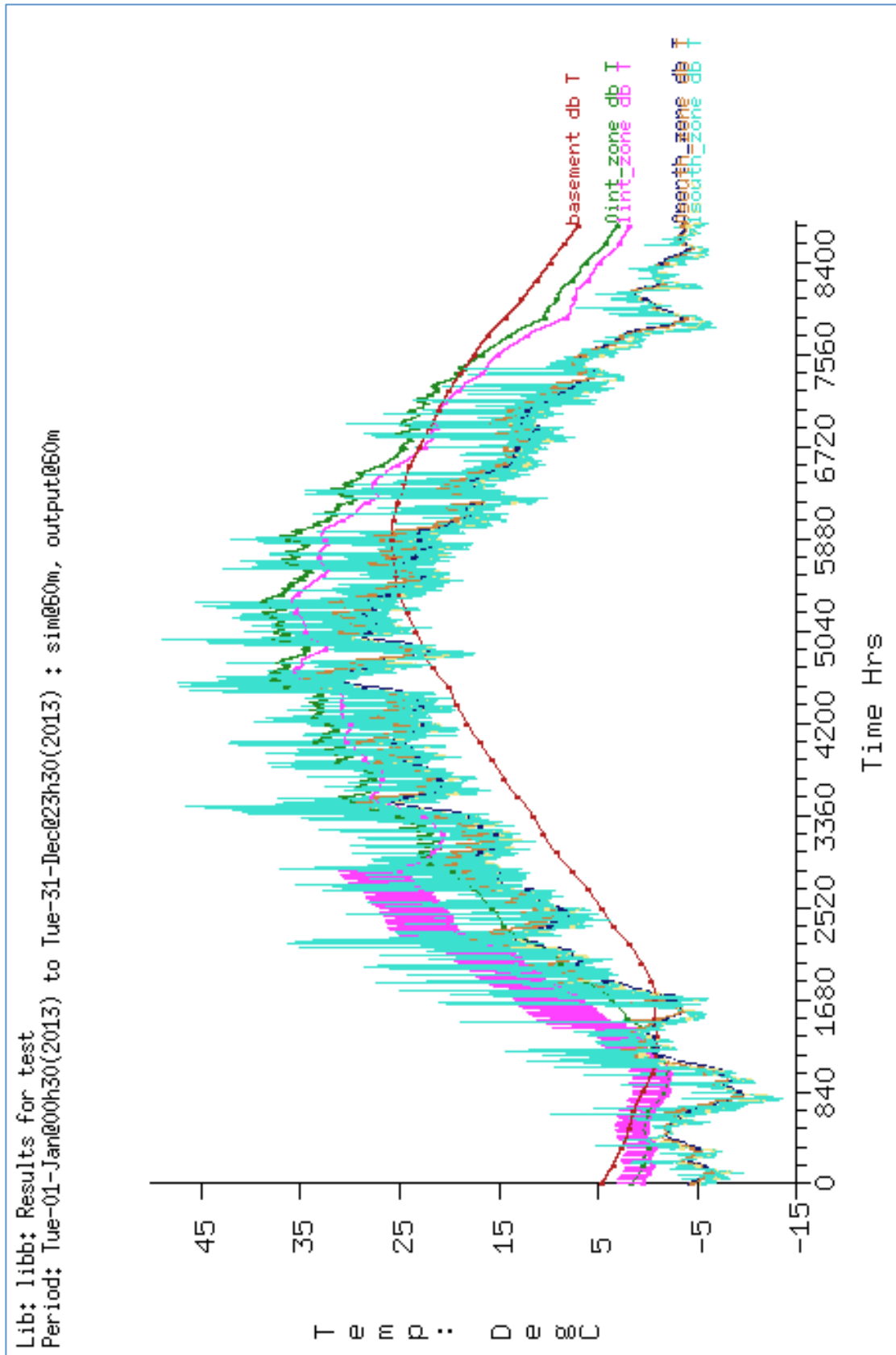
C.6 Case 6



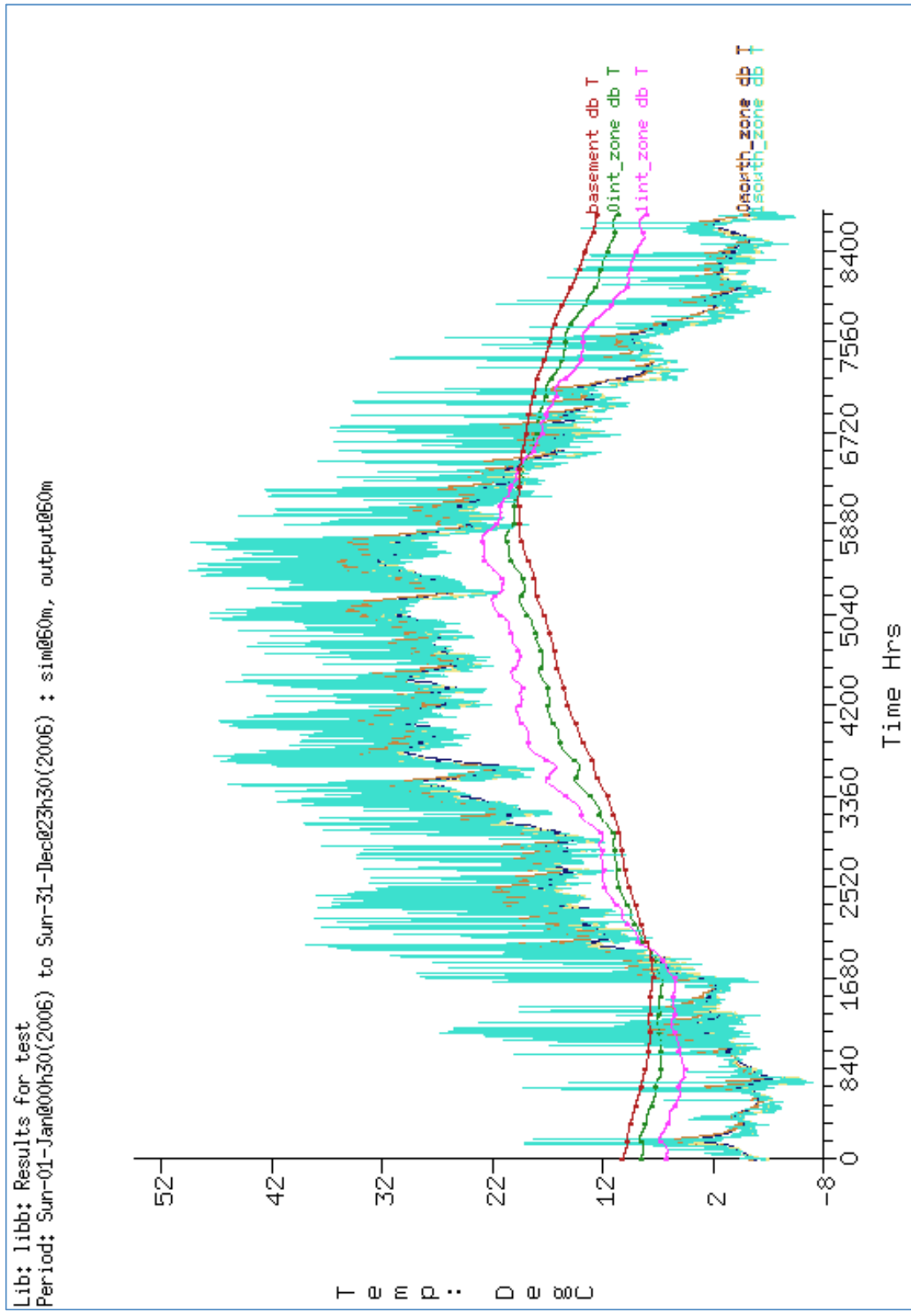
C.7 Case 7a



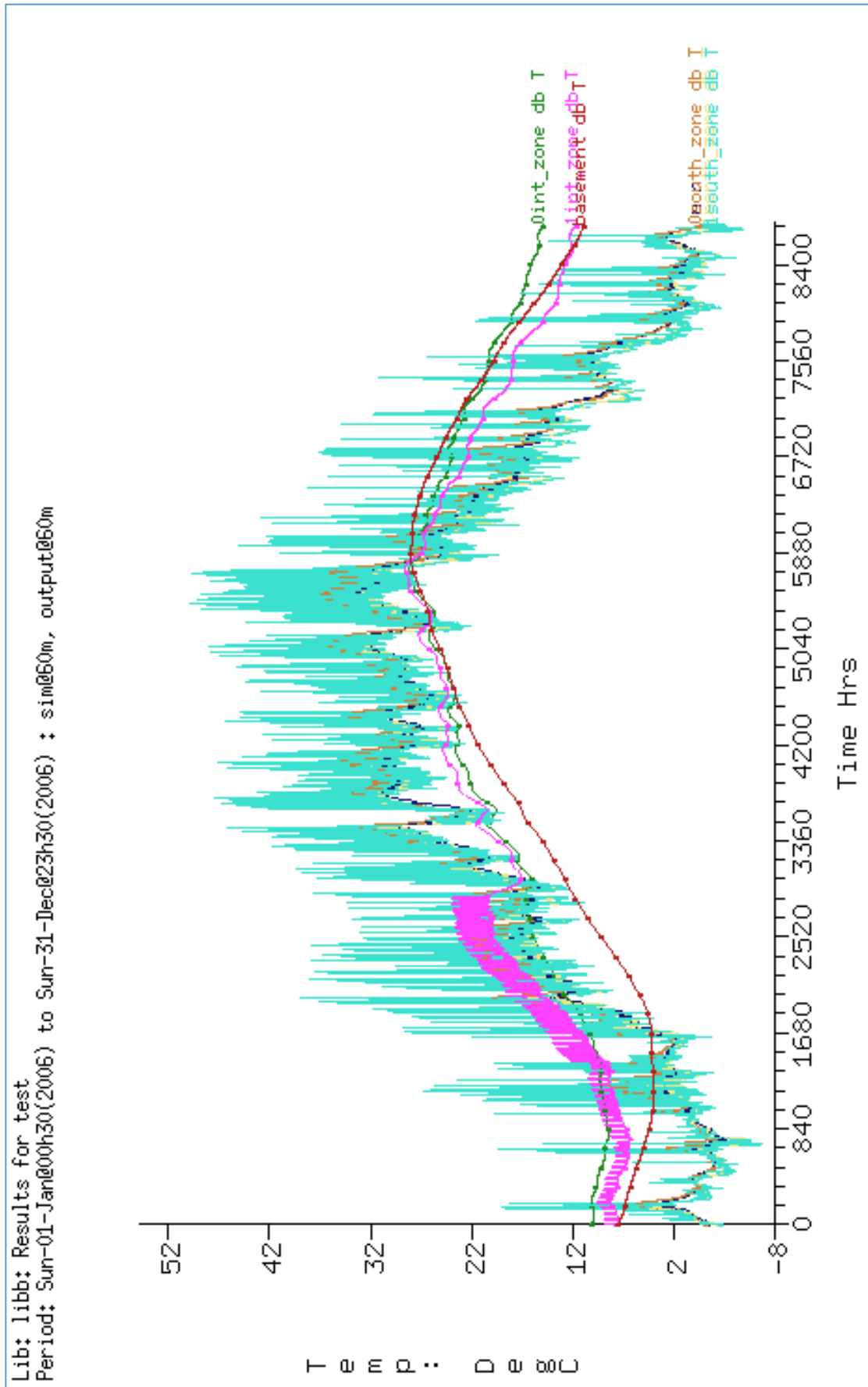
C.8 Case 7b



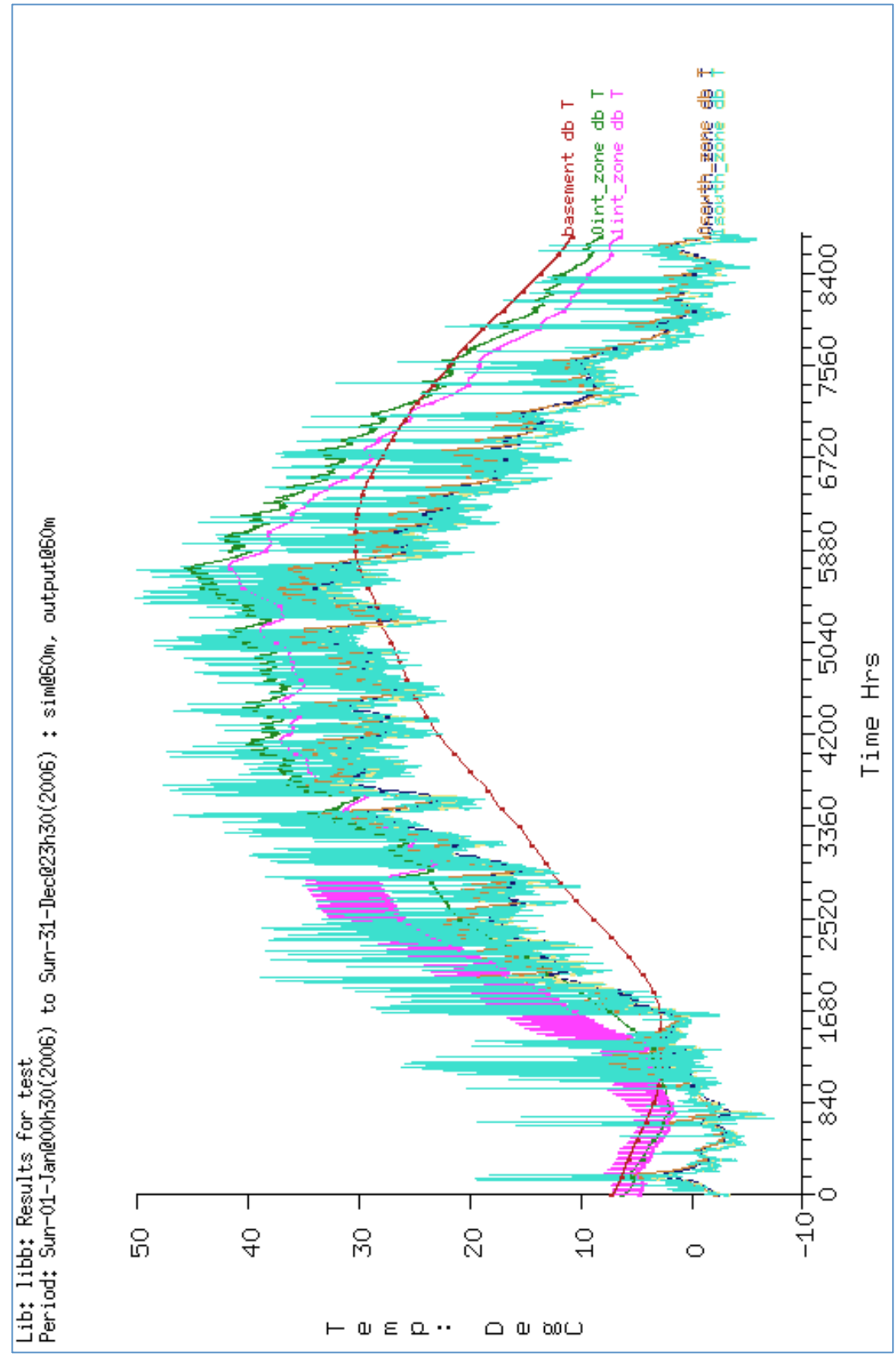
C.9 Case 8



C.10 Case 9



C.11 Case 10



Appendix D

Challenges with ESP-r

D.1 Challenges with ESP-r

ESP-r is under active development. Because of the open source policy, on any given day there may be a half dozen commits of code, documentation or updates to the software. One of the weaknesses in ESP-r is that it is a very advanced simulation tool often requiring expert knowledge. However, this can also be seen as a strength for expert users, as they may be able to offer more thorough and realistic results than that of other simulation tools. The user manual places emphasis on the importance of learning through workshops under close supervision of experts. The user manual also suggests repeatedly that there are “several dragons lurking around in the code”.

One problem encountered in this report was to set up the solar heating system consisting of plant components. An approach used by former student at NTNU, Are Siljan Børset was attempted replicated, but failed at first with several warning messages. After several attempts, it was discovered that there was most likely a *dragon lurking around in the code* in this version of ESP-r or that it had been installed incorrectly. A model in ESP-r is built up of a number of databases, and the default plant database for creating the solar heating system did not seem to work. The model was tested on four different computers using the same version of ESP-r and the same problem was found on all of them. Eventually a fifth computer with an older version of Linux and ESP-r was tested. The model had to be built up from scratch, as the two versions were incompatible. The problem encountered on the four initial computers did not seem to be a problem in the old version. The plants database was found with all the available components listed. However, the model still did not work as intended using the old version.

When trying to define the control strategy there was no option to select the two components (solar collector and tank) subject to the temperature difference sensor. An email was sent to ESP-r users and developers asking for help with the control strategy. A few suggestions were given in reply, but none of which had not already been tried. Yet another version of ESP-r was installed on the computer to see if that would fix the problem. Both the plants database and the temperature difference option for the control strategy was included in this version and the simulations would finally run.

